Detection, Documentation and Homogenization of Urban Heat Island Effects in Long Temperature Time Series

Dissertation

zur Erlangung des Grades

„Doktor der Naturwissenschaften“

im Promotionsfach Geographie

am Fachbereich Chemie, Pharmazie und Geowissenschaften

der Johannes Gutenberg-Universität Mainz

Manuel Dienst

geboren in Neuss

Mainz, den 31.08.2018

Tag der mündlichen Prüfung: 07.11.2018

Summary

Particularly in the light of current global warming, we trust in meteorological station data to quantify recent changes in the climate system. This data also forms the foundation of paleoclimatic reconstructions as well as climate models, confirming the importance of its reliability and representativeness to allow glimpses in past and future climate variability. Unfortunately, non-climatic impacts are sometimes incorporated in temperature records, hence biasing them. This thesis addresses the effect of urban heat islands (UHIs) on temperature readings, tackling the question of how to detect and remove this influence in long temperature series. Furthermore, it sheds a light on whether it is legitimate to characterise small settlements and associated weather stations as rural, thus regarding the urban bias negligible. In order to approach these questions, temperature readings with a high spatio-temporal resolution from sensor networks in several European villages and one city have been analysed. A first investigation showed the formation of significant urban heat islands in the villages Haparanda (Sweden), Geisenheim (Germany), and Cazorla (Spain). Minimum temperatures are most affected and display a decreasing UHI maximum intensity from North (1.4 °C) to South (0.9 °C). Land cover analysis revealed warming to be strongly correlated with nearby built-up area in all villages. In a second study, this relationship was also confirmed for the city of Brno (Czech Republic). The additional warming was quantified for all past measurement sites of the more than 200-year-old local meteorological station. A unique approach enabled the assessment of an urban heat island related bias at different times in the corresponding temperature record, allowing for a removal of this inadvertent influence. A correction led to a steeper warming trend particularly in minimum temperatures, with the strongest implications for spring (+0.3 °C / century). Similar results are found in Haparanda if correcting for site-related anthropogenic influence. For this study, measurements were conducted at each historical measurement location to exactly quantify site-specific warming features. Since Haparanda has a more than 150 year long temperature record and is situated remotely, relative homogenization based on reference data is not applicable here, hence boosting the importance of this data enhancement approach. Applying the same technique in the Spanish village Tivissa led to a substantial trend increase in minimum temperatures of up to 1 °C / century, while maximum temperatures were less, though inversely, affected. As the time series has been partly homogenized, results could be compared to the aforementioned method. While the new method's strength is the exact consideration of break points in the time series due to relocations as well as the allowance for site-specific climatology, its weaknesses are to disregard other non-climatic factors as well as to display limitations if relocations are not well documented.

Zusammenfassung

Besonders in Anbetracht der globalen Erwärmung vertrauen wir auf Daten meteorologischer Stationen, um aktuelle Veränderungen im Klimasystem zu erfassen. Eben jene Daten bilden die Grundlage für paläoklimatische Rekonstruktionen und Klimamodelle, was die Wichtigkeit ihrer Zuverlässigkeit und Repräsentativität im Hinblick auf die Abbildung vergangener und zukünftiger Klimavariabilität bestärkt. Allerdings sind bisweilen nichtklimatische Effekte in den Temperaturzeitreihen enthalten, die sie fehlerhaft machen. Diese Dissertation setzt sich mit den Auswirkungen städtischer Wärmeinseln auf Temperaturmessdaten auseinander, wobei sie der Frage nachgeht, wie sich dieser Einfluss in langen Zeitreihen detektieren und entfernen lässt. Zudem untersucht sie das Problem, ob kleinere Ortschaften und ihre assoziierten Wetterstationen tatsächlich als ländlich charakterisiert werden können, was bedeuten würde, dass jeglicher urbaner Einfluss vernachlässigbar ist. Um diese Fragen zu klären wurden Temperaturmessungen mit hoher raum-zeitlicher Auflösung von Sensornetzwerken in mehreren europäischen Dörfern und einer Stadt analysiert. Eine erste Untersuchung zeigte die Bildung ausgeprägter Wärmeinseln in den Dörfern Haparanda (Schweden), Geisenheim (Deutschland) und Cazorla (Spanien). Am stärksten tritt dieser Effekt in Minimumtemperaturen auf und zeigt darin einen Rückgang in der maximalen Intensität von Nord (1,4 °C) nach Süd (0,9 °C). Eine Analyse der Bodenbedeckung aller Orte machte deutlich, dass die Erwärmung stark mit der bebauten Fläche in der Umgebung korreliert. Eine zweite Untersuchung bestätigte diesen Zusammenhang für die Stadt Brünn (Tschechien). Die zusätzliche Erwärmung wurde dort für alle vergangenen Messstandorte der über 200 Jahre alten meteorologischen Station bestimmt. Dieser einzigartige Ansatz macht es möglich, den Fehler, der durch den städtischen Wärmeeffekt verursacht wird, im Nachgang aus der Temperaturzeitreihe herauszurechnen. Diese Korrektur führt zu einem Anstieg des Erwärmungstrends in Maximum- aber vor allem Minimumtemperaturen, wobei der Frühling am stärksten betroffen ist (+0,3 °C / Jahrhundert). Ähnliche Ergebnisse zeigt auch die Zeitreihe aus Haparanda auf, wenn der anthropogene Einfluss an den einzelnen Messstellen herausgenommen wird. Für diese Untersuchung wurden Messungen an jeder historischen Position der meteorologischen Station durchgeführt, um lokale Erwärmungsmuster zu quantifizieren. Die Wichtigkeit einer Verbesserung der Daten wird bestärkt durch den Umstand, dass Haparanda eine mehr als 150 Jahre lange Temperaturzeitreihe aufweist und die Station sehr abgeschieden liegt, was eine relative Homogenisierung der Daten basierend auf Referenzwerten anderer Stationen unmöglich macht. Bei Anwendung derselben Methode im spanischen Ort Tivissa ergibt sich ein Trendanstieg in Minimumtemperaturen von 1 °C / Jahrhundert, wobei sich die Maximumtemperaturen invers

verhalten und weniger stark betroffen sind. Da die Zeitreihe teilweise homogenisiert wurde, lassen sich die Resultate mit der hier neu eingeführten Methode vergleichen. Stärken der neuen Methode sind die genaue Berücksichtigung von Umbrüchen in der Zeitreihe aufgrund von Änderungen der Messstelle sowie die genaue Berücksichtigung der lokalen Klimatologie. Die fehlende Beachtung anderer, nicht-klimatischer Faktoren sowie die begrenzte Anwendbarkeit bei mangelnder Dokumentation von Änderungen der Messstelle sind hingegen erkennbare Schwächen.

Acknowledgements

Not available in online version.

Not available in online version.

Table of Contents

Summary I

Zusammenfassung II

Acknowledgements IV

Table of Contents VI

1. Introduction 1

2. Determination of the urban heat island intensity in villages and its connection to land cover in three European climate zones 8

2.1. Introduction 9

2.2. Study sites and methods 10

2.2.1. Study sites 10

2.2.2. Temperature sensor network 12

2.2.3. Digitization 13

2.2.4. Data analysis 14

2.3. Results 16

2.3.1. Spatial temperature patterns 16

2.3.2. Correlation of land cover and temperature 18

2.3.3. Regression analysis 19

2.4. Discussion 21

2.4.1. Topography 21

2.4.2. Village UHIs 22

2.4.3. Land cover effects 24

2.4.4. Implications of village UHI 26

2.5. Conclusion 27

2.6. References 27

3. Addressing the relocation bias in a long temperature record by means of land cover assessment 34

3.1. Introduction 35

3.2. Methods 36
3.2.1. Study area 36
3.2.2. Measurements 36
3.2.3. Land Use and Land Cover change 39
3.2.4. Historical temperature data 40
3.3. Results 41
3.4. Discussion and conclusions 46
3.4.1. Temperatures and their connection to settlement structure 47
3.4.2. The relocation bias 48
3.4.3. Time series corrections 48
3.5. References 50

4. Removing the relocation bias from the 155-year Haparanda temperature record in Northern Europe 56
4.1. Introduction 57
4.2. Research sites and methods 59
4.2.1. Study area 59
4.2.2. Met station history 60
4.2.3. Application of HOMER for bias identification 62
4.2.4. Temperature sensor network 64
4.2.5. Data analysis 65
4.2.6. Correction for relocation bias 66
4.3. Results 67
4.3.1. Haparanda temperature differences 67
4.3.2. Adjustment of the long Haparanda station record 69
4.4. Discussion 72
4.4.1. Suitability of the rural reference 72
4.4.2. Determining the urban bias 73
4.4.3. Adjusting the long Haparanda temperature record 75
4.5. Conclusions 77
4.6. References 77

5. Detection and elimination of UHI effects in long temperature records from villages – A case study from Tivissa, Spain 84
5.1. Introduction 85
5.2. Study area and methods 86
5.2.1. Study area 86
5.2.2. Meteorological station history and dataset 87
5.2.3. Current measurements 89
5.2.4. The correction approach 90
5.2.5. Comparison to HOMER output 91
5.3. Results 91
5.3.1. Spatial temperature patterns 92
5.3.2. Eliminating the relocation bias 94
5.3.3. Comparison of correction and homogenization approach 96
5.4. Discussion 98
5.4.1. Urban warming in Tivissa 98
5.4.2. Implications of time series adjustment 99
5.4.3. Evaluating the correction approach 101
5.5. Conclusions 103
5.6. References 104

6. Conclusions and Prospects 109

Bibliography 112
List of Figures 120
List of Tables 123
Curriculum vitae 124

1 Introduction

Urbanization and the urban heat island

Today's world is experiencing a rapid and extensive urbanization. The main reason for this development is the high population growth of more than 80 million people every year, which will most likely result in the world's population exceeding eight billion before 2030 (United Nations, 2017). Another cause is the enhanced tendency to live in cities, resulting in 55 % of the entire population residing in urban areas (United Nations, 2018). As these trends are more likely to increase rather than decrease, positive as well as negative developments will intensify accordingly.

Among other implications, the aforementioned trends create a change in environment and dominating land cover, gradually replacing natural and cultivated landscapes with urban ones. This can be observed all over the planet, for example in the United States of America (Homer *et al.*, 2015), Mexico (López *et al.*, 2001), Bangladesh (Dewan and Yamaguchi, 2009), and in various developing countries (Döös, 2002). This conversion not only poses a great threat to biodiversity and contributes to biotic homogenization (McKinney, 2006), it also eventuates in an alteration of climatic conditions, for example influencing regional thunderstorm dynamics (Bornstein and Lin, 2000; Niyogi *et al.*, 2011) and amplifying the amount of precipitation (Vogel and Huff, 1978; Dixon and Mote, 2003). The presumably most prominent feature is the development of an urban heat island (UHI), referring to a rise in temperatures in the urban area compared to the rural surroundings as detailed by Landsberg (1981).

The transition from a rural to an urban area is mainly characterised by a change in materials and geometry entailed in the introduction of houses, industrial complexes, walls, paved surfaces, and other urban structures that usually contribute to additional warming. One major aspect in that regard is the alteration of the Sky View Factor (SF) and the related change in radiation balance. The urban geometry often forms street canyons that lead to enhanced radiation trapping, preventing a cooling especially at night when sensible heat in rural areas leaves the system more easily (Hamdi and Schayes, 2008). Introducing materials like concrete, bricks, and others, while removing natural surfaces and vegetation might drastically lower the heat capacities and surface albedos of a site, contributing to accelerated warming as shown by Kolokotroni and Giridharan (2008). The replacement of bare soil and vegetation by urban

surfaces has other implications as well, one being the reduction of evapotranspiration and hence a decrease in latent heat flux (Grimmond and Oke, 2002). In consequence, park areas have proved to develop cool islands within the urban areas (Spronken-Smith and Oke, 1998; Chang *et al.*, 2007). Another contribution to higher urban temperatures is the anthropogenic heat release generated by, for example, industrial production, domestic heating, air conditioning, and traffic. The magnitude of such emissions shows a strong seasonality due to the varying demand for heating and cooling, respectively, as detailed in many studies all over the world, e.g. for Singapore (Quah and Roth, 2012), Toulouse, France (Pigeon *et al.*, 2007), and São Paulo, Brazil (Ferreira *et al.*, 2010).

Finally, embodying an obstacle and hence blocking or redirecting the wind flow (Oke, 1987), urban structures generally lead to decreased wind velocities of up to 20-30 % within cities in comparison to the rural surroundings (Lee, 1979). As a result, ventilation in cities is disturbed, implying less potential to counteract UHI effects (Morris *et al.*, 2001; Lopes *et al.*, 2011) and to remediate air pollution (Berkowicz *et al.*, 1996; Elminir, 2005). This increases the risk of affecting human health, as heat stress in urban areas might cause higher mortality rates (Conti *et al.*, 2005; Tan *et al.*, 2010). Moreover, pollutants and particle matter are known to cause respiratory diseases (Künzli *et al.*, 2000; Brunekreef and Holgate, 2002).

UHI variations and the negligence of smaller settlements

Even though the factors influencing the formation of UHIs are the same, the intensity varies from region to region and from city to city. Most important in that regard are the regional climate as well as the size and structure of the urban area. In addition to that, measurement procedures vary among the studies as well as the meteorological conditions investigated.

In terms of measurements, it is possible to split existing studies in two main groups. The first one uses satellite based data to mainly assess surface temperature (e.g. Lo and Quattrochi, 2003; Chen *et al.*, 2006). The second one relies on in situ meteorological measurements to depict air temperature UHI intensities, with some sensors being stationary (e.g. Jauregui, 1997; Giridharan *et al.*, 2004; Chow and Roth, 2006; Yang *et al.*, 2013) and some being installed on vehicles for mobile application (e.g. Kumar *et al.*, 2001; Devadas and Rose, 2009). Apart from that, some research only focusses on a certain season (e.g. Bornstein and Lin, 2000; Giridharan and Kolokotroni, 2009; Coseo and Larsen, 2014) or time of day (e.g. Alcoforado and Andrade, 2005; Maragogiannis *et al.*, 2011), while other research depicts the UHI considering different weather events and weather activity (e.g. Unger, 1996; Szymanowski, 2005). These differences

make it hard to compare results with one another. Regardless of the measurement procedure, there are certain implications for urban climate that seem to be related to regional climatic conditions. While Wienert and Kuttler (2005) showed UHI intensity to be dependent on latitude, they also stated that only small part of the variation could be explained by this approach. Local characteristics seem to be more important as they influence the UHI and cause spatial differences. Topography is a major issue in that regard, substantially contributing to warming or cooling at different sites, as shown by Zhang *et al.* (2005) for Bejing. The sea-breeze might also alter the UHI as modelled by Yoshikado (1994), or proven for Korea, where several coastal cities develop less severe maximum UHI intensities than inland cities (Kim and Baik, 2004). The overall regional climate seems to intensify the UHI or mitigate it at certain times, as we see maximum nighttime intensities in Central Europe during summer (Klysik and Fortuniak, 1999; Ketterer and Matzarakis, 2015) and in Southern Europe during winter (Montávez *et al.*, 2000; Saaroni *et al.*, 2000), while Hua *et al.* (2008) show cities in northern China developing stronger overall UHIs than those in the south.

Nevertheless, UHI intensity is also dependent on size and structure of a city. The usually densely built centres contribute more to warming than loosely built residential areas or areas with a significant amount of vegetated surfaces (Maragogiannis *et al.*, 2011; Tomlinson *et al.*, 2012; Dimoudi *et al.*, 2013). In consequence, these findings also hold true for not only spatial variations within, but also between different cities. Besides, an early study by Oke (1973) reported that the rise in average UHI can be expressed as a linear regression in respect of increasing population size. Steeneveld *et al.* (2011) shows for the Netherlands that population density is better correlated with the intensity of UHI than population size. While nightlights explain urban related warming better than population estimates in the U.S. (Kalnay and Cai, 2003), Lindén *et al.* (2015) prove both parameters to be almost equally reliable based on meteorological data from Germany. Although there is disagreement about which characteristic might be best suitable to address that issue, all studies reveal that the more severe urbanization is, the more intense is warming.

As cities are the most prominent feature of urbanization and hence bear most potential to affect local climate, the aforementioned studies focus on them. However, small towns and villages are also characterised by urban structures and therefore might cause additional warming. Studies from Alaska (Hinkel *et al.*, 2003), Australia (Torok *et al.*, 2001) and Hungary (Szegedi *et al.*, 2013) show that smaller settlements might develop substantial UHIs as well. Unfortunately, studies considering this issue are still rare and further research needs to be

carried out in order to better assess the magnitude of anthropogenic warming and its implications in small urban areas.

Anthropogenic influence in meteorological measurements

The urban climate does not only have implications for the well-being of cities' inhabitants, it also might affect meteorological measurements, hence posing a threat to the reliability of recent climate data. Temperature data derived from meteorological observations is not only crucial to quantify and evaluate latest climate changes, it also enables models to project future climate conditions (Meehl *et al.*, 2007; Randall *et al.*, 2007) as well as it serves as a calibration tool for paleoclimatic research fields such as dendrochronology (Esper *et al.*, 2002), speleothem research (Scholz *et al.*, 2012), or palynology (Nakagawa *et al.*, 2002). In consequence, ensuring the quality of temperature data is of utmost importance, especially regarding long time series.

Ideally, all variations in a temperature record are caused by climate exclusively (Aguilar *et al.*, 2003). Although instrumental data depicts directly measured air temperature and hence offers absolute values, other factors do have an impact on temperature readings. These include changes in instruments, screening, observing staff, time of read-out, and relocations, any of them possibly leading to biases in the time series that need to be addressed (Böhm *et al.*, 2009). To ensure good accessibility, early measurements of long temperature series often started within urban areas, later being moved in accordance to changes in observing staff or to lessen urban influence. Relocations usually have the most severe impact on measurements (Tuomenvirta, 2001; Begert *et al.*, 2005), which is, above all, related to the drastic change in station surroundings and hence local climate in general. Apart from the site-related anthropogenic influence, temperature data might also contain an urban bias as a result of urban growth, manifesting itself as an additional gradual increase in temperatures as referred to by Kukla *et al.* (1986). While the effect of urbanization on temperature trends on a global scale is estimated rather low (Parker, 2004; Parker, 2010), it might have severe implications for regional datasets (Quereda Sala *et al.*, 2000; Stone, 2007; Fujibe, 2009).

The most common and recent way of detecting and eliminating the mentioned biases are homogenization procedures. These measures usually perform a quality control and delete erroneous data, identify break points and inhomogeneities by comparing a record to other station data from the region, and adjust the record accordingly, as summarized by Peterson *et al.* (1998) and deployed by Mestre *et al.* (2013). Processing data with homogenization tools offers the advantage of being able to handle a great amount of climate data at the same time and

adjust various records during the process, as Brunet *et al.* (2006) shows for a Spanish dataset. Nevertheless, relative homogenization is dependent on other suitable time series, possibly limiting its application for specific periods in time.

The question of urban and rural

Since cities are known to have an impact on temperature measurements, time series originating from these severely urbanized areas are considered biased and hence, this anthropogenic influence is quantified as shown for Vienna (Böhm, 1998) or is also eliminated as done for Uppsala and Stockholm (Moberg and Bergström, 1997). To differentiate whether a temperature record is likely affected or not, the stations are usually characterised as either urban or rural stations in climate databases. This characterisation often relies on population, with 10,000 inhabitants being the limit for a station to be considered as rural in the Global Historical Climatological Network (Hansen *et al.*, 2001) or in the KNMI explorer (Trouet and Van Oldenborgh, 2013). Rural station data is often used to assess the warm bias contained in the urban station data, as shown by Jones *et al.* (1990) or Parker (2010).

As mentioned earlier, several smaller urban areas (<10,000 inhabitants) did establish UHIs, raising the question of reliability and representativeness of the rural dataset. While this is of no importance for time series provided by stations without any urbanized areas close to the measurements site, a more thorough investigation of rural station data is nonetheless essential in order to quantify potential urbanization impacts in records associated with small settlements.

Objectives and outline

The main objective of this thesis is the assessment and removal of UHI related influence in long temperature records in order to enhance the dataset for climate reconstruction and prediction. Another main feature will be the investigation of anthropogenic warming in small settlements and the implications this might have for meteorological data originating from these locations. Each of the in total four following chapters will be introduced by describing the main problem it tackles, explaining the methods used to address it, and discussing the outcome of data analysis.

Since measurement procedures usually vary a lot and villages as such have been disregarded for most part in the scientific examination of UHI effects, the first chapter aims at addressing these issues. The study presented quantifies the UHI in three different villages throughout

Europe, one in northern Sweden (boreal zone), one in central Germany (temperate zone), and one in south-eastern Spain (Mediterranean). Measurement procedures and devices are the same to achieve the best comparability among the villages and the various climate zones. In a second step, spatial temperature differences are linked to land cover in order to estimate the implications of, for example, vegetated or urban surfaces for local warming or cooling, respectively. As all villages host meteorological stations characterised as rural, the study should proof whether this holds true in the light of possible UHI formation.

The second chapter focusses on the more than 200 years long temperature record from the city of Brno in the Czech Republic. Being one of the longest instrumental records depicting climate in Eastern Europe, the record's quality is of utmost importance. As the station was relocated several times, first moving within the city and later outside of it, the time series is likely affected by different extents of anthropogenic warming. To remove this varying impact, recent temperature readings from many stations in the Brno area are linked to land cover to estimate the additional warming caused by urban structures, as introduced in the chapter before. Following this, historical maps and satellite images are used to assess the urban structures next to all past locations of the meteorological station, allowing for a quantification of the corresponding warming. A correction is then performed for each time period by subtracting the detected warming from the original temperature data, allowing for a new assessment of climate variability during the last centuries.

Haparanda, a village in Northern Sweden, is central to the third chapter, because it provides a time series starting in 1859 and hence being one of the longest temperature records in the subarctic region. With villages potentially developing UHIs, the dataset needs to be checked for anthropogenic warming and, if necessary, corrected for this bias. Because of the remote location of the station as well as its long history, relative homogenization techniques are not applicable due to the lack of reference station data nearby. The study introduces a completely new approach to detect the UHI effect by quantifying it based on recent temperature measurements at the exact historical sites of the original meteorological station. Removing the warming, and hence the bias associated with relocations, is critical for a more precise evaluation of 19th and 20th century warming.

In the last chapter, the new method to assess and eliminate the relocation bias in long temperature records is applied to a century long time series from north-eastern Spain. Since the record has been homogenized relying on reference records to eliminate supposedly non-climatic signals, the dataset offers the possibility to compare the relocation bias free data with the overall

homogenized time series, evaluating differences as well as similarities between both approaches. With homogenization not being performed before 1950, the new correction method also offers a tool to address anthropogenic warming in the first half of the 20th century that might be contained in the time series.

2 Determination of the urban heat island intensity in villages and its connection to land cover in three European climate zones

Manuel Dienst[1], Jenny Lindén[2], Jan Esper[1]

[1]Department of Geography, Johannes Gutenberg University, Mainz, Germany

[2]IVL – Swedish Environmental Research Institute, Gothenburg, Sweden

Climate Research, 2018 – published

2.1 Introduction

An alteration of the landscape eventuates in a change of local climatology detectable in various meteorological parameters. The urbanization of an area is one example for such a conversion, implying a gradual replacement of vegetation and bare soil by buildings and paved surfaces. Among other implications, urbanization increases temperatures and leads to the establishment of an urban heat island (UHI) if compared to the rural surroundings (e.g. Landsberg, 1981; Oke, 1987). This difference is usually strongest in summer and at night (Oke, 1982; Morris *et al.*, 2001). Arnfield (2003) summarized several important factors influencing urban temperatures positively including reduced evapotranspiration as a result of sealed surfaces and missing vegetation, a lowered exchange of air masses and increased multiple reflection and radiative heating due to urban structures and anthropogenic heat release. Because of the heterogeneity of the urban landscape, climate varies within a city (Unger, 2004; Thorsson *et al.*, 2010), and UHI intensity (UHII) is affected by factors such as regional climate or adaption strategies as well. Rapid urbanization has been connected to an increased UHI (Chen *et al.*, 2006) and this urban warming has been found to be positively correlated with population density (Steeneveld *et al.*, 2011). UHI studies were primarily focused on larger cities, e.g. Nanjing, (Huang *et al.*, 2008), Thessaloniki (Kantzioura *et al.*, 2012), Bejing (Zhao *et al.*, 2011), or Melbourne (Morris *et al.*, 2001). However, smaller settlements with a population ≤10,000 inhabitants have been linked to increased urban temperatures as well (e.g. Torok *et al.*, 2001; Hinkel *et al.*, 2003).

Because the microclimate of a location is strongly influenced by its surroundings, meteorological stations should be placed with great care to be representative for a region (Aguilar *et al.*, 2003). In an urban area, this implies regarding the occurrence of nearby structures such as buildings, streets, trees, etc., as factors that alter radiation, humidity, and wind patterns. Accordingly, a strong relation was detected between temperatures measured in cities and the surrounding land cover (e.g. Lo and Quattrochi, 2003; Chen *et al.*, 2006), an issue that still needs to be assessed for smaller settlements as well.

The assessment of urban temperatures is of high importance, not only with regard to human comfort and well-being (Mayer and Höppe, 1987), but also concerning representative temperature measurements for specific regions. The anthropogenic influence on climate alters temperature trends (Jones and Wigley, 2010), thereby adding critical information to the interpretation of 20th century global warming. Even though Parker (2010) considered the UHI effect on temperature trends to be small, Hansen *et al.* (2001) and Ren *et al.* (2008) detected a significant impact in the US and Chinese networks, respectively. Therefore, approaches to

homogenize temperature data have become vital to ensure their reliability (Brunet *et al.*, 2006; Venema *et al.*, 2012). Albeit aiming at removing all non-climatic impact in the temperature data, homogenization and correction of time series might as well have inadvertent implications like the recovery of urban warming bias (Zhang *et al.*, 2014; Dienst *et al.*, 2017), emphasizing the need to adjust records with special diligence. Cities contain the highest potential to affect the representativity of meteorological station measurements due to their large extension, but even smaller towns and villages influence the observations. Since studies vary vastly with respect to measurement periods, instrumentation, and data selection, there is need to establish a suitable dataset for different villages in varying climate zones.

The aim of this study is to assess the impact of land cover on urban air temperatures in 3 smaller settlements in Sweden (boreal Northern Europe), Germany (temperate Central Europe), and Spain (Mediterranean Southern Europe). Previous work confirmed the existence of an UHI in the Swedish and the German villages (Lindén *et al.*, 2015b), which we here compare with the newly assessed Spanish village. The main goal of this study is to analyze which land covers contribute most to warming and cooling and whether the impact is different in the various climate zones.

2.2 Study sites and methods

2.2.1 Study sites

The study sites are located in Haparanda in northern Sweden near the Arctic Circle, Geisenheim in western Germany in the temperate zone, and Cazorla in southern Spain in the Mediterranean (Fig. 2-1). We refer to these settlements as villages considering the widely applied population threshold of <10,000 inhabitants as utilized by the KNMI Climate Explorer introduced by Trouet and Van Oldenborgh (2013) and the Global Historical Climatological Network (Peterson and Russell, 1997; Hansen *et al.*, 2001). While this criterion separates the study sites from towns and cities, we want to emphasize that Haparanda, Geisenheim, and Cazorla are nonetheless urban areas as a settlement with several thousand inhabitants implies substantial built-up areas, infrastructure, traffic, etc. The term urban is therefore used in this paper especially to acknowledge the dominant land cover (streets, buildings, paved surfaces). Haparanda and Geisenheim gained town privileges in the past and are administratively considered as towns in Sweden and Germany, respectively.

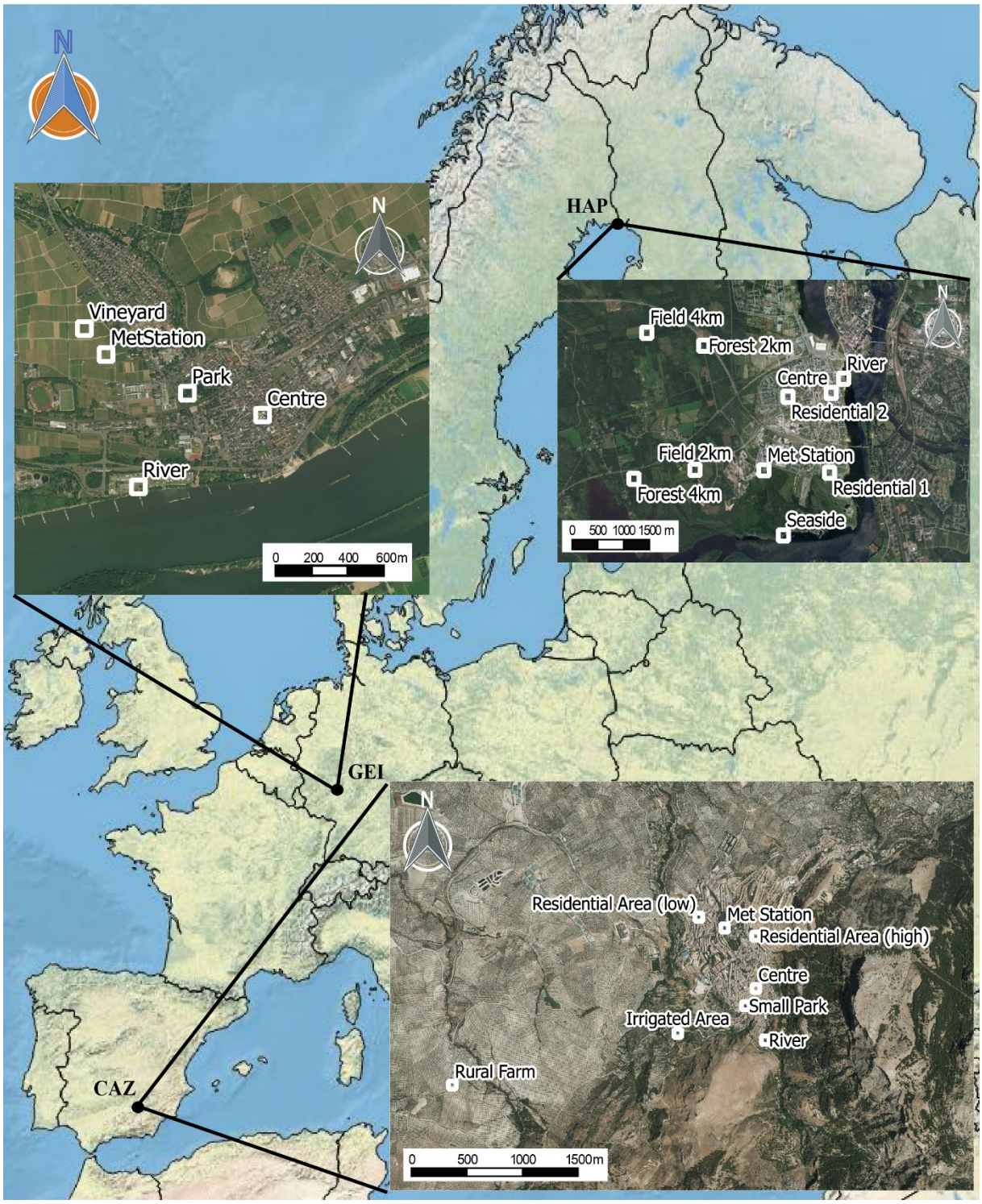

Figure 2-1 Sensor set-up in the three villages. The white squares indicate the sensor locations. Satellite images for Geisenheim and Cazorla have been derived from *Microsoft Bing maps 2017* and for Cazorla from *ESRI map services 2017*. CAZ: Cazorla, GEI: Geisenheim, HAP: Haparanda.

Cazorla is situated at the western boarder of the Sierras de Cazorla, Segura y Las Villas national park in south-eastern Spain and has a population size of about 8,000. The climate is temperate with dry and hot summers, characterised by maximum temperatures exceeding 22 °C at least in

one month of a year (Köppen & Geiger: Csa; Kottek *et al.* (2006)). Since the village is located on a mountainside in hilly terrain, it extends from 720 to 900 m above sea level (a.s.l.). The small river Cerezuelo (width ~10 m) originates in the nearby mountain range and runs through the settlement. The building pattern is homogeneous, with light coloured buildings of 2 to 3 storeys and small streets. Bare rock and forests surround Cazorla to the east and south whereas to the north and west, olive plantations dominate the landscape.

Geisenheim is located in central Germany on the eastern banks of the river Rhine (width ~400 m) and south of the Taunus mountain ridge. The village stretches along the hillside, resulting in a height difference of 55m from the river (80 m a.s.l.) to the topmost point (135 m a.s.l.). Characterised by fully humid, temperate climate with warm summers (Köppen & Geiger: Cfb), the region is dominated by agriculture, especially wine growing. Geisenheim consists of an old and dense medieval centre with timber-framed one-storey houses and small streets, surrounded by residential areas with 1 to 3 storey buildings. Today, although the Geisenheim administrative region is home to ~11,500 people, the village as such has ~7,500 inhabitants.

Haparanda is situated in northern Sweden on the border with Finland and its climate is dominated by fully humid conditions characterized by ample snow and cool summers (Köppen & Geiger: Dfc). The village is situated north of the Baltic Sea, with the river Torneo (width ~350 m) running to its eastern side entering the nearby sea. The surrounding landscape is flat and close to sea level, and is primarily covered by forests and some meadows. A square forms the centre of Haparanda, with mostly old wooden buildings in its vicinity. Residential areas mainly consisting of wooden one-storey houses have been constructed to the west and south of the centre and are home to ~7,000 inhabitants. The building pattern is rather loose, including widely spaced streets even in the centre. Small industrial areas are found north and south-west of the village.

2.2.2 Temperature sensor network

A network of temperature sensors was established in each village and its surroundings (Fig. 2-1), originally to detect the urban warming effect on historical temperature measurements (Lindén *et al.*, 2015b; Dienst *et al.*, 2017). We closely followed the WMO guidelines for sensor installation in urban climate studies (Oke, 2008), though a completely standardized placement, e.g. on unified posts, was not feasible because of the complexity of the sites, nearby urban structures and human activity.Nevertheless, all sensors were placed inside a protection against insolation at 2.5 m height above the ground, usually on existing posts or trees as detailed in

Table 1-1. All sensors were installed so that a free air flow is guaranteed, no walls or buildings are too close, and sensors are north-facing to avoid direct solar radiation. Each sensor was placed in a different microenvironment to support a good comparison regarding the impact of varying land cover. The villages were endued with a core set of air temperature sensors covered by radiation shields and additionally measure relative humidity (HOBO Pro v2 U23-001 in radiation shields RS1, Onset Computer). During a 3 wk inter-sensor comparison, considering 10 min measurement intervals, differences were <0.05 °C on average, including <5 % of values exceeding a difference of 0.1 °C, and could therefore be ignored in the analysis.

In each village, 1 sensor was established in the centre and 1 outside the urban area to assess the UHI magnitude. Since villages in general are often located at rivers or streams like the ones investigated here, another core sensor was placed at the riverside. In Haparanda and Cazorla, additional smaller air temperature sensors (HOBO TidbiT v2 data logger, Onset Computer) were installed to increase coverage of the varying surroundings and topography, since the areas are more diverse than in Geisenheim with mostly cropland and the river surrounding the village. These smaller sensors were equipped with a white plastic cover and placed on the shaded northern side of trees to minimize the impact of direct insolation. The common measurement period started in September 2015 and lasted 1 yr. The sensors were set to measure in 30min intervals to achieve a high temporal resolution. In total, 5 U23-sensors were installed in Geisenheim and Haparanda, and 3 in Cazorla. In addition, 5 TidbiT sensors were installed in Haparanda, and 5 in Cazorla (see Table 2-1).

2.2.3 Digitization

To assess the influence of land cover on air temperatures, the surroundings of each temperature sensor were manually digitized based on satellite images (*Microsoft Bing maps 2017, ESRI map services 2017*) using the open source GIS software QGIS (QGIS Development Team, 2017) to achieve the best results possible in terms of accuracy and spatial resolution (up to 0.2m/pixel). Five categories were introduced to account for different types of land cover found in the three study areas: buildings, impervious surfaces, vegetation, water bodies, and bare soil/gravel/sand. The type of natural vegetation as well as crops grown varies because of different climatic conditions and cultivation practices. High vegetation implies dense conifer forests in Haparanda and dense woodland in Geisenheim, respectively, whereas in Cazorla, it refers to open evergreen forests of limited height. As stated in Section 2.2.1, cultivated areas are dominated by wine-growing in Geisenheim and are more or less limited to olive plantations in Cazorla, while Haparanda has no cropland at all. Low vegetation refers to mainly grassland and bushes in all 3 villages. Since a distinction is not always possible using satellite photography, and there

are no clear definitions for different vegetation types, all were combined in the category vegetation.

Other studies have demonstrated the immediate surrounding up to a distance of 1000 m to the measurement site to be influential (e.g. Li and Roth, 2009; Lindén *et al.*, 2015a) and, considering these findings, land cover was digitalized in 50, 100, 500 and 1000 m distance to the sensors. For each sensor and radius, the area covered by 1 single type of land cover within a certain radius was compared to the total area covered by all types within this radius, thus providing the proportion of 1 land cover type within a defined radius. These values were later used for the correlation and regression analysis including all sensors and radii.

2.2.4 Data analysis

For each sensor, 48 measurements d^{-1} over 365 d were available to evaluate daily mean, minimum, and maximum (TM, TN, and TX, respectively) air temperatures. Even though the set-up allows for very high temporal resolution and robust daily means, the actual minimum and maximum temperatures could not be estimated, as the recorded values likely occurred in between the measurement intervals. A height correction was not applied to the data, since differences in elevation are either small (Haparanda, Geisenheim) or topography is complex (Cazorla) so that a correction might as well amplify differences caused by elevation, especially regarding TN. The data were used to calculate daily, monthly, and seasonal values. Since the main goal of this study is to assess the impact of land cover on temperatures, seasonal temperatures were correlated against different land covers surrounding the sensors and a 2-tailed t-test was performed to estimate significance ($p < 0.10$). A subset of data was used in a regression analysis to estimate the temperature change per unit land cover change.

Most of the TidbiT sensors installed proved to be biased by direct solar radiation, revealing the white plastic coverage and north-exposed placement was insufficient to prevent this bias. While data in Sweden is insignificantly influenced mostly because of shading by other vegetation, several sensors in Cazorla display a strong impact. Since an approach to correct the biased data might overly alter the site-specific differences, daytime data were disregarded from analysis, and only the properly shielded core measurements (centre, rural reference, river) were used. To support spatial coverage in the correlation and regression analyses, additional data were exclusively selected from measurements of TN and hence are not biased.

	LOCATION	SENSOR	SITE DESCRIPTION	ALT
HAPARANDA (SWEDEN)	Village Centre	U23	On lamp post on lawn, small wooden buildings and some vegetation around; paved streets	5m
	River	U23	On lamp post on lawn, next to riverside, grass surrounding spot, greater buildings in some distance	2m
	Residential area 1	U23	On old meteorological station post in garden with lawns and small wooden houses	4m
	Residential area 2	U23	On tree in backyard with lawns and small wooden houses around	10m
	Met Station	U23	On gate of AWS, outside city (about 200m away from buildings), on grass/gravel next to forest	9m
	Seashore	Tidbit	On tree 15m away from sea, wet ground, forest/bushy area	1m
	Field 2km	Tidbit	On small tree in ditch with some more trees between fields with high grass, 1km away from sea	8m
	Field 4km	Tidbit	On small tree in ditch with some more trees between fields with high grass, 4km away from sea	10m
	Forest 2km	Tidbit	On tree in forest, widely spaced large trees, bushes and tall grass in openings, 3km away from sea	10m
	Forest 4km	Tidbit	On tree in forest, widely spaced large trees, bushes and tall grass in openings, 0.5km away from sea	4m
GEISENHEIM (GERMANY)	Village Centre	U23	On lamp post near camping site; lawn and gravel paths with some trees; 30m away from river	93m
	River	U23	On lamp post in town centre square; paved ground; square is surrounded by buildings made of stone	84m
	Park	U23	On tree in the park of the University of Applied Sciences; lawn and trees; parking lot/street nearby	101m
	Vineyard	U23	On post in the vineyards outside the town; vine branches; smaller paths nearby	120m
	Met Station	U23	On fence of official automatic weather station in the vineyards outside town; lawn; paths and vine branches nearby	110m
CAZORLA (SPAIN)	Village Centre	U23	On balcony in narrow street with 3 storey buildings; streets and similar buildings nearby	823m
	River	U23	On post in garden of a house next to the river; grass; bushes and trees next to river; few houses	818m
	Rural Farmhouse	U23	On tree of rural farmhouse; olive plantations around	823m
	Small Park	Tidbit	On tree in bushes; next to parking lot	785m
	Met Station	Tidbit	Within the screen of the met station; gravel; one or two storey buildings around	813m
	Irrigated Area	Tidbit	On tree in irrigated plant area	843m
	Chorro	Tidbit	On tree in Nature Park; bushes and trees; rocks	1321 m
	Residential area (low)	Tidbit	On tree in small open area in middle of residential area; one or two storey buildings; some trees	742m
	Residential area (high)	Tidbit	On tree in small open area in middle of residential area; one or two storey buildings; some trees	853m
	Rural area (high)	Tidbit	On tree; olive plantations around	907m
	Rural area (low)	Tidbit	On tree; olive plantations around	735m

Table 2-1 Overview on the different sensors positioned in every village.

2.3 Results

2.3.1 Spatial temperature patterns

To assess the possible formation of UHI and the effect of nearby rivers in the 3 European climate zones, spatial differences in seasonal TN and TM were analyzed. In each village, a subset of 3 fully protected U23 sensors representing urban, rural, and riverside locations was used for comparison.

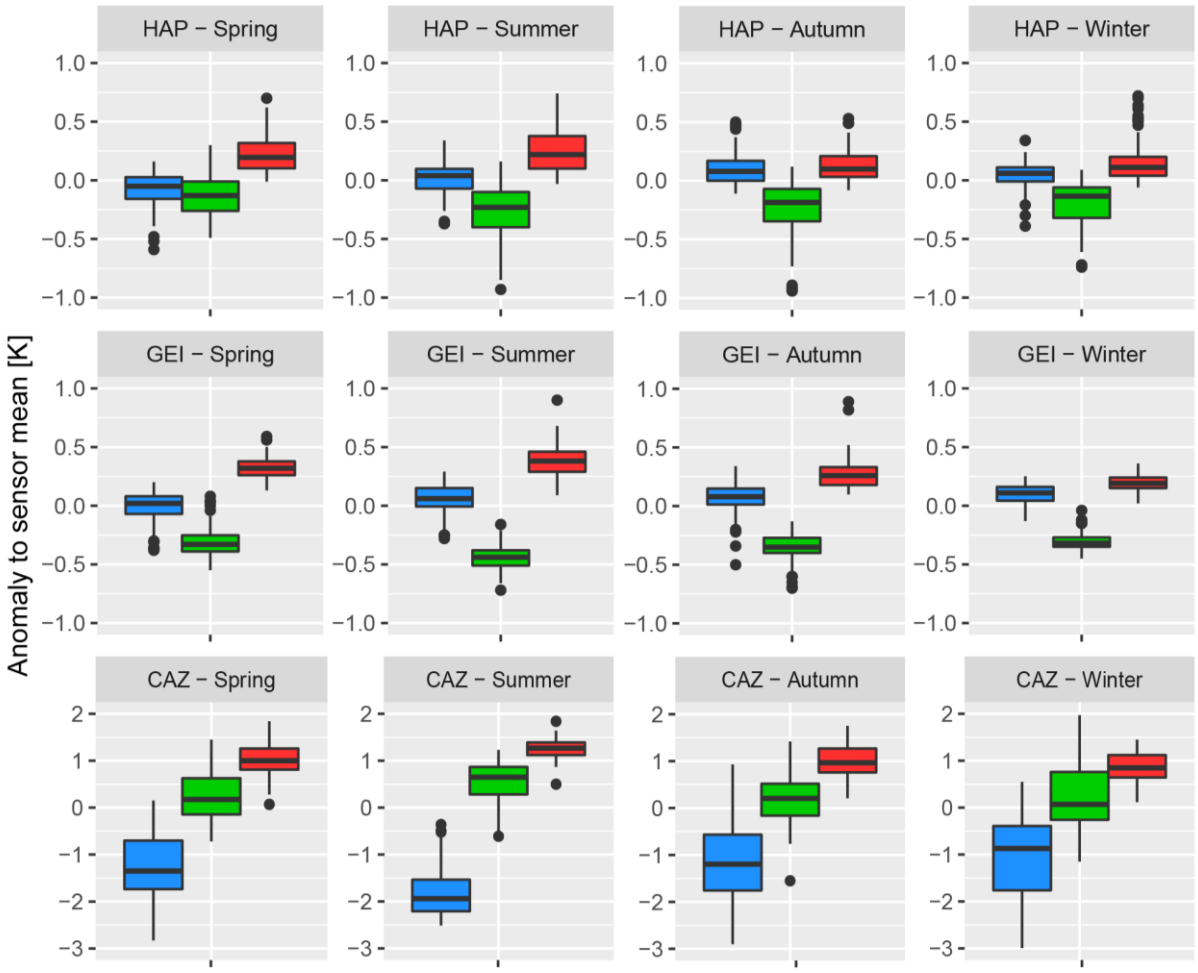

Figure 2-2 Seasonal mean temperature values for river, centre and rural U23 sensors in each village. Temperatures are shown as differences to the mean of all sensors. Boxplots display the median (black middle line), the upper and lower quartile including 50% of the data (coloured box) and whiskers (vertical lines) including the other 50%. If a value lies beyond 1.5 times the interquartile range, it is plotted as an outlier and excluded from the whiskers, reducing the amount of data within.

Figure 2-2 reveals the existence of UHI in every village with the general pattern of spatial differences in TM being persistent throughout the seasons, though at varying magnitudes. The urban-rural temperature patterns are similar in Haparanda and Geisenheim, whereas Cazorla displays a different pattern. The median difference is largest during summer in Geisenheim

(0.8 °C) and Haparanda (0.5 °C), and smallest during winter reaching 0.5 °C and 0.3 °C, respectively. In both villages, the river site remains cooler than the urban site but is still warmer than the rural site. This pattern is most pronounced in summer and spring. In Cazorla, the urban site is also the warmest, with smallest differences in summer (0.6 °C), and larger differences in all other seasons (~0.8 °C). In addition, the location next to the river is cooler than both the urban and rural site, especially in summer (-3.2 °C in comparison to the centre).

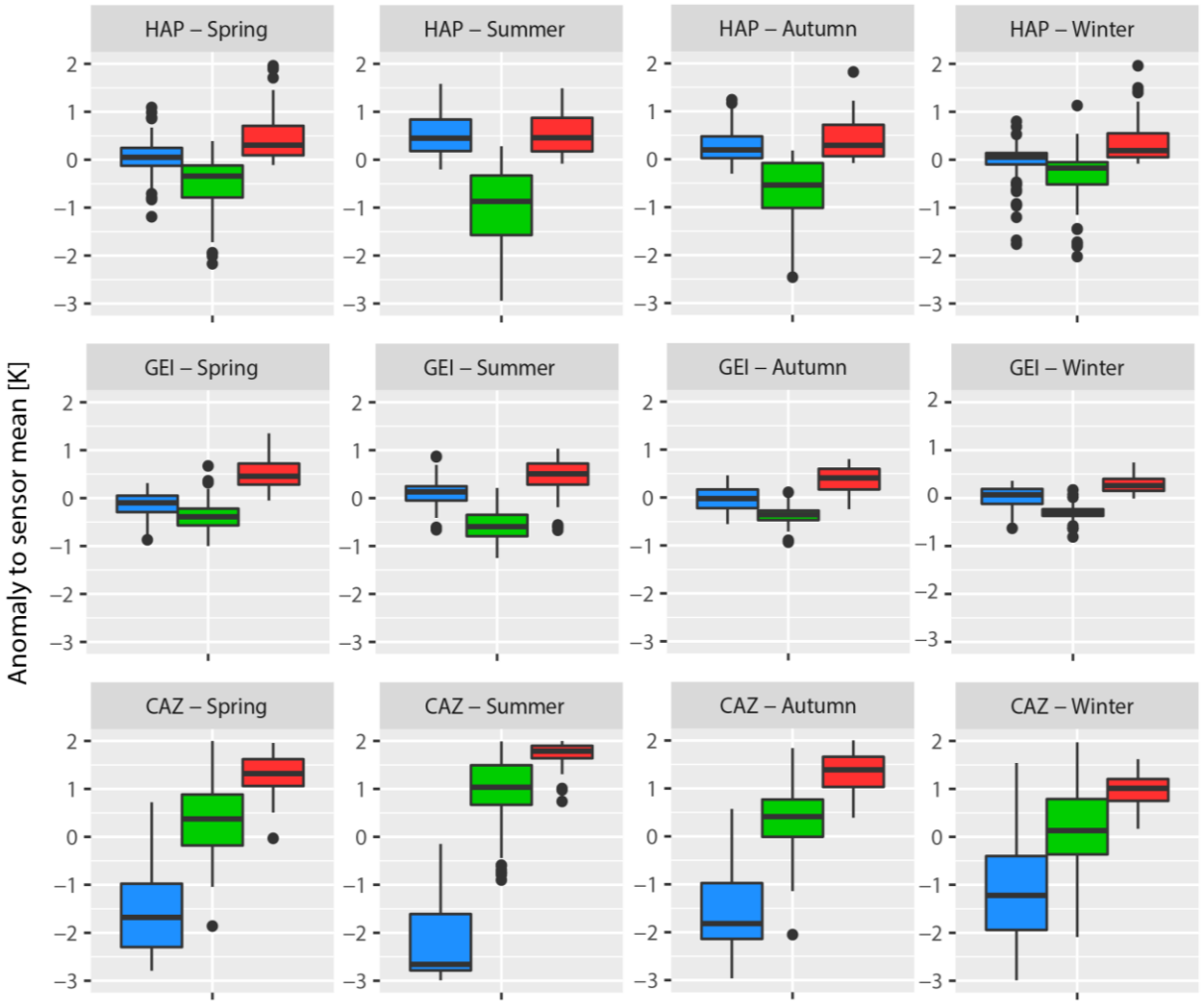

Figure 2-3 Seasonal minimum temperature values for river, centre and rural U23 sensors in each village. Temperatures are shown as differences to the mean of all sensors. Boxplots display the median (black middle line), the upper and lower quartile including 50% of the data (coloured box) and whiskers (vertical lines) including the other 50%. If a value lies beyond 1.5 times the interquartile range, it is plotted as an outlier and excluded from the whiskers, reducing the amount of data within.

Patterns in TN are very similar to TM, although differences are more distinct and variable in TN (Fig. 2-3). Regarding the UHII, Haparanda centre shows a warming of 0.4 °C in winter and 1.4 °C in summer. In Geisenheim, the magnitude is larger in winter (0.6 °C), but slightly smaller

in summer (1.1 °C). Cooler temperatures at the riverside when compared to the centre are present in TN as well, which is especially true for spring but not for summer in Haparanda, when both locations show the same temperature values. The Cazorla river site is substantially cooler if TN is considered, exceeding even -4 °C in summer relative to the centre, whereas the rural-urban difference is stronger in the colder seasons (~0.9 °C) just like in TM.

2.3.2 Correlation of land cover and temperatures

To analyze the influence of land cover on local temperatures, a regression analysis was performed between the sensor measurements (TN of each season) and the land cover considering different radii. This analysis indicates complex associations, including smaller variations among seasons but stronger ones among the villages in the different climate zones. Strong correlations between temperature and water bodies are recorded in Cazorla and even more so in Haparanda and Geisenheim if buildings or vegetation are considered instead of water. Figure 2-4 shows the coefficients of determination for TN for the most important land cover classes. A significant warming influence of buildings on minimum temperatures is recorded in Geisenheim and Haparanda, particularly for the smallest radii (<100 m) in Geisenheim ($R^2 > 0.7$ for all seasons), whereas in Haparanda, the 500 and 1000 m radii reveal highest coefficients ($R^2 > 0.5$ for all seasons). Even though buildings have no distinct impact on TN in Cazorla, except for the closest radius of 50 m, water bodies do. Spring, summer, and autumn temperatures are negatively correlated with water bodies in up to 100 m proximity, but the relation decreases with distance. An inverse pattern is revealed in the 2 other villages. Whereas in Haparanda the coefficients of determination increase with distance, though on an overall low level, the values are higher in Geisenheim, particularly in the 1 km radius and during summer ($R^2 = 0.72$). Summer temperatures in Haparanda are (negatively) influenced by vegetation, which is most prominent in 500 to 1000 m radii. In Geisenheim, the pattern is reversed, since the correlations are strongest for the close surroundings and decrease with distance. The same is true for Cazorla, where significant relations were recorded up to a distance of 100 m. During summer, temperatures are neither significantly correlated with vegetation nor with buildings.

Although other findings are not shown, both other types of land cover need mentioning in addition to the results displayed in Figure 2-4. Impervious surfaces cause warming in all villages, particularly in Haparanda ($R^2 \approx 0.7$). These patterns are similar to the ones detected for the building land cover and merely confirm the uniform performance of urban surfaces. The bare soil/sand/gravel land cover is negligible in terms of its occurrence within the digitized radii if compared to the other types of land cover, particularly in Haparanda and Geisenheim. The

poor correlation results might simply be caused by this circumstance and a reliable statement on how temperatures could be affected is not possible.

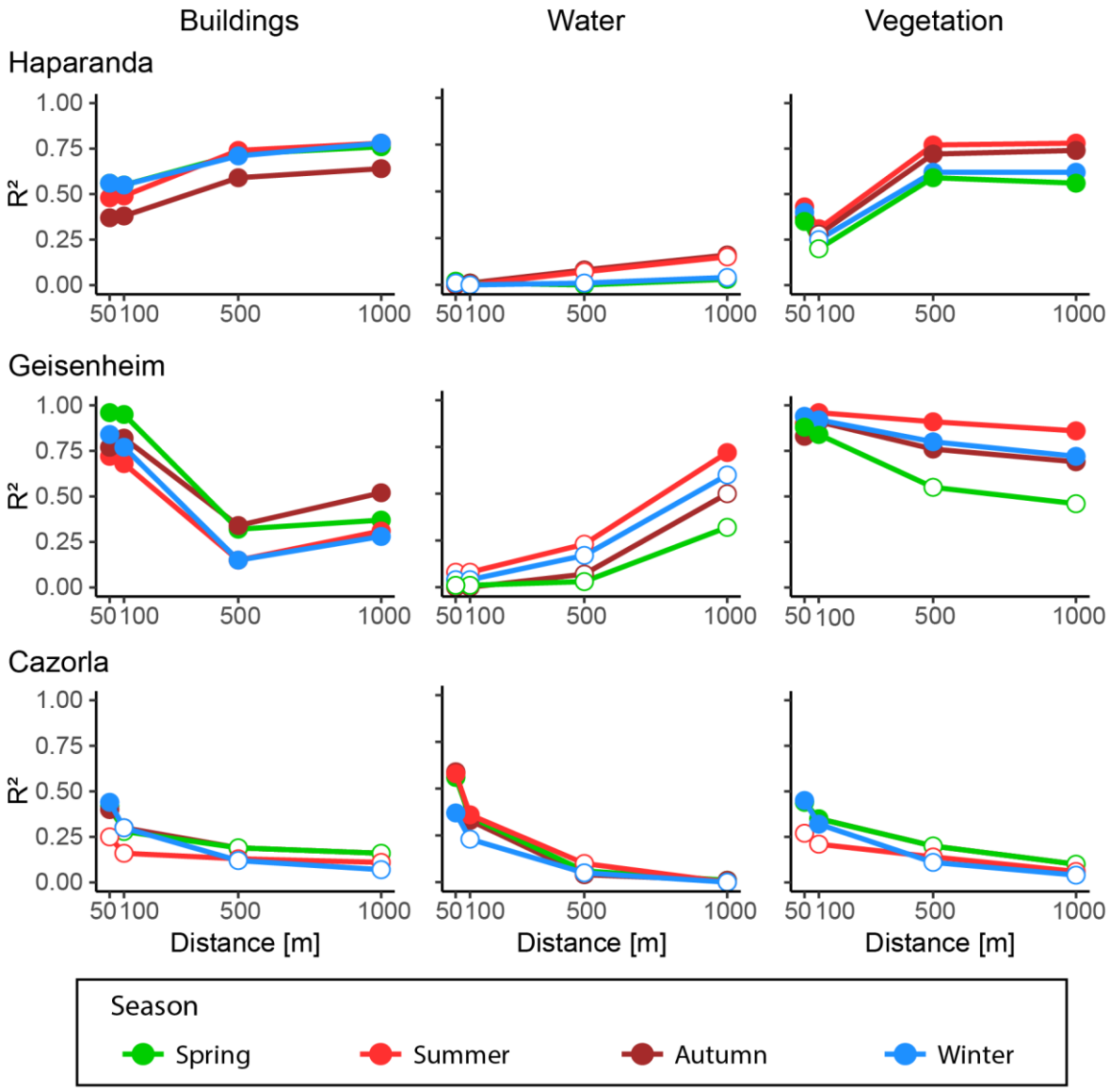

Figure 2-4 Coefficients of determination shown for three different types of land cover in each village. Seasonal temperatures were correlated with the specific land cover in four different radii. Filled dots indicate significant correlations on a 90%-level.

2.3.3 Regression analysis

Several of the significant correlations have been selected and are shown as a regression analysis in Fig. 2-5 to estimate the degree of warming and cooling in association with land cover. We here focus on minimum spring temperatures to increase comparability among the sites. The analysis includes the dominant warming caused by buildings in all villages as well as the dominant cooling related to vegetation, even though water had a significant impact as well in the Mediterranean village. In a radius of 500 m, spring TN in Haparanda is considerably

lowered if the area is covered with high vegetation (-0.2 °C per 10 % land cover increase). An even stronger, but inverse, trend is recorded for building density, even if building density is less than 30 %. The 100 m radius pattern in Geisenheim is quite similar to that in Haparanda, although the rate of warming (0.2 °C per 10 % buildings) and cooling (-0.1 °C per 10 % vegetated area) are lower. While vegetation cover is generally well distributed, building density is below 20 % for all locations but one, possibly limiting the reliability of the indicated trend. However, building density is more evenly distributed for other radii, and the relation with temperatures remains similar, substantiating the validity of this result. In Cazorla, the cooling caused by vegetation reaches -0.3 °C per 10 % land cover increase in a radius of 50 m. For the same radius, a smaller but positive trend is revealed by correlating building density and spring temperatures, demonstrating a warming influence similar to the other two villages. All regression analyses displayed in Fig. 2-5 are statistically significant ($p < 0.1$).

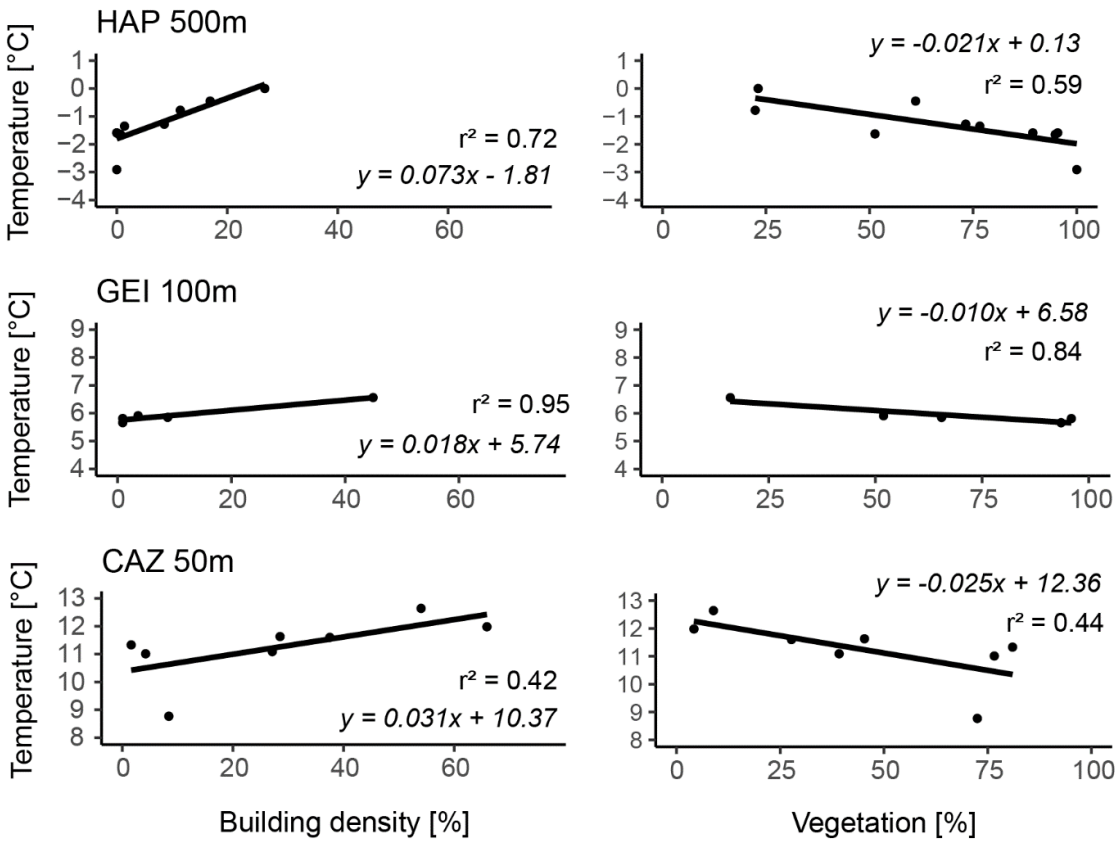

Figure 2-5 Regression analysis for selected types of land cover in a specific radius which revealed strong and significant ($p < 0.1$) correlations with temperature. The equations display the rise or decrease in temperature per percent increase in type of land cover. CAZ: Cazorla, GEI: Geisenheim, HAP: Haparanda.

2.4 Discussion

The results of this study showed that villages in Sweden, Germany, and Spain develop a substantial UHI with regard to size as well as building pattern of the urban areas considered and that maximum UHII weakens from north to south, as previously presented by Wienert and Kuttler (2005). The UHI persists throughout all seasons, and building density contributed most to the warming. Vegetation provides significant cooling in all villages, but is less prominent in Cazorla, where water is most influential. In the following, we first discuss the influence of topography and sensor set-up on the temperature network. We then address the seasonal UHI course in the villages in northern, central, and southern Europe, and compare our findings with other studies. Last, we address the similarities and differences in the relation between land cover and temperatures in the 3 different European climate zones.

2.4.1 Topography

Topography is a minor factor in Geisenheim and especially in Haparanda, but is an important one in Mediterranean Cazorla. Cazorla is situated in a mountainous region and the differences in height between the sensors reach up to 100m. Assessing influences due to topography remains complicated, particularly for TN. For instance, the steepness of a slope has an impact on how deep surface-induced cooling penetrates into the atmospheric layer (Jarvis and Stuart, 2001). Particularly on clear-calm days, west-exposed mountain slopes are expected to become warmer during daytime, whereas at night, they cool faster and a downhill wind establishes, cooling the village further down the slope (e.g. Barry, 2008; Poulos and Zhong, 2008). This likely mitigates UHI in Cazorla, particularly in TN.

Consequently, the data were not adjusted for elevation, as an adequate correction would need to be based on a precise understanding of the local climatology, and might otherwise alter site-specific differences and even increase biases. Even though sensors were placed at different elevations in Cazorla, no distinct warming or cooling patterns associated with topography were found that could be used for correction purposes. This might be because the landscape continues to slope westbound and no real valley situation is present. Nevertheless, in the complex terrain of Cazorla, temperatures are less dependent on surrounding land cover. This situation is further complicated by shading effects caused by the nearby mountains in the east. Sunlight reaches the rural areas earlier, thereby shifting the diurnal curve in comparison to the village sensors which are shaded by the mountains for a longer time, e.g. during summer, there is a 1.5 h delay in the centre. Since only TN has been used, data are not influenced by shading patterns.

Although the dataset from Cazorla contains uncertainties due to topography, 6 of 8 sensors are located within an altitudinal range of < 50 m, and the core sensors (centre, river, rural farmhouse) are all placed at the same elevation. Furthermore, since the analysis is based on seasonal median temperatures, specific meteorological features only have minor effects on the data.

In general, cloudiness reduces spatial variations and is often linked to higher wind speeds that have similar mitigating effects on UHII (e.g. Unger, 1996; Kim and Baik, 2002). Inversions might also alter the altitudinal patterns. Influences like these should be negligible though, since the analyses performed here to detect spatial warming and cooling patterns are not based on selected days but can be regarded as an all-weather approach including all data available, allowing for a robust estimation of urban warming.

2.4.2 Village UHIs

The 3 sheltered core sensors (centre, river, rural farmhouse) allow for a good comparison even in Cazorla, as these were placed at the same elevation. In Haparanda and Geisenheim, UHII was highest in summer minimum temperatures in agreement with other studies summarized by Arnfield (2003), reaching 1.4 °C and 1.1 °C, respectively. UHII is generally lower in the villages assessed here compared to studies in larger cities: Klysik and Fortuniak (1999) report night time UHII during summer to reach 3 to 4 °C in Lodz (700.000 inhabitants), and Bottyán *et al.* (2005) document a mean maximum intensity of 2.5 °C in Debrecen (200.000 inhabitants) during the non-heating season. However, given the relatively low population density, low building density and size of the villages, the additional warming amounting to up to half of the warming in the cities mentioned above is to be characterised as a substantial change in local climate. In addition, our study presents seasonal median minimum temperatures including all weather conditions. An investigation on maximum UHII, considering a selection of clear sky conditions and calm days, would naturally reveal greater urban-rural discrepancies. Nevertheless, the values reported here confirm an increase in UHII in line with urban growth as noted elsewhere (Torok *et al.*, 2001; Chen *et al.*, 2006; Szegedi *et al.*, 2013). Our study thereby adds information at the lower end of the scale, assuming temperatures to rise significantly even in sparsely urbanized areas.

Other studies on village UHIs report findings connecting well to this study. Szegedi *et al.* (2013) showed for a similar-sized village in Hungary (9,500 inhabitants) that UHII is lower (0.6 °C) than that found in our study if the whole year is considered. However, maximum UHIIs of almost 2 °C are reached on clear and calm days. Hinkel and Nelson (2007) confirm higher wind

speeds to mitigate the UHI significantly in a village in Alaska (4,500 inhabitants), but they also report a consistent urban-rural difference of 2 °C during winter. While they emphasize the importance of anthropogenic heat release as the reason for pronounced winter UHII, the effect is much stronger than in Haparanda (0.3 °C in winter), although the Swedish village is close to the Arctic Circle as well. This is likely because the building pattern is very dense, heating is more intense and the difference between ambient air temperature and the heated structures is more distinct at the Alaskan site. Several villages (<10,000 inhabitants) at the south-eastern Australian coast develop a substantial urban warming reaching 2 to 3.5 °C on selected days in summer when the effect tends to be strongest (Torok *et al.*, 2001). Additionally, Steeneveld *et al.* (2011) showed for 2 villages in the Netherlands a mean maximum UHII of 1 to 2.3 °C. Although a comparison might be difficult since various climate zones, village sizes, and building patterns are considered, we estimate our results to be similar to these studies nonetheless, particularly since single days exceeded 2 °C in all three European villages examined here.

A stronger cold season UHII as observed in Cazorla is supported by other studies from the Mediterranean (Montávez *et al.*, 2000; Papanastasiou and Kittas, 2012). The smaller warm season difference is likely related to the fact that evaporative cooling at the rural site is particularly low when the vegetation suffers from drought stress and closes the stomata to mitigate water losses. This conclusion is supported by work revealing unirrigated lawns contributing less to regional cooling compared to their irrigated counterparts in Colorado (USA) urban areas (Bonan, 2000). The rural sensor in Cazorla is mostly surrounded by olive plantations, and a study by Ben Ahmed *et al.* (2007) concluded that even irrigated olive trees in the Mediterranean basin reveal significant decreases in photosynthetic activity and hence transpiration. This would also support the increase in UHII during autumn and spring, when conditions are less stressful for the vegetation in terms of temperature and humidity. Several studies addressing similar latitudes as the Mediterranean region in East Asia confirm the existence of stronger nighttime UHIIs in winter (e.g. Kim and Baik, 2002; Shen, 2015). However, maximum UHIIs have also often been observed during daytime in summer (Zhang *et al.*, 2005; Chan, 2011), contradicting the finding from the Mediterranean that stressed vegetation contributes to lower urban-rural differences. Since the areas in East Asia discussed in this paragraph are highly urbanized, Zhang *et al.* (2005) explain the substantial warming during daytime in summer with an increase in anthropogenic heat sources like air conditioning, while Shen (2015) refers to severe air pollution coupled with low wind speeds as the main reason for a strong nighttime UHI in winter. Hua *et al.* (2008) find a regional pattern in UHIIs

over China, with more severe urban warming in TN during winter in the north than in the south. Since the regional climate in the Mediterranean and East Asia is very different, this might as well be the reason for varying spatio-temporal intensities in UHI.

Proximity to open water could affect wind patterns and air temperatures, hence altering the UHII (Zhou *et al.*, 2016). The small river Cerezuelo proved to be of great influence in Mediterranean Cazorla, reaching >4 °C cooling in summer TN compared to the centre, but this phenomenon is substantially less important in temperate Geisenheim and boreal Haparanda. Hathway and Sharples (2012) showed the cooling by rivers to be dependent on relative humidity, and ambient air as well as river temperature, with more effective cooling recorded if the river is cold and the ambient air warm. Not only are air temperatures considerably higher in summer in Cazorla (mean = 26.4 °C) than in Haparanda (mean = 15.3 °C) and Geisenheim (mean = 18.7 °C), but the arid conditions contribute to lower relative humidity as well. In addition, the water originates from a nearby spring in the Cazorla mountain range and hence is very cold, whereas the 2 other villages are located hundreds of kilometres downstream with water passing by that was already heated. As a result, a significant contribution to cooling in the Spanish Cazorla origins from the cold river Cerezuelo, a phenomenon that is substantially reduced in German Geisenheim and Swedish Haparanda as is consistent with the study by Hathway and Sharples (2012).

2.4.3 Land cover effects

Some of the patterns found in European villages could be explained by circumstances already mentioned in the Sections 2.4.1 and 2.4.2. This includes a weaker correlation between land cover and temperatures in Cazorla in general, likely caused by the complex terrain. Even though differences in elevation have been kept within a certain range, recent work indicated that topographic structures might have a significant influence on TN (e.g. Lindén *et al.*, 2015a). Besides, during the warm season, the limited transpiration cooling from vegetation suffering from stomatal closure in Cazorla likely causes a reduction in the discrepancy between urban and rural sites. Significant interdependencies between temperature and vegetation are only detectable in close to the sensors, decreasing rapidly with distance, and defining the influential source area in Cazorla to <100 m. During the colder seasons, windy conditions and thick cloud cover in such mountainous regions might lower differences as well. Further work including the addition of more sensors in key locations and the analysis of wind conditions in different sites would be needed to address these issues and clarify the underlying reasons.

In Haparanda, vegetation contributes most substantially to cooling, with the effect being most pronounced in an area of 500 and 1000 m surrounding the sensors. The strongest effect occurs in summer, when vegetation is most productive and in this case not limited by soil water capacity due to the humid climate, although it is even detectable in the colder seasons with a cooling of -0.2 °C per 10 % vegetation coverage in spring, for example. If the vegetated area is considered for correlation in Geisenheim, a cooling could be confirmed that is most distinct in summer because transpiration is highest during that time. The cooling rate is presumably overall low in Geisenheim (-0.1 °C per 10 % vegetation coverage), because vineyards are characterized by lower photosynthetic rates compared to trees and forests as a whole. Model simulations (Dimoudi and Nikolopoulou, 2003) as well as satellite-based investigations (Buyantuyev and Wu, 2010) confirmed vegetation to lower temperatures significantly in urban areas.

In Haparanda as well as Geisenheim, exclusively significant coefficients are recorded if buildings were correlated with temperatures. The regression analysis confirmed a substantial warming caused by the built-up area as reported in other studies (Zhou *et al.*, 2011; Coseo and Larsen, 2014). In Haparanda, the coefficients of determination are highest in 500 and 1000 m radii, whereas in Geisenheim they decrease in these distances. Several other studies found a radius up to 500 m to be most relevant for spatial differences in urban temperatures (Hart and Sailor, 2009; Yokobori and Ohta, 2009). The 0.7 °C warming per 10 % building coverage calculated in Haparanda during spring is high if compared to Geisenheim (0.2 °C per 10 % building coverage). Because daytime in Sweden, and hence solar radiation, is massively prolonged in the warm season, a stronger impact caused by enhanced heating through urban geometry and materials is expected in late spring and early summer. This is likely coupled with a substantial anthropogenic heat release as is common for urban areas (Pigeon *et al.*, 2007), more specifically being enhanced during wintertime as a consequence of mainly domestic heating, which stops in Geisenheim during spring. This might even lead to a greater UHII during the cold season compared to the season mainly influenced by radiation, as observed in Alaska (Hinkel2007) and Hungary (Szgedi2013). Apart from that, Cazorla reveals less significant correlations and warming is solely notable in a radius of up to 50m, which confirms temperatures to be more decoupled from land cover in this region.

As stated in Section 2.3.2, water bodies proved to have limited effect on cooling except for the river Cerezuelo. However, since this effect diminishes with increasing distance to a water body (Oswald *et al.*, 2012), it appeared reasonable that significant correlations are constrained to a radius of up to 100 m considering the small size of the river. Steeneveld *et al.* (2011) found no significant correlation and showed that water bodies did not mitigate the UHI in several cities

and towns in the Netherlands. A later study by Steeneveld *et al.* (2014) revealed that water bodies might support the maximum UHI because of the high heat capacity of water, lowering maximum temperatures during the day but contributing to warmer temperatures at night. While Geisenheim and Haparanda are in line with these findings from central Europe, the Mediterranean Cazorla is an example for the mitigating effect water bodies might have for ambient temperatures as described in other studies (e.g. Murakawa *et al.*, 1991; Sun and Chen, 2012).

Our analysis revealed correlation patterns to be predominantly decoupled from seasons. Even though absolute seasonal R^2-values between temperatures and land cover types vary, the seasons largely agree whether correlations are significant and which radii contribute most to a cooling or warming of local temperatures. With the reliability of the results from Cazorla being questionable because of the complex terrain, further work needs to be carried out to address the site-specific climatology and avoid additional heating by sunlight and to compare the results to another Mediterranean site with less complex terrain.

2.4.4 Implications of village UHI

The UHI and its intensity heavily depend on the rural reference. If the rural reference is already affected by anthropogenic influence, the UHII could perhaps be even larger than recorded. In earlier studies, stations located in settlements with several thousand inhabitants were considered rural and used to quantify the additional warming in larger cities (e.g. Gallo *et al.*, 1993; Ezber *et al.*, 2007). Since our study revealed a strong influence of small built-up areas in radii up to 1km, many references likely underestimate the UHI in cities by overestimating temperatures measured in assumed ‘rural’ locations. Consequently, airport stations used as reference (e.g. Street *et al.*, 2013; Ketterer and Matzarakis, 2014) might be biased too as paved surfaces and buildings are nearby, although the pattern of built-up areas, paved surfaces and vegetation is different from that in a city. A better approach of classifying rural stations in terms of a possible urban temperature bias is based on remote sensing, i.e. using night-light data (Kalnay and Cai, 2003).

We showed that the formation of an UHI is real in Haparanda and Geisenheim as well as in Cazorla, mainly caused by building density contributing to a substantial warming. This additional warming is very likely preserved as a bias in the records of all meteorological stations from these villages. Since the station in Cazorla is still positioned within the village and has not moved gradually from inside town to the surrounding rural area, as is the case in Haparanda and Geisenheim, even current measurements are affected and need to be used with caution.

2.5 Conclusion

A significant UHI was found in 3 European villages. The intensity is strongest in summer TN in temperate Geisenheim (1.1 °C) and boreal Haparanda (1.4 °C), whereas in Mediterranean Cazorla, other seasons show the greatest urban-rural temperature differences (~0.9 °C). Limited plant activity due to warm and arid summer conditions likely limits cooling through transpiration in Cazorla, thereby leading to a less prominent discrepancy in summer compared to central and northern Europe, where summer temperature and moisture conditions are more favourable for plant growth.

Local TN were found to be positively linked to surrounding building density in all 3 villages. In the boreal as well as in the temperate villages, the relationship is highly significant regardless of season and distance (ranging from 50 to 1000 m). In the Mediterranean climate, the relationship is strong close to the sensors, but less so with increasing distance. Increasing building coverage by 10% resulted in a warming of spring TN by 0.3 °C and 0.2 °C in Cazorla and Geisenheim, respectively. The warming is stronger in Haparanda (0.7 °C per 10 % increase in buildings during spring) and highest in summer, likely due to long lasting solar radiation. Vegetation also contributed significantly to cooling in Haparanda (-0.2 °C per 10 % vegetation) and Geisenheim (-0.1 °C per 10 % vegetation). In Cazorla, the regression analysis indicated a significant cooling influence of vegetation solely in distances <100 m, except for summer, possibly due to the complexity of the terrain as well as the drought-stressed vegetation.

A distinct drop in summer TN by 4 °C near the mountain river was detected in Cazorla, where temperatures are significantly affected in radii of 50 and 100 m. Similar effects are absent in Haparanda and Geisenheim, likely because ambient air temperatures are lower and water temperatures are higher. Although the strength and intensity of land cover influence on temperature seem to weaken with decreasing latitude from Haparanda to Geisenheim to Cazorla, all villages are affected by urban warming. This leads to a potential UHI bias in meteorological observations recorded in these locations and may affect the well-being of the inhabitants.

2.6 References

Aguilar E, Auer I, Brunet M, Peterson TC,Wieringa J (2003). Guidelines on climate metadata and homogenization. *WMO/TD* **1186**.

Arnfield AJ (2003). Two decades of urban climate research: a review of turbulence, exchanges of energy and water, and the urban heat island. *International Journal of Climatology* **23**: 1-26.

Barry RG (2008). Mountain weather and climate. Cambridge University Press, Cambridge.

Ben Ahmed C, Ben Rouina B, Boukhris M (2007). Effects of water deficit on olive trees cv. Chemlali under field conditions in arid region in Tunisia. *Scientia Horticulturae* **113**: 267-277.

Bonan GB (2000). The microclimates of a suburban Colorado (USA) landscape and implications for planning and design. *Landscape and Urban Planning* **49**: 97-114.

Bottyán Z, Kircsi A, Szegedi S, Unger J (2005). The relationship between built-up areas and the spatial development of the mean maximum urban heat island in Debrecen, Hungary. *International Journal of Climatology* **25**: 405-418.

Brunet M, Saladié O, Jones P, Sigró J, Aguilar E, Moberg A, Lister D, Walther A, Almarza C (2006). A case-study/guidance on the development of long-term daily adjusted temperature datasets. *WMO/TD* **1425**.

Buyantuyev A, Wu J (2010). Urban heat islands and landscape heterogeneity: linking spatiotemporal variations in surface temperatures to land-cover and socioeconomic patterns. *Landscape Ecology* **25**: 17-33.

Chan ALS (2011). Developing a modified typical meteorological year weather file for Hong Kong taking into account the urban heat island effect. *Building and Environment* **46**: 2434-2441.

Chen X-L, Zhao H-M, Li P-X, Yin Z-Y (2006). Remote sensing image-based analysis of the relationship between urban heat island and land use/cover changes. *Remote Sensing of Environment* **104**: 133-146.

Coseo P, Larsen L (2014). How factors of land use/land cover, building configuration, and adjacent heat sources and sinks explain Urban Heat Islands in Chicago. *Landscape and Urban Planning* **125**: 117-129.

Dienst M, Lindén J, Engström E, Esper J (2017). Removing the relocation bias from the 155-year Haparanda temperature record in Northern Europe. *International Journal of Climatology* **37**: 4015-4026.

Dimoudi A, Nikolopoulou M (2003). Vegetation in the urban environment: microclimatic analysis and benefits. *Energy and Buildings* **35**: 69-76.

Ezber Y, Sen OL, Kindap T, Karaca M (2007). Climatic effects of urbanization in Istanbul: a statistical and modeling analysis. *International Journal of Climatology* **27**: 667-679.

Gallo KP, McNab AL, Karl TR, Brown JF, Hood JJ, Tarpley JD (1993). The use of a vegetation index for assessment of the urban heat island effect. *International Journal of Remote Sensing* **14**: 2223-2230.

Hansen J, Ruedy R, Sato M, Imhoff W, Lawrence D, Easterling DR, Peterson TC, Karl T (2001). A closer look at United States and global surface temperature change. *Journal of Geophysical Research* **106**: 23947-23963.

Hart MA, Sailor DJ (2009). Quantifying the influence of land-use and surface characteristics on spatial variability in the urban heat island. *Theoretical and Applied Climatology* **95**: 397-406.

Hathway EA, Sharples S (2012). The interaction of rivers and urban form in mitigating the Urban Heat Island effect: A UK case study. *Building and Environment* **58**: 14-22.

Hinkel KM, Nelson FE (2007). Anthropogenic heat island at Barrow, Alaska, during winter: 2001–2005. *Journal of Geophysical Research* **112**: 1-12.

Hinkel KM, Nelson FE, Klene AE, Bell JH (2003). The urban heat island in winter at Barrow, Alaska. *International Journal of Climatology* **23**: 1889-1905.

Hua LJ, Ma ZG, Guo WD (2008). The impact of urbanization on air temperature across China. *Theoretical and Applied Climatology* **93**: 179-194.

Huang L, Li J, Zhao D, Zhu J (2008). A fieldwork study on the diurnal changes of urban microclimate in four types of ground cover and urban heat island of Nanjing, China. *Building and Environment* **43**: 7-17.

Jarvis CH, Stuart N (2001). A comparison among strategies for interpolating maximum and minimum daily air temperatures. *Journal of Applied Meteorology* **40**: 1060-1074.

Jones PD, Wigley TML (2010). Estimation of global temperature trends: what's important and what isn't. *Climatic Change* **100**: 59-68.

Kalnay E, Cai M (2003). Impact of urbanization and land-use change on climate. *Nature* **423**: 528-531.

Kantzioura A, Kosmopoulos P, Zoras S (2012). Urban surface temperature and microclimate measurements in Thessaloniki. *Energy and Buildings* **44**: 63-72.

Ketterer C, Matzarakis A (2014). Human-biometeorological assessment of the urban heat island in a city with complex topography – The case of Stuttgart, Germany. *Urban Climate* **10**: 573-584.

Kim Y-H, Baik J-J (2002). Maximum Urban Heat Island Intensity in Seoul. *Journal of Applied Meteorology* **41**: 651-659.

Klysik K, Fortuniak K (1999). Temporal and spatial characteristics of the urban heat island of Lodz, Poland. *Atmospheric Environment* **33**: 3885-3895.

Kottek M, Grieser J, Beck C, Rudolf B, Rubel F (2006). World Map of the Köppen-Geiger climate classification updated. *Meteorologische Zeitschrift* **15**: 259-263.

Landsberg HE (1981). The Urban Climate. New York, Academic Press.

Li RM, Roth M (2009). Spatial variation of the canopy-level urban heat island in Signapore. *The seventh International Conference on Urban Climate*. Yokohama, Japan, International Association for Urban Climate.

Lindén J, Esper J, Holmer B (2015a). Using Land Cover, Population, and Night Light Data for Assessing Local Temperature Differences in Mainz, Germany. *Journal of Applied Meteorology and Climatology* **54**: 658-670.

Lindén J, Grimmond CSB, Esper J (2015b). Urban warming in villages. *14th EMS Annual Meeting & 10th European Conference on Applied Climatology (ECAC)*. Auer, I. Prague, Czech Republic, Advances in Science & Research.

Lo CP, Quattrochi DA (2003). Land-Use and Land-Cover Change, Urban Heat Island Phenomenon, and Health Implications: A Remote Sensing Approach. *Photogrammetric Engineering & Remote Sensing* **69**: 1053-1063.

Mayer H, Höppe P (1987). Thermal Comfort of Man in Different Urban Environments. *Theoretical and Applied Climatology* **38**: 43-49.

Montávez JP, Rodríguez A, Jiménez JI (2000). A study of the urban heat island of Granada. *International Journal of Climatology* **20**: 899-911.

Morris CJG, Simmonds I, Plummer N (2001). Qualification of the Influences of Wind and Cloud on the Nocturnal Urban Heat Island of a Large City. *Journal of Applied Meteorology* **40**: 169-182.

Murakawa S, Sekine T, Narita K, Nishina D (1991). Study of the effects of a river on the thermal environment in an urban area. *Energy and Buildings* **16**: 993-1001.

Oke TR (1982). The energetic basis of the urban heat island. *Quarterly Journal of the Royal Meteorological Society* **108**: 1-24.

Oke TR (1987). Boundary Layer Climates. Routledge, London.

Oke TR (2008). Urban Observations. *Guide to meteorological instruments and methods of observation*. WMO. Geneva. **WMO-No. 8**.

Oswald EM, Rood RB, Zhang K, Gronlund CJ, O'Neill MS, White-Newsome JL, Brines SJ, Brown DG (2012). An Investigation into the Spatial Variability of Near-Surface Air Temperatures in the Detroit, Michigan, Metropolitan Region. *Journal of Applied Meteorology and Climatology* **51**: 1290-1304.

Papanastasiou DK, Kittas C (2012). Maximum urban heat island intensity in a medium-sized coastal Mediterranean city. *Theoretical and Applied Climatology* **107**: 407-416.

Parker DE (2010) Urban heat island effects on estimates of observed climate change. *WIREs Climate Change* **1**, 123-133.

Peterson TC, Vose RS (1997). An Overview of the Global Historical Climatology Network Temperature Database. *Bulletin of the American Meteorological Society* **78**: 2837-2849.

Pigeon G, Legain D, Durand P, Masson V (2007). Anthropogenic heat release in an old European agglomeration (Toulouse, France). *International Journal of Climatology* **27**: 1969-1981.

Poulos G, Zhong S (2008). An observational history of small-scale katabatic winds in Mid-Latitudes. *Geography Compass* **2**: 1798-1821.

QGIS Development Team (2017). QGIS Geographic Information System. Open Source Geospatial Foundation Project. http://qgis.osgeo.org/

Ren G, Zhou Y, Chu Z, Zhou J, Zhang A, Guo J, Liu X (2008). Urbanization Effects on Observed Surface Air Temperature Trends in North China. *Journal of Climate* **21**: 1333-1348.

Shen T (2015). Evaluation of urban heat island situation in developed cities of Zhejiang province. *Department of Architecture and Built Environment*. Nottingham, University of Nottingham. **PhD**.

Steeneveld GJ, Koopmans S, Heusinkveld BG, Theeuwes NE (2014). Refreshing the role of open water surfaces on mitigating the maximum urban heat island effect. *Landscape and Urban Planning* **121**: 92-96.

Steeneveld GJ, Koopmans S, Heusinkveld BG, van Hove LWA, Holtslag AAM (2011). Quantifying urban heat island effects and human comfort for cities of variable size and urban morphology in the Netherlands. *Journal of Geophysical Research* **116**: 1-14.

Street M, Reinhart C, Norford L, Ochsendorf J (2013). Urban Heat Island in Boston – an Evaluation of Urban Airtemperature Models for Predicting Building Energy Use. *13th Conference of International Building Performance Simulation Association*. Chambéry, France.

Sun R,Chen L (2012). How can urban water bodies be designed for climate adaptation? *Landscape and Urban Planning* **105**: 27-33.

Szegedi S, Toth T, Kapocska L, Gyarmati R (2013). Examinations on the meteorological factors of urban heat island developement in small and medium-sized towns in Hungary. *Carpathian Journal of Earth and Environmental Sciences* **8**: 209-214.

Thorsson S, Lindberg F, Björklund J, Holmer B, Rayner D (2010). Potential changes in outdoor thermal comfort conditions in Gothenburg, Sweden due to climate change: the influence of urban geometry. *International Journal of Climatology* **31**: 324-335.

Torok SJ, Morris CJG, Skinner C, Plummer N (2001). Urban heat island features of southeast Australian. *Australian Meteorological Magazine* **50**: 1-13.

Trouet V, Van Oldenborgh GJ (2013). KNMI Climate Explorer: A Web-Based Research Tool for High-Resolution Paleoclimatology. *Tree-Ring Research* **69**: 3-13.

Unger J (1996). Heat Island intesity with different meteorological conditions in a medium-sized town: Szeged, Hungary. *Theoretical and Applied Climatology* **54**: 147-151.

Unger J (2004). Intra-urban relationship between surface geometry and urban heat island: review and new approach. *Climate Research* **27**: 253-264.

Venema V, Mestre O, Aguilar E, Guijarro J, Domonkos P, Vertachnik G, Szentimrey T, Stepanek P, Zahradnicek P, Viarre J, Müller-Westermeier G, Lakatos M, Williams CN, Menne MJ, Lindau R, Rasol D, Rustemeier E, Kolokythas K, Marinova T, Andresen L, Acquaotta F, Fratianni S, Cheval S, Klancar M, Brunet M, Gruber C, Prohom M, Likso T, Esteban P,

Brandsma T, Willet K (2012). Detecting and repairing inhomogeneities in datasets, assessing current capabilities. *Bulletin of the American Meteorological Society* **93**: 951-954.

Wienert U, uttler W (2005). The dependence of the urban heat island intensity on latitude - A statistical approach. *Meteorologische Zeitschrift* **14**: 677-686.

Yokobori T, Ohta S (2009). Effect of land cover on air temperatures involved in the development of an intra-urban heat island. *Climate Research* **39**: 61-73.

Zhang J-H, Hou Y, Li G, Yan H, Yang L, Yao F (2005). The diurnal and seasonal characteristics of urban heat island variation in Beijing city and surrounding areas and impact factors based on remote sensing satellite data. *Science in China. Ser. D Earth Sciences* **48**: 220-229.

Zhang L, Ren G, Ren Y, Zhang A, Chu Z, Zhou Y (2014). Effect of data homogenization on estimate of temperature trend: a case of Huairou station in Bejing Municipality. *Theoretical and Applied Climatology* **115**: 365-373.

Zhao C, Fu G, Liu X, Fu F (2011). Urban planning indicators, morphology and climate indicators: A case study for a north-south transect of Beijing, China. *Building and Environment* **46**: 1174-1183.

Zhou W, Huang G, Cadenasso ML (2011). Does spatial configuration matter? Understanding the effects of land cover pattern on land surface temperature in urban landscapes. *Landscape and Urban Planning* **102**: 54-63.

Zhou X, Ooka R, Chen H, Kawamoto Y, Kikumoto H (2016). Impacts of inland water area changes on the local climate of Wuhan, China. *Indoor and Built Environment* **25**: 296-313.

3 Addressing the relocation bias in a long temperature record by means of land cover assessment

Isabel Knerr[1,2], Manuel Dienst[2], Jenny Lindén[3], Petr Dobrovolný[4], Jan Geletic[5], Ulf Büntgen[4,5,6], Jan Esper[2]

[1]Faculty of Geography, Philipps-University, Marburg, Germany

[2]Department of Geography, Johannes Gutenberg University, Mainz, Germany

[3]IVL – Swedish Environmental Research Institute, Gothenburg, Sweden

[4]Department of Geography, Masaryk University, Brno, Czech Republic

[5]Institute of Computer Science, Czech Academy of Sciences, Brno, Czech Republic

[6]Department of Geography, University of Cambridge, Cambridge, United Kingdom

Theoretical and Applied Climatology – in review

3.1 Introduction

High-quality, long-term meteorological measurements form the backbone of modern climate research (Auer *et al.*, 2005), including proxy-based paleoclimatology (Esper *et al.*, 2007) and model-based climate change prediction and evaluation (e.g. Cox *et al.*, 1999; Leach, 2007; Voldoire *et al.*, 2012). The term high quality implies that the data is homogenous, i.e. variability and trends are exclusively caused by weather and climate (Aguilar *et al.*, 2003; Venema *et al.*, 2012b). Even though continuous efforts to reduce non-climatic biases in meteorological measurements are improving data homogeneity, biases due to changes in observing practices, instrumentation or station surroundings are found in long station records (Moberg and Bergström, 1997; Auer *et al.*, 2005; Brunet *et al.*, 2006a). Many studies report that the most important inhomogeneities are related to station relocations and its implications, i.e. a change in site conditions and hence microclimate (e.g. Tuomenvirta, 2001; Brunet *et al.*, 2006a; Rahimzadeh and Zavareh, 2014).

Long meteorological stations were often originally placed within cities to ensure good accessibility, but these cities gradually grew to become larger and were modernized, frequently leading to changes in station surroundings and thus triggering relocations (Allen *et al.*, 2011). The potential influence of an urban-induced temperature trend in these records has been examined in numerous studies (e.g. Goodridge, 1992; Portman, 1993; Jones *et al.*, 2008; Parker, 2010; Wigley and Santer, 2013). The main concern is the influence of the urban heat island – the warming effect caused by limited radiative and advective cooling due to urban geometry, increased thermal admittance of construction materials, reduced latent heat storage as a result of sealed surfaces, and limited vegetation coverage (Arnfield, 2003). Studies have shown that differences in LULC can explain a significant part of the spatial variability in temperatures, not only with regard to urban/rural differences but also among urban sites per se (Chen *et al.*, 2006; Lindén, 2011). Although the thermal source area influencing temperatures can extend upwind for metres to kilometres (Stewart and Oke, 2012), the most effective influences occur within 500 m horizontal distance or less in urban environments (Hart and Sailor, 2009; Li and Roth, 2009; Yokobori and Ohta, 2009; Lindén, 2011).

In order to reduce inhomogeneities in long time-series of meteorological observations (e.g. Begert *et al.*, 2005; Auer *et al.*, 2007), homogenization methods are often applied (Brunet *et al.*, 2006b; Štěpánek *et al.*, 2009), with ACMANT, CLIMATOL or HOMER being some popular examples (Venema *et al.*, 2012a; Pérez-Zanón *et al.*, 2015). These approaches integrate statistical tests to identify break points and use relative homogenisation approaches to compare

one candidate time series with other records from nearby stations (Vincent, 1998; Zhen and Zhong-Wei, 2015). However, temperature records that cover more than 100 years or more are seldom and rarely close to nearby stations with records of similar length, thus restricting possibilities for relative homogenisation. Alternative methods are therefore needed to assess and correct potential biases due to station relocations and other factors. Any attempt to do so relies on the availability of metadata in order to understand and consider the station history (Aguilar *et al.*, 2003). Crucial information include observation hours, relocation dates, changes in instrumentation and environment.

Here, we assess the influence of LULC and other factors on spatial temperature differences in and around Brno, the second largest city of the Czech Republic. We therefore use a 3.5-year-long network of daily measurements from 11 stations in different urban and sub-urban environments. Our findings allow us to assess past temperature patterns in Brno based on historical maps. By considering former locations of old meteorological stations, the LULC analysis enables quantification of the urban heat island effect at each of these sites at different points in time. To correct for relocation biases in Brno's climate record, site-specific effects are removed from the original time-series, presumably allowing for an enhanced view on warming within the last two centuries.

3.2 Methods

3.2.1 Study area

Brno is located in the south-east of the Czech Republic in southern Moravia. Even though most part of the city extends within a basin, huge difference in altitude of more than 250 m occur between different parts of the urban area due to the otherwise hilly terrain. Considering the Köppen climate classification (Peel *et al.*, 2007), Brno exhibits a mixture of oceanic, temperate (Cfb) and humid, continental climate (Dfb), with cold winters and warm summers. The average annual precipitation is 509 mm and the average annual air temperature is 9.3 °C based on the period from 1961 until 1990 (Brázdil *et al.*, 2006).

3.2.2 Measurements

We use a network of eleven meteorological stations in the city of Brno to quantify spatial temperature differences. The network was established by the Masaryk University in Brno in cooperation with the Czech Hydrometeorological Institute (Dobrovolný *et al.*, 2012). Since several studies reveal a distinct influence on station readings in a radius of 500 m or less (e.g.

Chow and Roth, 2006; Li and Roth, 2009; Lindén *et al.*, 2015), the dominating land surface within 500 m radius was first considered to assign the stations to three different descriptive classes based on the percentage of sealed areas surrounding the stations in order to evaluate whether an Urban Heat Island (UHI) is existent in Brno (Fig. 3-1).

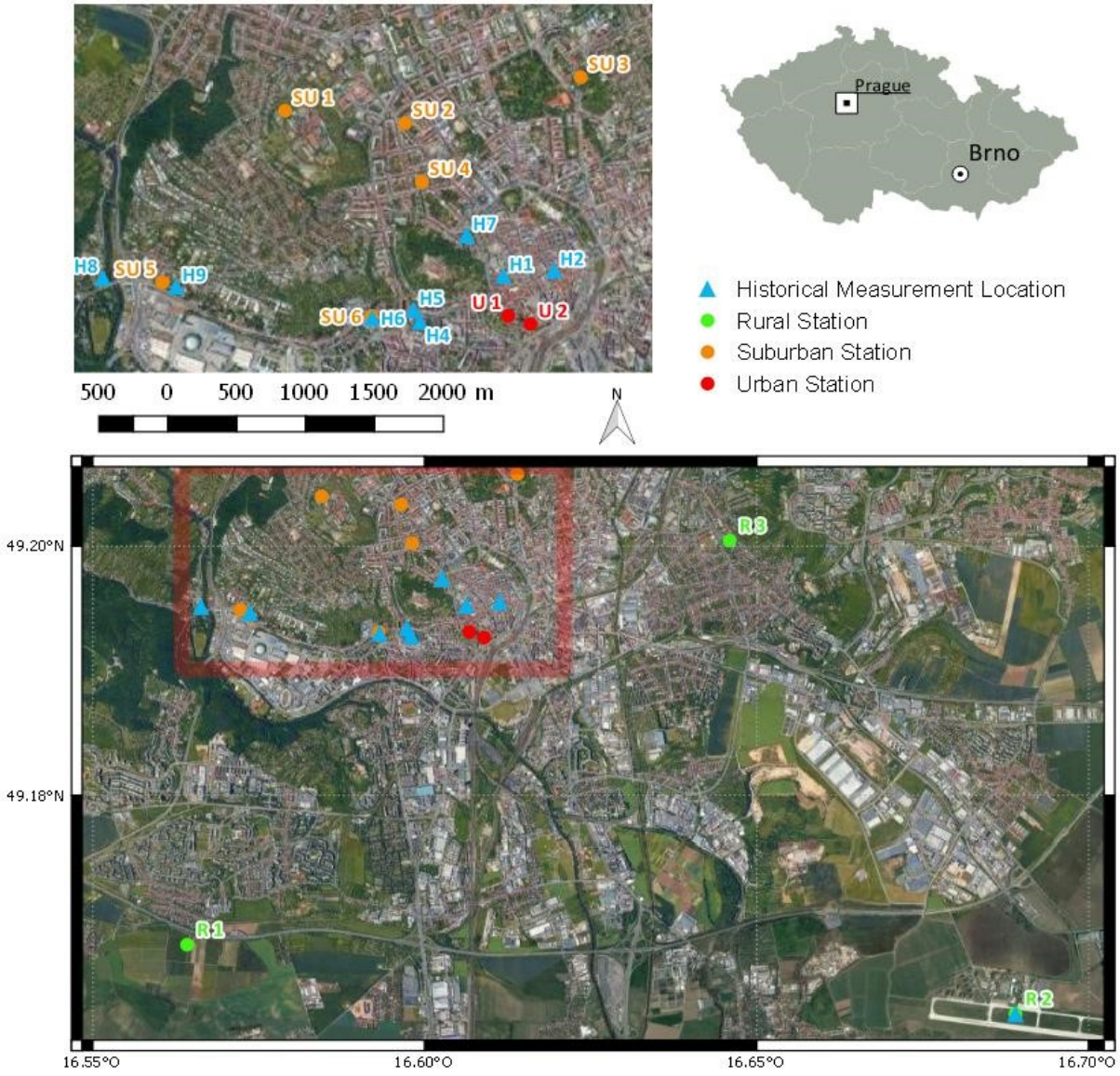

Figure 3-1 Location of the 11 current measurement stations and historical measurement sites in the area of Brno.

The first class contains two urban stations (U) in the historical city centre with more than 75 % of sealed areas, the second class includes three rural stations (R) outside of the city with 40 % or less of sealed areas (R) and the third class consists of six suburban stations with a percentage of sealed areas between 41 % and 75 % (SU), all within a radius of 500 m around the measurement stations. Sites and classifications of the stations are displayed in Figure 3-1, along

with the locations of the historical station setup through time (cf. Table 3-4). A counter-check relying on the Local Climate Zones introduced by Stewart and Oke (2012) revealed the classification based on digitization to match the given categories very well (cf. Table 3-1).

Name	Coordinates		Elevation [m a.s.l.]	Local Climate Zones (LCZ)
	LAT	LON		
U 1	49.191389	16.606667	245	Compact midrise (2)
U 2	49.190833	16.608889	227	Compact midrise (2)
R 1	49.16	16.564167	244	Sparsely built (9)
R 2	49.153056	16.688889	241	Large low-rise with low plants (8D)
R 3	49.200556	16.645833	216	Sparsely built (9)
SU 1	49.205	16.584444	298	Open midrise (5)
SU 2	49.204167	16.596389	242	Open midrise (5)
SU 3	49.207222	16.613889	225	Open midrise (5)
SU 4	49.200278	16.598056	234	Open midrise (5)
SU 5	49.193611	16.572222	214	Open midrise (5)
SU 6	49.191389	16.593056	206	Open midrise (5)

Table 3-1 Location of the 11 current measurement stations and historical measurement sites in the area of Brno.

Temperatures were recorded at 10-minute intervals from June 2011 to February 2015. A total of 35 days were missing in the final dataset, though all stations still reach a data coverage >96%. Daily arithmetic means were calculated based on the 10-min measurements, and an altitude correction of 0.6 K/100 m (e.g. Mullet, 1987; Paulsen *et al.*, 2000) was applied. A determination of daily maximum and minimum temperatures was performed by selecting the highest and lowest 10-minute values per day. Because of the intricacy that is inherent to an altitude correction for minimum and maximum values (Unwin, 1980), these values have not been processed. Seasonal values were determined using the arithmetic mean of the daily values, whereas for minimum and maximum, the median was considered to reduce the influence of extremes. The seasonal values were correlated against all types of LC within each radius considered (50 m, 100 m, 300 m, 500 m, 800 m, 1000 m) to determine the most influential source area and LC types. In order to estimate the amount of temperature change associated to LC, a regression analysis was performed.

To better clarify whether certain sites are distinctly warmer or cooler than others, ΔT was used in the first analysis instead of absolute values. The ΔT values were calculated according to equation 1:

$$\Delta T_1 = T_1 - T_{all}$$

with T_{all} being the average of the temperature values for all 11 stations used in the analysis.

By means of equation 1, boxplot diagrams were created to detect a possible UHI effect as well as to check the distribution of the data available. A student's t-test was performed to assess whether differences are significant on a 0.05 level.

3.2.3 Land Use and Land Cover change

To investigate the influence of LULC change in Brno, areas within a radius of 50 m, 100 m, 300 m, 500 m, 800 m and 1000 m around the measurement stations were digitalised, using ArcGIS 10.3 and aerial photographs. The settlement structure and density (right) was classified into six representative categories in order to include all possible surfaces, though two of these (water bodies, gravel/sand) were excluded from analysis due to insignificant occurrences. An overview of the remaining four classes and an additional combination into sealed areas (SA) and total vegetation (TV) are shown in Table 3-2.

Buildings * (BU)	all building structures
Paved Areas * (PA)	impermeable surfaces
Low Vegetation ** (LV)	agricultural fields, gardens, meadows and similar
High Vegetation ** (HV)	forests, but also visible grove in gardens or along streets

* combined in the category "Sealed Areas" (SA)

** combined in the category "Total Vegetation" (TV)

Table 3-2 Classification of those land cover types in the wider area of Brno that have been considered in this study.

Especially in cities, a subdivision between low and high vegetation is important. Depending on the moisture content, large areas with low vegetation might absorb heat during day and emit it during nigh, similar to paved surfaces, i.e. these areas do not necessarily contribute to cooling (TAHA, 1997; WANG *ET AL.*, 2016). Since a differentiation between low and high vegetation solely by interpreting an aerial photo is difficult, the combined category TV was generated. To

quantify the aggregated warming effect of buildings and paved areas, these were integrated in the SA (TAHA, 1997; WANG *ET AL.*, 2016).

3.2.4 Historical temperature data

Other than our recent measurements with a temporal resolution of 10 minutes at each location, the historical data gathered has far less data available each day. Since historical measurements required manual read out, most temperature observations were scheduled to be checked at least three times a day. This was usually done in the morning, at noon and in the evening, trying to capture daily minimum and maximum as well as a reasonable daily mean as best as possible. In the following, measurement procedures and calculations of daily averages are detailed for the Brno meteorological station.

Regarding the first station location H1 (period from 1800 to 1812, see Figure 3-1 for locations), the provided data consists of daily values derived from the mean of five daily observations (Brázdil *et al.*, 2006). For the next two measurement sites, either no values (H2) or no exact location and no values are reported (H3). In the period from 01/1848 to 12/1878 (H4 and H5), temperature was measured at 6 am, 2 pm and 10 pm. Even though these times do not match exactly, a calculation of daily values was performed or conducted using the "Mannheimer Stunden". Since 01/1879, measuring times were adopted to the "Mannheimer Stunden" 7 am, 2 pm and 9 pm of mean local time, though recording shifted for a short period of time (06/1885 - 12/1889) to 6 am, 1 pm and 9 pm. The otherwise continuous dataset contains a total of 207 days with missing or incorrect temperature values in the period from 1878 to 1890.

In order to quantify a possible bias from historical relocations, the current effect of land cover on local temperatures was assessed and linked with information derived from digitalized historical maps provided by the Moravian Land Archive, Brno, Czech Republic. Building density in various radii (50 m, 100 m, 300 m, 500 m, 800 m, 1000 m) was determined for each time interval the stations experienced a change in location. The relationship between building cover and temperature variation established in the analysis of the current station network was used to remove the bias caused by the varying building cover at the historical measuring sites. Since other types of LC such as sealed areas or vegetation were not part of the historical maps, this analysis was exclusively based on building cover.

3.3 Results

In order to identify a possible UHI effect, an overview on spatial temperature patterns is presented in figure 3-2. The overall largest discrepancies among the station groups become apparent for mean and minimum temperatures in summer. Mean temperatures are significantly higher at urban sites (U) compared to rural sites (R) reaching 0.9 K in summer, 0.8 K in spring and 0.5 K in autumn. Winter temperatures display the highest variability in the data and differences among sites are almost negligible. Even though minimum temperatures are certainly characterised by a larger variability compared to mean temperatures, they emphasize the fact that rural areas are characterised by cooler conditions compared to the urban sites during all seasons (~1.2 K) except for winter. Splitting the urban stations into two groups reveals an even enhanced warming if sealed areas account for more than 75% of the surrounding land cover. Since maximum temperatures did not display significant differences among the sensor groups and hence did not show any connection to land cover, it was disregarded from further analysis.

As a second step, a correlation of mean and minimum temperatures with various categories of land cover was performed, revealing several strong relations especially in the 300 m and 500 m radii (Fig. 3-3). For mean temperatures, highest correlations among all LC were found for BU when spring temperatures and a 300 m radius were considered ($R^2 = 0.80$). The inter-seasonal patterns are very similar, with larger radii leading to decreases correlation strength, although remaining significant. The combined category (TV) displays prominent correlations and a significant relationship during all seasons but winter, even though seasonal R^2-values of LV and HV did not exceed 0.4 when considered separately in a pre-analysis. With 500 m being the most influential radius, the highest coefficients of determination are again linked to temperatures in spring. Since SA and PA revealed a very similar pattern compared to BU, these land cover classes were omitted from the figure.

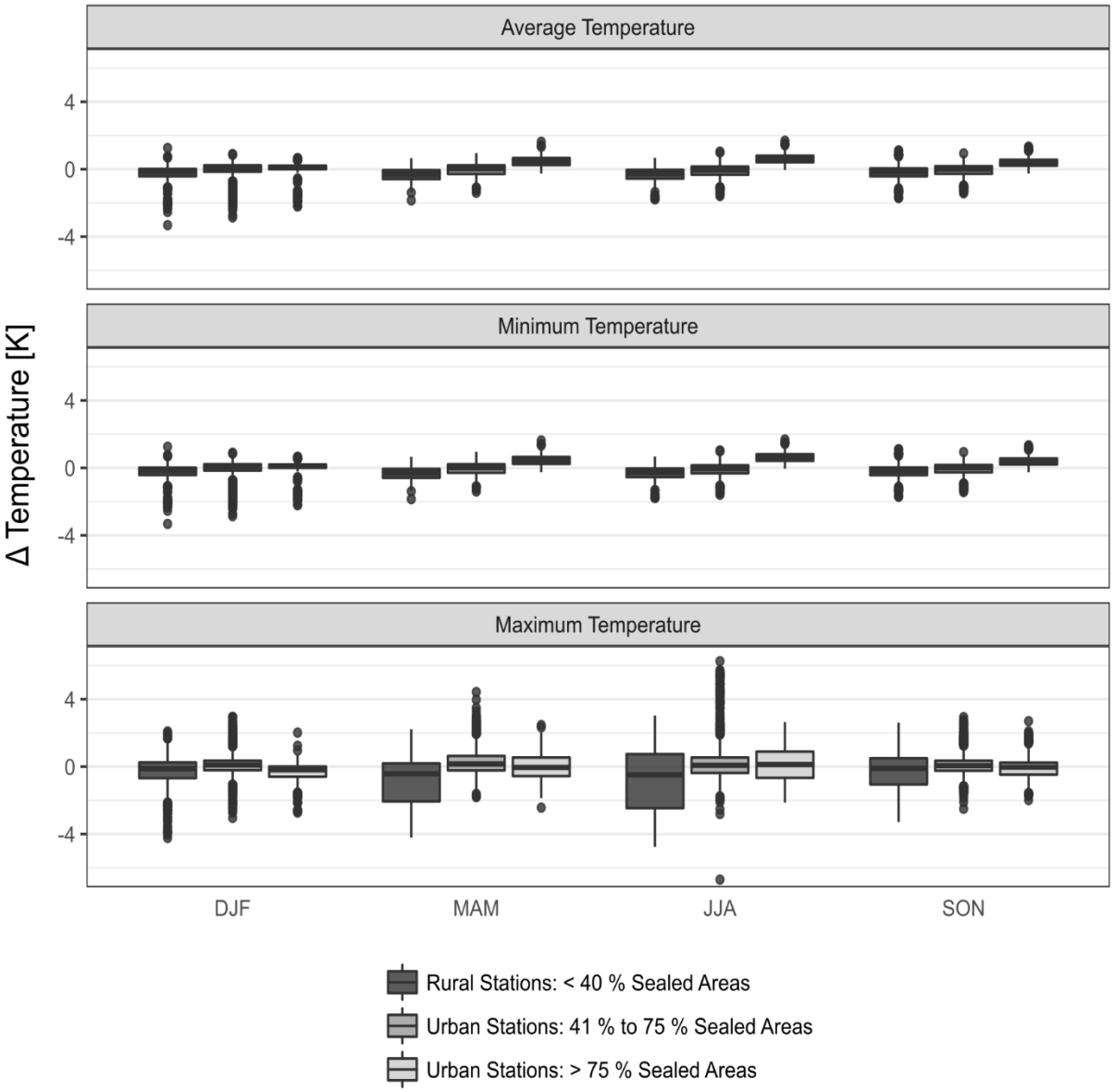

Figure 3-2 Seasonal air temperature variability based on daily data from June 2011 to February 2015 of rural (n=3, left) as well as urban stations with 41-75% (n=6, middle) and >75% sealed areas (n=2, right), respectively. Temperatures are displayed as anomalies, more specifically as differences to the mean of all sensors. Data exceeding 1.5 times the interquartile range are removed from the whiskers and shown as outliers.

For minimum temperatures, correlations are diverse in close vicinity of the stations and decrease if radii of more than 300 m are considered. The course is almost identical throughout all seasons with autumn displaying the highest values. Similar to mean temperatures, BU revealed significant correlations for all seasons (average R^2 ~0.5), although the explained variance is lower in minimum temperatures. Other than for mean temperatures, SA and PA (not shown here) reveal similar patterns including significant correlations during all seasons in radii of 100 m and more. Regardless of the season, the coefficients of determination display peak

values for the 100-500 m radii, and all correlations are significant if TV is considered. A pre-analysis revealed this to be caused by a strong influence of HV while LV showed very low R^2-values compared to other parameters tested. Overall, correlation strength is lower than for mean temperatures with peak values of R^2=0.6.

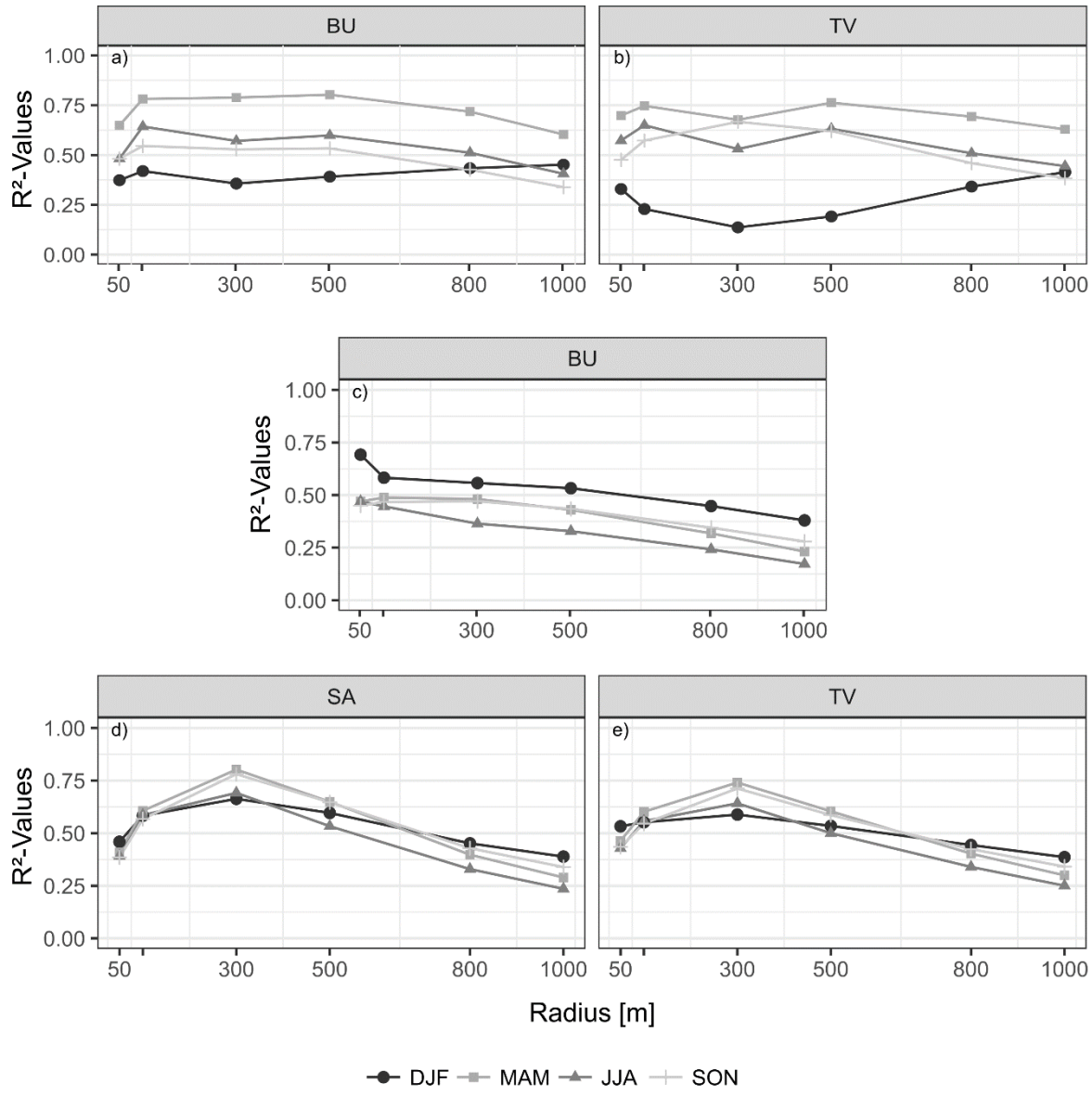

Figure 3-3 Coefficients of determination for seasonal average (a, b) und minimum temperatures (c, d, e) correlated with selected types of land cover (BU = Building, TV= Total Vegetation and SA= Sealed Areas) relative to different distances to the stations. Selection was based on the correlation strength and importance of each land cover for later analysis.

Since building coverage is crucial for the determination of the relocation bias, and correlations for mean and minimum temperatures were high during spring in the 500 m and 300 m radii, Figure 3-4 serves as an example for the analyses applied to all seasons. Mean temperatures

reveal an increase of 0.2 °C/10 % building coverage while displaying very low variance at the same time. By comparison, minimum temperatures show increased variability but a steeper trend (0.4 °C/10 % buildings).

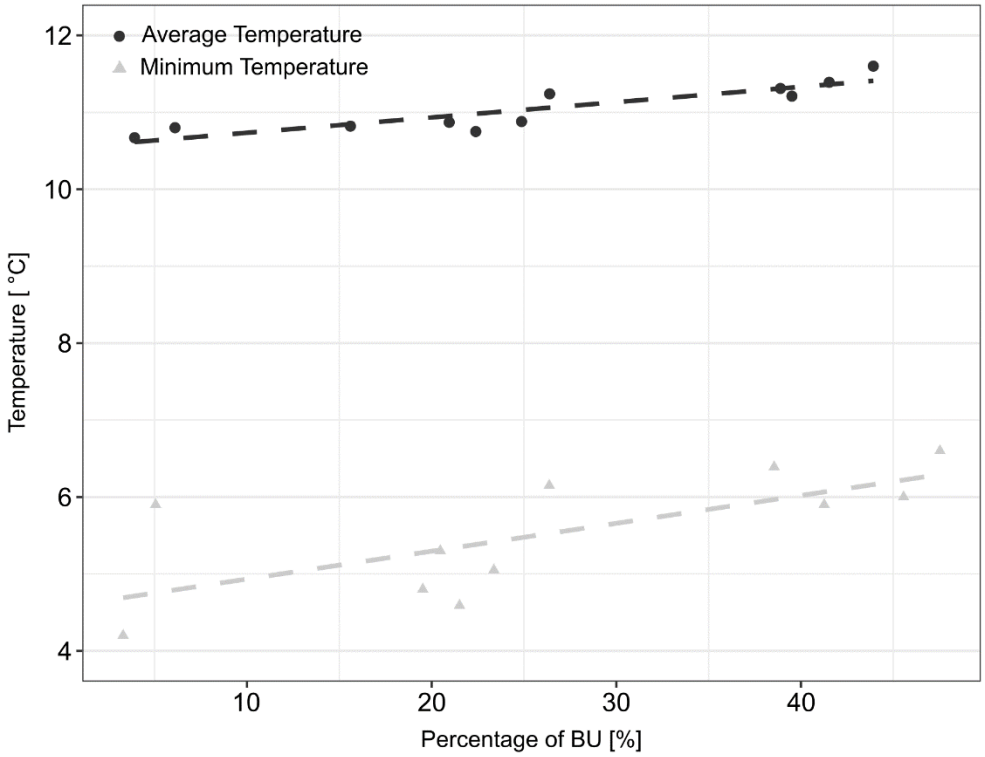

Figure 3-4 Regression analysis based on the relation between the percentage of built-up area within the station surroundings of 300 m radius and spring TN (R^2-Value 0.48*) and 500 m radius and TM (R^2-Value 0.80**), respectively. Spring temperatures were selected due to exceptionally high R^2-values.

Table 3-3 summarizes the regression functions for every season as well as the correlation coefficients, revealing significant relations exceeding $p<0.05$. Average temperatures display the strongest correlations whereas the increase in temperature per % buildings is highest in minimum temperatures, thus confirming the minima to be closely controlled by additional warming caused by urban structures. Based on former building density, the equations were used to quantify the urban bias at each historical measurement site (Table 3-4), enabling a correction by subtracting the values from the measured ones during the corresponding time intervals.

With spring temperatures having the strongest relation to building density ($R^2=0.8$), Figure 3-5 shows the annual average temperature during spring as an example of the original and adjusted records in comparison. Even though measuring started in 1799, temperatures are displayed since 1848 because the first 50 years of data are incomplete. Most striking is the fact that until 1890, the relocation bias is considerably higher than during any time later.

TM		
	function	**R²**
DJF	y = 0,0079 x + 0,9931	0,39 *
MAM	y = 0,0199 x + 10,5351	0,80 **
JJA	y = 0,0211 x + 19,7696	0,60 **
SON	y = 0,0141 x + 10,0381	0,53 *

TN		
	function	**R²**
DJF	y = 0,0210 x -1,6360	0,56 **
MAM	y = 0,0362 x + 4,5718	0,48 *
JJA	y = 0,0282 x + 13,2244	0,36 *
SON	y = 0,0305 x + 5,5001	0,47 *

Table 3-3 Regression equations and R²-values for LC buildings and temperature relation

Before 1890, the meteorological stations were established near the city centre, where building density was relatively high (30 % within a 500 m radius), especially biasing the period from 1884 to 1890 (cf. Table 3-4) at 0.58K. The station was then moved to the periphery of the city 1890, where building density is lower, reaching only 2-3 % within a radius of 500 m, and constraining the relocation bias to only 0.02 K.

Name	Duration	Map of Year	Built Fraction (500 m)	Bias DJF	Bias MAM	Bias JJA	Bias SON
H 1	1800 – 1812	1824	32%	0,25	0,63	0,67	0,44
H2	1813 - 1815; 1819	1824	30%	Missing Temperature Values			
H 4	1848 – 1853	1858	18%	0,14	0,35	0,37	0,25
H 5	1853 – 1878	1858	17%	0,12	0,33	0,35	0,23
H 6	1878 – 1883	1909	17%	0,12	0,35	0,37	0,24
H 7	1884 – 1890	1909	29%	0,23	0,58	0,62	0,41
H 8	1890 – 1922	1929	2%	0,02	0,05	0,06	0,04
H 9	1923 – 1960	1929	3%	0,02	0,06	0,06	0,04
H 10	1961 – 2005	2013	3%	0,03	0,08	0,08	0,05

Table 3-4 Overview of the historical measurement periods of the Brno meteorological station, together with the built fraction in a 500 m radius around the past measuring locations derived from historical maps drawn in the years listed in column three. Columns 4-8 display the quantified heat bias in different seasons caused by nearby buildings based on the equations shown in table 2-3.

As the relocation bias decreases towards recent times, the corrections increase the overall warming trend from 0.77 °C/100 y to 1.05 °C/100 y. If the 1850-1900 interval is considered, the changes are even stronger reaching 0.96 °C/100 y for the original and 1.34 °C/100 y for the corrected record. As the temperature bias due to building cover is mainly negligible in the 20th century, both time series line up closely during the past around 100 years (Figure 3-5).

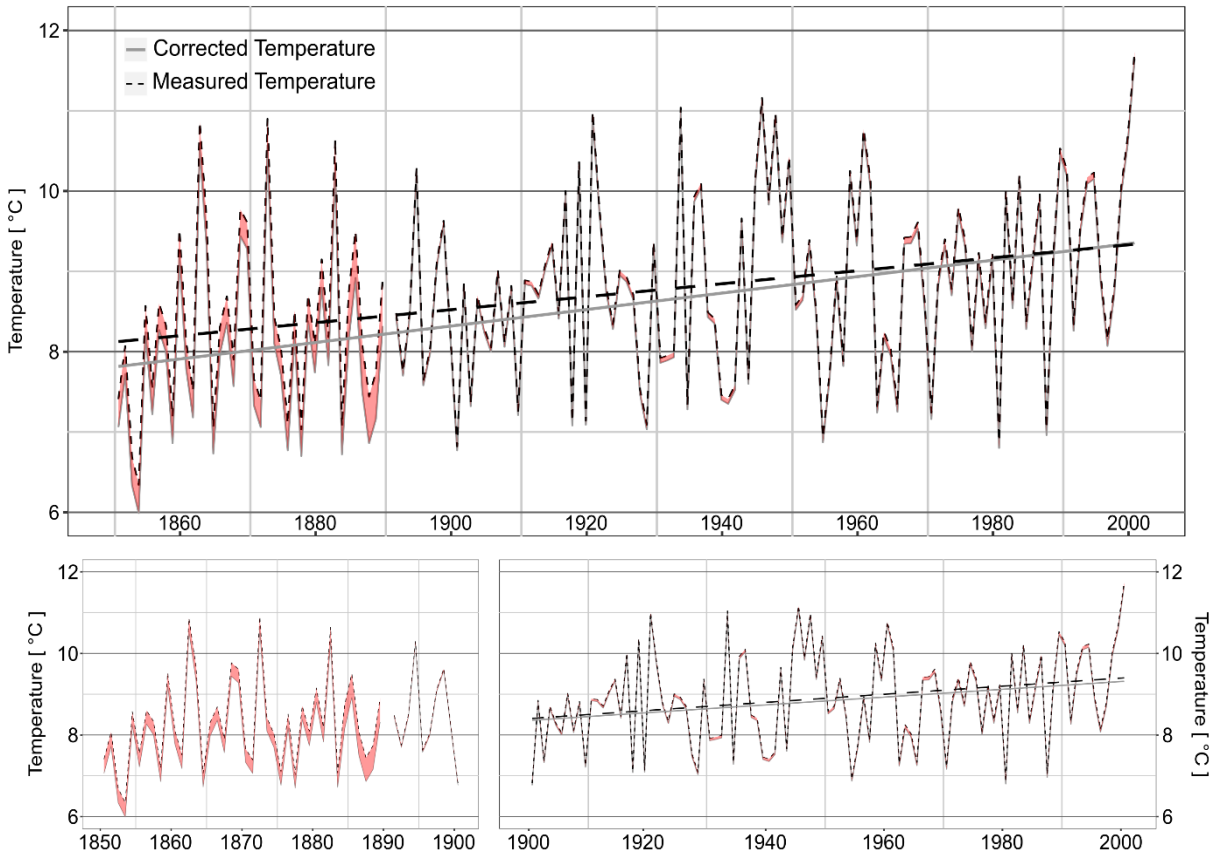

Figure 3-5 Measured and corrected Brno MAM record from 1850 until 2000. Data from the 19th century (left) and 20th century (right) are displayed separately to illustrate the strong corrections in the beginning and the minor changes in the later part. Spring season was selected due to the strongest relation to building density.

3.4 Discussion and conclusions

This study reveals a distinct UHI in the city of Brno that is most pronounced in summer but persistent throughout the whole year. Warming was strongly related to building coverage and sealed areas while vegetation provides significant cooling for urban temperatures. By employing a regression analysis for building density and temperatures, we applied a correction for the UHI intensity to the 150-year Brno meteorological measurements to eliminate the influence of relocations. In the following section, we explain the patterns and intensities of the UHI in different seasons as well as its connection to various types of land cover, followed by a

discussion of the relocation bias during different periods and its removal, as well as a comparison between the corrected and original time series.

3.4.1 Temperatures and their connection to settlement structure

A distinct UHI effect was found in Brno, with greatest differences detected during summer in mean and minimum temperatures and overall minor effects during winter. These seasonal variations are also reported from other cities (e.g. Morris *et al.*, 2001; Kolokotsa *et al.*, 2009), though some climate conditions yield inverted situations (Yang *et al.*, 2013). As suggested by Giridharan *et al.* (2007), the seasonal pattern can be explained by stronger summertime solar radiation amplifying the heating effect of urban materials and geometry. In addition, higher wind speeds and cloudy weather usually prevent the formation of a strong and lasting UHI in winter, however minor warming could still be detected as is true for London (Giridharan and Kolokotroni, 2009). Our results revealed the necessity of eliminating relocation biases in Brno considering different seasons.

Apart from these seasonal changes, the most distinct urban warming influence in minimum temperatures is in line with other studies. Kalnay and Cai (2003) report minimum temperature trends in the United States to be most affected due to urbanization, and studies from Nanjing (Huang *et al.*, 2008) or New York (Gaffin *et al.*, 2008) support a decline in UHI intensity after sunrise. The main reason for this is energy, which was stored during the day through solar radiation, remains longer in the city due to multiple release heat and uptake processes of the now emerged sensible heat as well as anthropogenic heat sources (Oke, 1982; Taha, 1997).

Land cover was used to identify the structures and surfaces contributing most to cooling and warming, respectively. Overall, temperatures were strongly and significantly correlated with buildings, sealed areas and vegetation. These findings confirmed source areas to influence radii of up to 1000 m as also found in other studies (e.g. Lindén *et al.*, 2015). The coefficients tended to decrease with increasing distance from the measurement locations. The strengths of correlations varied with season, with lowest influence of land cover in winter. Regression analyses showed the increasing amount of vegetation leading to lower temperature values. This is likely due to shading and evaporative cooling, which is most pronounced during the warmer months (Dimoudi and Nikolopoulou, 2003; Weng *et al.*, 2004). In contrast, the thermal properties of paved areas and buildings cause higher temperatures in their surroundings, generally most effective during summer when solar radiation is strongest (e.g. Lo and Quattrochi, 2003). Both factors, low evapotranspiration as well as limited solar radiation, explain the weak correlation values in the cold season.

3.4.2 The relocation bias

The quantification of the relocation bias and hence the quality of the correction is determined by mainly two different factors: the dependence of temperatures on building density, and the representativeness and reliability of the current measurements. In the previous section, we showed that spatial temperature differences are significantly related to land cover, with buildings and sealed areas explaining most of the additional warming at urban sites. As this analysis is based on more than 1300 days of high resolution data from 11 stations in and around Brno, we value the dataset to be very robust. As no significant changes were found in historical building cover compared to today, the current analysis is likely representative for the past 150 years. Being preserved as a site of historical importance, this is particularly true for the city centre, where most relocations took place. However, in the vicinity of the station locations H8 and H9, at the border of the city, several new buildings have been constructed in the course of urban growth population increase. We assume the influence of these changes to be negligible, however, since the percentage of buildings rose by less than 7% in the surroundings of sites H8 and H9.

Other uncertainties arise from the historical maps. The drawing as such might be imprecise, and since vegetation and surface cover was rarely included, only building cover could be used to assess the warming bias. This problem is likely less significant as only few areas were paved in the 19th century and, after that, the station moved to locations with almost no sealed and built-up surfaces.

Another aspect in cities is the concern of a possible anthropogenic warming due to direct heating effects. Even though most houses are heated in the winter season today, only a fraction of heat is emitted due to good insulation. In contrast, only minor insulation materials were used in former times allowing a great part of the heat to be transferred through the walls and windows to the outside. Consequently, Bozaky (2011) assumes the influence of heating to be relatively balanced over time as the amount of heating was much lower 200 years ago. Nevertheless, this is an important issue especially during the 19th century when the station was installed in substantially urbanized areas, emphasizing the need to concentrate on the possible impact in further studies.

3.4.3 Time series correction

When dealing with long temperature datasets, other issues than relocations that might have had an impact on the historical measurements need to be considered. In particular, these are changes in the instrumentation and sheltering, in observing times and temperature mean calculations

(e.g. Böhm *et al.*, 2009). Since 1799, more sophisticated instruments were introduced and replaced by new ones several times. The impact of these changes on the data is hard to quantify, because information on exact dates is missing. For other changes, historical evidence is existent, e.g. a shift in recording daily maximum values (Brázdil *et al.*, 2006). Since this change took place before 1850, it does not influence the later part of the record chosen for correction. Varying observing times and mean calculations (see chapter 2.5) surely had an impact on data, but might overall be negligible as Moberg and Bergström (1997) pointed out for a temperature dataset from Sweden. Such influences are, however, generally difficult to estimate if parallel measurements are not available. Despite not being able to account for all these possible impacts and uncertainties, other studies detailed relocations to be the most severe influence in long temperature records (e.g. Tuomenvirta, 2001; Syrakova and Stefanova, 2008). Hence, by addressing them, we offer an improvement for the dataset. Nevertheless, further studies need to be carried out in order to include additional correction for less severe biases resulting from further interferences other than relocations.

Applying the correction causes minimum and mean temperatures to drop regardless of the season, as all historical locations were affected by a varying number of nearby buildings and hence by a corresponding warm bias. The larger corrections in the early part of the record were necessary because measurements took place in the centre and surrounding building density was high. This situation changed with the relocation in 1890, moving the station to a location almost free of built-up surfaces. Reducing the early temperature values led to an increase in the overall warming trend, a common effect after applying a homogenization to long station records (Begert *et al.*, 2005; Brunet *et al.*, 2006a). 20th century warming remains almost un-affected though, as building cover did not exceed 3% in the stations' vicinity and changes to the time series remained marginal after 1890. A comparable study by Dienst *et al.* (2017) of a 150 year long record from Sweden showed similar results. In consequence, the results insinuate that warming has been underestimated. However, Zhang *et al.* (2014) offer another explanation for these findings, stating that a correction for relocation biases typically increases warming trends, since the gradual warming due to urbanization is recovered. Relocating the station to more rural surroundings towards today lowers temperatures because of the decrease in nearby buildings and sealed surface. Therefore, this procedure weakens the otherwise increasing background warming inherent in the time series due to city growth. According to them, by removing all influences only connected to warming by nearby land cover, this background urban warming is still present in the time series.

An elimination of the relocation bias in long term temperature records using the approach presented here, is feasible only if a dense network of recent temperature is established and sufficient historical information on the original measurement sites and conditions are available. Even though other factors were excluded from this correction approach, this study clearly documents the severity of non-climatic, anthropogenic influences in one of the longest meteorological records from Europe, while at the same time proving its reliability in the 20th century.

3.5 References

Aguilar E, Auer I, Brunet M, Peterson TC, Wieringa J (2003). Guidelines on climate metadata and homogenization. *WMO/TD* **1186**.

Allen L, Lindberg F, Grimmond CSB (2011). Global to city scale urban anthropogenic heat flux: model and variability. *International Journal of Climatology* **31**: 1990-2005.

Arnfield AJ (2003). Two decades of urban climate research: a review of turbulence, exchanges of energy and water, and the urban heat island. *International Journal of Climatology* **23**: 1-26.

Auer I, Böhm R, Jurkovi A, Orlik A, Potzmann R, Schöner W, Ungersböck M, Brunetti M, Nanni T, Maugeri M, Briffa K, Jones P, Efthymiadis D, Mestre O, Moisselin J-M, Begert M, Brazdil R, Bochnicek O, Cegnar T, Gajic-capka M, Zaninovi K, Majstorovi E, Szalai S, Szentimrey T, Mercalli L (2005). A new instrumental precipitation dataset for the greater alpine region for the period 1800-2002. *International Journal of Climatology* **25**: 139-166.

Auer I, Böhm R, Jurkovic A, Lipa W, Orlik A, Potzmann R, Schöner W, Ungersböck M, Matulla C, Briffa K, Jones P, Efthymiadis D, Brunetti M, Nanni T, Maugeri M, Mercalli L, Mestre O, Moisselin J-M, Begert M, Müller-Westermeier G, Kveton V, Bochnicek O, Stastny P, Lapin M, Szalai S, Szentimrey T, Cegnar T, Dolinar M, Gajic-Capka M, Zaninovic K, Majstorovic Z, Nieplova E (2007). HISTALP—historical instrumental climatological surface time series of the Greater Alpine Region. *International Journal of Climatology* **27**: 17-46.

Begert M, Schlegel T, Kirchhofer W (2005). Homogeneous temperature and precipitation series of Switzerland from 1864 to 2000. *International Journal of Climatology* **25**: 65-80.

Böhm R, Jones PD, Hiebl J, Frank D, Brunetti M, Maugeri M (2009). The early instrumental warm-bias: a solution for long central European temperature series 1760–2007. *Climatic Change* **101**: 41-67.

Bozaky D (2011). The historical development of thermal insulation materials. *Periodica Polytechnica Architecture* **41**: 49-56.

Brázdil R, Řezníčková L, Valášek H (2006). Early instrumental meteorological observations in the Czech Lands I: Ferdinand Knittelmayer, Brno, 1799-1812. *Meteorologický časopis* **9**: 59-71.

Brunet M, Saladié O, Jones P, Sigró J, Aguilar E, Moberg A, Lister D, Walther A, Almarza C (2006a). A case-study/guidance on the development of long-term daily adjusted temperature datasets. *WMO/TD* **1425**.

Brunet M, SaladiÉ O, Jones P, SigrÓ J, Aguilar E, Moberg A, Lister D, Walther A, Lopez D, Almarza C (2006b). The development of a new dataset of Spanish Daily Adjusted Temperature Series (SDATS) (1850–2003). *International Journal of Climatology* **26**: 1777-1802.

Chen X-L, Zhao H-M, Li P-X, Yin Z-Y (2006). Remote sensing image-based analysis of the relationship between urban heat island and land use/cover changes. *Remote Sensing of Environment* **104**: 133-146.

Chow W, Roth M (2006). Temporal dynamics of the urban heat island of Singapore. *International Journal of Climatology* **26**: 2243-2260.

Cox PM, Betts RA, Bunton CB, Essery RLH, Rowntree PR, Smith J (1999). The impact of new land surface physics on the GCM simulation of climate and climate sensitivity. *Climate Dynamics* **15**: 183-203.

Dienst M, Lindén J, Engström E, Esper J (2017). Removing the relocation bias from the 155-year Haparanda temperature record in Northern Europe. *International Journal of Climatology* **37**: 4015-4026.

Dimoudi A, Nikolopoulou M (2003). Vegetation in the urban environment: microclimatic analysis and benefits. *Energy and Buildings* **35**: 69-76.

Dobrovolný P, Řezníčková L, Brázdil R, Krahula L, Zahradníček P, Hradil M, Doleželová M, Šálek M, Štěpánek P, Rožnovský J, Valášek H, Kirchner K, Kolejka J (2012). Klima Brna. Víceúrovňová analýza městského klimatu. Brno.

Esper J, Frank D, Büntgen U (2007). On selected issues and challenges in dendroclimatology. *A changing world: challenges for landscape research*. Kienast, F, Wildi, O,Ghosh, S, Springer**:** 113-132.

Gaffin SR, Rosenzweig C, Khanbilvardi R, Parshall L, Mahani S, Glickman H, Goldberg R, Blake R, Slosberg RB, Hillel D (2008). Variations in New York city's urban heat island strength over time and space. *Theoretical and Applied Climatology* **94**: 1-11.

Giridharan R, Kolokotroni M (2009). Urban heat island characteristics in London during winter. *Solar Energy* **83**: 1668-1682.

Giridharan R, Lau SSY, Ganesan S, Givoni B (2007). Urban design factors influencing heat island intensity in high-rise high-density environments of Hong Kong. *Building and Environment* **42**: 3669-3684.

Goodridge JD (1992). Urban bias influences on long-term California air temperature trends. *Atmospheric Environment. Part B. Urban Atmosphere* **26**: 1-7.

Hart MA, Sailor DJ (2009). Quantifying the influence of land-use and surface characteristics on spatial variability in the urban heat island. *Theoretical and Applied Climatology* **95**: 397-406.

Huang L, Li J, Zhao D, Zhu J (2008). A fieldwork study on the diurnal changes of urban microclimate in four types of ground cover and urban heat island of Nanjing, China. *Building and Environment* **43**: 7-17.

Jones PD, Lister D, Li Q (2008). Urbanization effects in large-scale temperature records, with an emphasis on China. *Journal of Geophysical Research* **113**: 1-12.

Kalnay E, Cai M (2003). Impact of urbanization and land-use change on climate. *Nature* **423**: 528-531.

Kolokotsa D, Psomas A, Karapidakis E (2009). Urban heat island in southern Europe: The case study of Hania, Crete. *Solar Energy* **83**: 1871-1883.

Leach AJ (2007). The climate change learning curve. *Journal of Economic Dynamics and Control* **31**: 1728-1752.

Li RM, Roth M (2009). Spatial variation of the canopy-level urban heat island in Signapore. *The seventh International Conference on Urban Climate*. Yokohama, Japan, International Association for Urban Climate.

Lindén J (2011). Nocturnal Cool Island in the Sahelian city of Ouagadougou, Burkina Faso. *International Journal of Climatology* **31**: 605-620.

Lindén J, Esper J, Holmer B (2015). Using Land Cover, Population, and Night Light Data for Assessing Local Temperature Differences in Mainz, Germany. *Journal of Applied Meteorology and Climatology* **54**: 658-670.

Lo CP, Quattrochi DA (2003). Land-Use and Land-Cover Change, Urban Heat Island Phenomenon, and Health Implications: A Remote Sensing Approach. *Photogrammetric Engineering & Remote Sensing* **69**: 1053-1063.

Moberg A, Bergström H (1997). Homogenization of Swedish temperature data - Part III - The long temperature records from Uppsala and Stockholm. *International Journal of Climatology* **17**.

Morris CJG, Simmonds I, Plummer N (2001). Qualification of the Influences of Wind and Cloud on the Nocturnal Urban Heat Island of a Large City. *Journal of Applied Meteorology* **40**: 169-182.

Mullet LB (1987). The solar chimney - overall effciency, design and performance. *International Journal of Ambient Energy* **8**: 35-40.

Oke TR (1982). The energetic basis of the urban heat island. *Quarterly Journal of the Royal Meteorological Society* **108**: 1-24.

Parker DE (2010) Urban heat island effects on estimates of observed climate change. *WIREs Climate Change* **1**, 123-133.

Paulsen J, Weber UM, Körner C (2000). Tree Growth near Treeline: Abrupt or Gradual Reduction with Altitude? *Arctic, Antarctic, and Alpine Research* **32**: 14-20.

Peel MC, Finlayson BL, Mcmahon TA (2007). Updated world map of the Köppen-Geiger climate classification. *Hydrology and Earth System Sciences Discussions, EGU* **11**: 1633-1644.

Pérez-Zanón N, Sigró J, Domonkos P, Ashcroft L (2015). Comparison of HOMER and ACMANT homogenization methods using a central Pyrenees temperature dataset. *Advances in Science and Research* **12**: 111-119.

Portman DA (1993). Identifying and Correcting Urban Bias in Regional Time Series: Surface Temperature in China's Northern Plains. *Journal of Climate* **6**: 2298-2308.

Rahimzadeh F, Zavareh MN (2014). Effects of adjustment for non-climatic discontinuities on determination of temperature trends and variability over Iran. *International Journal of Climatology* **34**: 2079-2096.

Štěpánek P, Zahradníček P, Skalák P (2009). Data quality control and homogenization of air temperature and precipitation series in the area of the Czech Republic in the period 1961–2007. *Advances in Science and Research* **3**: 23-26.

Stewart ID, Oke TR (2012). Local Climate Zones for Urban Temperature Studies. *Bulletin of the American Meteorological Society* **93**: 1879-1900.

Syrakova M, Stefanova M (2008). Homogenization of Bulgarian temperature series. *International Journal of Climatology* **29**: 1835-1849.

Taha H (1997). Urban Climates and Heat Islands: Albedo, Evapotranspiration, and Anthropogenic Heat. *Energy and Buildings* **25**: 99-103.

Tuomenvirta H (2001). Homogeneity adjustments of temperature and precipitation series - Finnish and Nordic data. *International Journal of Climatology* **21**: 495-506.

Unwin DJ (1980). The synoptic climatology of Birmingham's urban heat island, 1965-74. *Weather* **35**: 43-50.

Venema V, Mestre O, Aguilar E, Auer I, Guijarro J, Domonkos P, Vertachnik G, Szentimrey T, Stepanek P, Zahradnicek P, Viarre J, Müller-Westermeier G, Lakatos M, Williams CN, Menne MJ, Lindau R, Rasol D, Rustemeier E, Kolokythas K, Marinova T, Andresen L, Acquaotta F, Fratianni S, Cheval S, Klancar M, Brunetti M, Gruber C, Prohom M, Likso T, Esteban P, Brandsma T (2012a). Benchmarking homogenization algorithms for monthly data. *Climate of the Past* **8**: 89-115.

Venema V, Mestre O, Aguilar E, Guijarro J, Domonkos P, Vertachnik G, Szentimrey T, Stepanek P, Zahradnicek P, Viarre J, Müller-Westermeier G, Lakatos M, Williams CN, Menne MJ, Lindau R, Rasol D, Rustemeier E, Kolokythas K, Marinova T, Andresen L, Acquaotta F, Fratianni S, Cheval S, Klancar M, Brunet M, Gruber C, Prohom M, Likso T, Esteban P, Brandsma T, Willet K (2012b). Detecting and repairing inhomogeneities in datasets, assessing current capabilities. *Bulletin of the American Meteorological Society* **93**: 951-954.

Vincent LA (1998). A Technique for the Identification of Inhomogeneities in Canadian Temperature Series. *Journal of Climate* **11**: 1094-1104.

Voldoire A, Sanchez-Gomez E, Salas y Mélia D, Decharme B, Cassou C, Sénési S, Valcke S, Beau I, Alias A, Chevallier M, Déqué M, Deshayes J, Douville H, Fernandez E, Madec G, Maisonnave E, Moine MP, Planton S, Saint-Martin D, Szopa S, Tyteca S, Alkama R, Belamari

S, Braun A, Coquart L, Chauvin F (2012). The CNRM-CM5.1 global climate model: description and basic evaluation. *Climate Dynamics* **40**: 2091-2121.

Wang ZH, Zhao X, Yang J, Song J (2016). Cooling and energy saving potentials of shade trees and urban lawns in a desert city. *Applied Energy* **161**: 437-444.

Weng Q, Lu D, Schubring J (2004). Estimation of land surface temperature–vegetation abundance relationship for urban heat island studies. *Remote Sensing of Environment* **89**: 467-483.

Wigley TML, Santer BD (2013). A probabilistic quantification of the anthropogenic component of twentieth century global warming. *Climate Dynamics* **40**: 1087-1102.

Yang P, Ren G, Liu W (2013). Spatial and Temporal Characteristics of Bejing Urban Heat Island Instensity. *Journal of Applied Meteorology and Climatology* **52**: 1803-1816.

Yokobori T, Ohta S (2009). Effect of land cover on air temperatures involved in the development of an intra-urban heat island. *Climate Research* **39**: 61-73.

Zhang L, Ren G, Ren Y, Zhang A, Chu Z, Zhou Y (2014). Effect of data homogenization on estimate of temperature trend: a case of Huairou station in Bejing Municipality. *Theoretical and Applied Climatology* **115**: 365-373.

Zhen L, Zhong-Wei Y (2015). Homogenized Daily Mean/Maximum/Minimum Temperature Series for China from 1960-2008. *Atmospheric and Oceanic Science Letters* **2**: 237-243.

4 Removing the relocation bias from the 155-year Haparanda temperature record in Northern Europe

Manuel Dienst[1], Jenny Lindén[2], Erik Engström[3], Jan Esper[1]

[1]Department of Geography, Johannes Gutenberg University, Mainz, Germany
[2]IVL – Swedish Environmental Research Institute, Gothenburg, Sweden
[3]Swedish Meteorological and Hydrological Institute, Norrköping, Sweden

International Journal for Climatology, 2017- published

4.1 Introduction

The analysis of past and current climate variability and trends requires long-term, high quality instrumental meteorological datasets (Auer *et al.*, 2005). Instrumental data benefit from very high – monthly or even daily – resolution, but also covers a relatively short time period, as most coordinated measurements did not start before the 19th century (Brunet *et al.*, 2006). Although proxy data, such as tree-rings, ice cores or lake/ocean sediments, can be used to reconstruct climate variability of thousands of years back in time, high quality instrumental data are essential for calibration and verification (Esper *et al.*, 2007).

High quality meteorological data imply that the readings are homogeneous, and that variability and trends in the data are exclusively caused by weather and climate (Aguilar *et al.*, 2003; Venema *et al.*, 2012b). Even though efforts, such as sheltering and regular maintenance of instruments are made with the aim to produce homogeneous data, several biases have been identified within temperature series, particularly in long datasets (Tuomenvirta, 2001).The biases are caused by various events and procedures, like relocations, changes in observing practices or the introduction of new instruments (Böhm *et al.*, 2009). Station relocations have been shown to cause the majority of the detected inhomogeneities (e.g. Tuomenvirta, 2001; Brunet *et al.*, 2006; Syrakova and Stefanova, 2008; Böhm *et al.*, 2009; Rahimzadeh and Zavareh, 2014). A relocation or change in the environmental conditions of the station surroundings (e.g. construction of new buildings or removal of trees etc.), may cause biases in the data due to alteration of the radiation balance and ventilation (Oke, 2006).

Prior to the introduction of automatic weather stations (AWS) some 15 years ago, meteorological observations required daily or sub-daily manual read outs. Due to the high labour intensity of this work, the stations were often positioned in connection to urban settlements to support accessibility. However, the data may thus contain an urban bias (Jones and Wigley, 2010). The urban bias is characterized as an intensified warming within urban areas which is typically most pronounced during night-time and in summer (Oke, 1982; Morris *et al.*, 2001), even though contrary results have been found as well, for example in Eastern Asia with a greater bias in winter (Yang *et al.*, 2013). This local warming phenomenon is called “urban heat island” (UHI) and has been subject of many studies (Arnfield, 2003; Rizwan *et al.*, 2008). Various factors have been identified to affect UHI including an increased thermal admittance of construction materials, restricted radiative and advective cooling due to the urban geometry, and reduced cooling through evapotranspiration by sealed surfaces and limited vegetation coverage (Oke, 1982; Dimoudi and Nikolopoulou, 2003).

The urban warming bias generally intensifies with the size, population and density of an urban area (e.g. Oke, 1982). An additional anthropogenic heat release induced by traffic, domestic heating and industry can enhance the magnitude of UHI (e.g. Arnfield, 2003), but the influence of these factors might be limited outside of dense urban centres of major cities, such as New York and Paris (Allen *et al.*, 2011). On a global scale, the urban bias has proved to be small if not negligible (e.g. Parker, 2005; Trenberth *et al.*, 2007; Parker, 2010), but other work indicated locally substantial biases in, for example, the rapidly urbanizing China (Jones *et al.*, 2008; Ren *et al.*, 2008; He *et al.*, 2013) and the United States (Hansen *et al.*, 2001). Most UHI studies focus on greater cities throughout the world (e.g. Morris *et al.*, 2001; Huang *et al.*, 2008; Weng and Lu, 2008). Smaller urban settlements are less studied, even though UHI effects have been found in towns (e.g. Magee *et al.*, 1999; Fujibe, 2009; Steeneveld *et al.*, 2011) and villages (e.g Hinkel *et al.*, 2003; Lindén *et al.*, 2015b) as well. The scarcity of studies focusing on smaller urban settlements limits the possibility to assess the potential urban heat island intensity (UHII) affecting instrumental stations located in such environments.

In order to assess the homogeneity of long station records, access to detailed meta information including descriptions of historical changes in instrumentation and surroundings are crucial (Aguilar *et al.*, 2003). Metadata should contain coordinates, relocation dates, instrumental alterations, changes in observation practices and surroundings. The knowledge gained from these data, in combination with statistical homogenization procedures, offer the possibility to apply justified and detailed corrections of long station records (Brunet *et al.*, 2006). Most homogenization procedures using statistical tests for break point detection rely on the assumption that climate signals in nearby stations are similar, enabling the assessment of inhomogeneities by means of comparison (Venema *et al.*, 2012a). One such method is HOMER, a script developed within a European COST action (Venema *et al.*, 2012a) that has since been applied in numerous studies (e.g. Freitas *et al.*, 2013; Mestre *et al.*, 2013; Vertachnik *et al.*, 2015). However, long station records including data from the early 20th century or even the 19th century are rare, limiting relative homogenization approaches particularly during the early periods.

In this paper we present an empirical approach to estimate and remove relocation biases from one of the longest temperature datasets in the Nordic region, the 155-year record from the village of Haparanda, Sweden. The correction is based on parallel measurements to identify the spatial field air temperature variations within this village over a two year period.

4.2 Research site and methods

4.2.1 Study area

Haparanda is situated in the north of Sweden at the river Torneälv together with the Finnish town Tornio to the east and the Baltic Sea to the south (Fig. 4-1). The climate is sub-arctic, with cold winters, cool and short summers, and no dry season (Köppen-Geiger classification: Dfc. Kottek *et al.* (2006)). The landscape is flat with altitude differences below 20m a.s.l. within a distance of 5km around Haparanda, and mainly covered by forest, wetlands and some agricultural fields.

Haparanda was first mentioned in the 17th century when it consisted of five homesteads. It gained town privileges with a population of approximately 550 in 1842, after having constructed a centre in the years before (Wasserman, 2009). The population grew to 2700 in the 1940, 4200 in 1970, and 4865 in 2010 (StatisticsSweden, www.scb.se). However, historical maps (LandmaterietSweden, https://www.lantmateriet.se/en/) show that the original structure of the centre remained unchanged. The economic map of Sweden reveals that the centre in 1946 was essentially identical to today's structures with many buildings still being intact, while the urban area surrounding has slowly grown (see Fig. 4-1). Historical photos from around 1940 indicate that also the construction materials remained similar including wood as the dominating building material (Odencrants, 1945; Hederyd, 1993). Street paving was introduced gradually with most roads in the centre being surfaced in the 1940's. Horses were exclusively used until the 1920's when they were progressively replaced by cars. Also electricity was introduced in 1920s, but many houses are still heated by wood burning nowadays. Growth of the village has mainly been in the form of residential and commercial areas constructed some distance from the centre. Trade has been the main source of income in Haparanda, i.e. no major industries are located in the village.

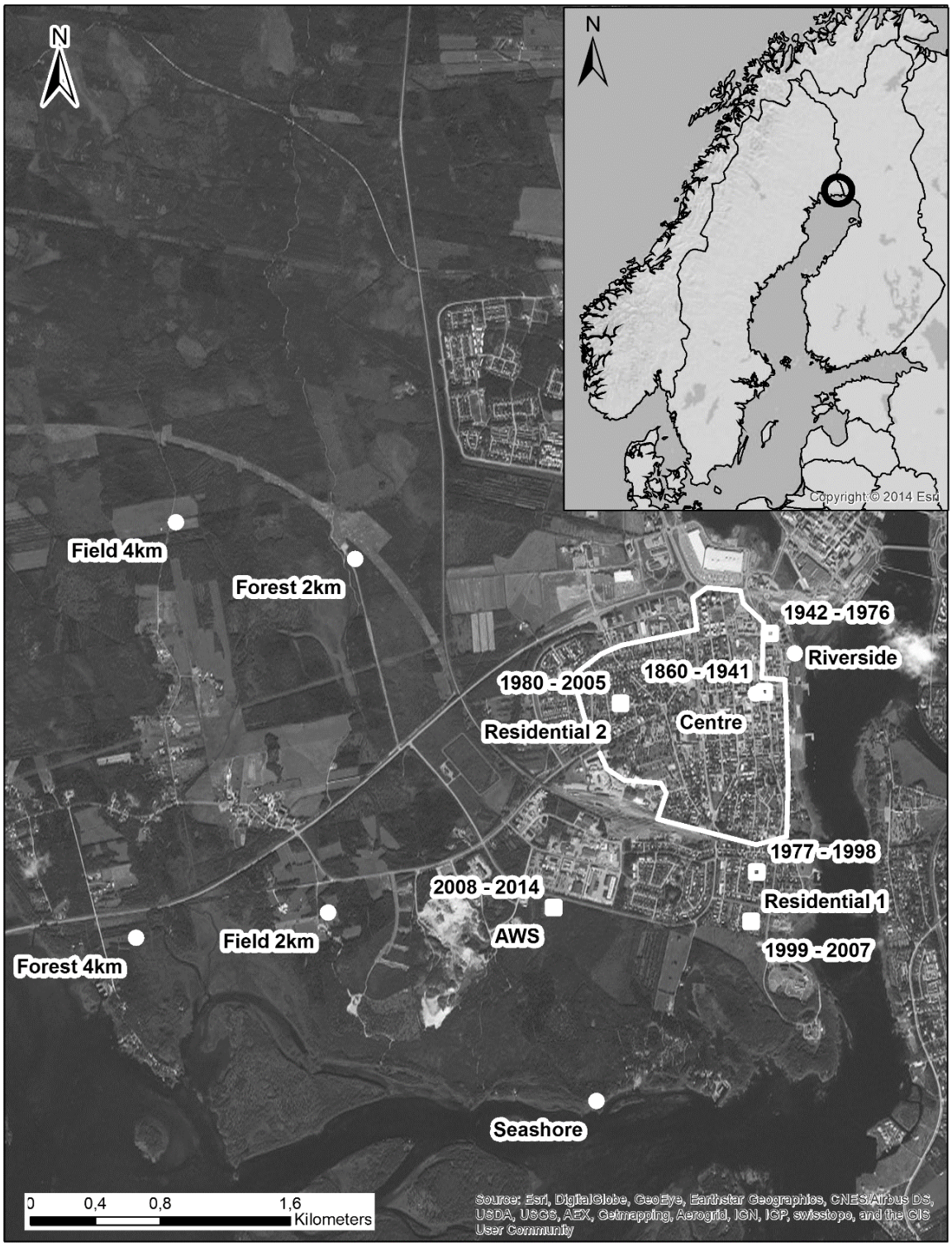

Figure 4-1 Meteorological station (white squares) and sensor locations (white dots) in Haparanda. Dates indicate periods of historical station positions including overlap periods among residential sites. AWS is the current station location. An outline of the urban area 1946 is displayed as well (white line). *Maps from ESRI 2014.*

4.2.2 Met station history

Meteorological measurements in Haparanda were initiated in 1859, making this one of the longest continuous temperature records in subarctic regions. However, metadata indicate

several relocations within the village. For the first 83 years of operation, the station was located in a north-facing window cage on a wooden house in the village centre. It then moved to a free-standing screen in a nearby, less urbanized riverside location (where several minor moves took place), where measurements were performed from 1942-1976. Between 1977 and 2008, the station moved to three different residential locations, before it arrived at its current location outside the residential area (Table 4-1, Fig. 4-1). The station measurements in the residential areas were used in parallel as well as combined to form the Haparanda series during that time. Several changes in the observing staff took place but since this is poorly documented, it was not taken into account. Certainly, changes in instrumentation have taken place as well but no information on this is available either.

	LOCATION	SITE DESCRIPTION	ALT	PERIOD
MET STATION	Village Centre	Instruments in cage outside a window of a north facing wall of a wooden house, small wooden buildings and some vegetation around, paved streets and walkways	4m	1859 - 1941
	Riverside	Station on lawn next to customs station, near town centre, next to the riverside	2m	1942 - 1976
	Residential area 1	Residential area, lawn, small houses with backyards	4m	1977 – 1998 1999 - 2007
	Residential area 2	*Parallel station! Residential area, lawn, small houses with backyards*	*10m*	*1980 - 2005*
	AWS	AWS station, outside city (about 200m away from buildings), on grass/gravel next to forest	9m	From 2008 on
U23 SENSORS	Village Centre	On lamp post on lawn, small wooden buildings and some vegetation around, paved streets and walkways	5m	From 2013 on
	Riverside	On lamp post on lawn, next to riverside, grass surrounding spot, greater buildings in some distance	2m	From 2013 on
	Residential area 1	On old met station post in garden with lawns and small wooden houses around	4m	From 2013 on
	Residential area 2	On tree in backyard with lawns and small wooden houses around	10m	From 2013 on
	AWS	On gate of AWS, outside city (about 200m away from buildings), on grass/gravel next to forest	9m	From 2013 on
TIDBIT SENSORS	Seashore	On tree 15m away from sea, wet ground, forest/bushy area	1m	From 2013 on
	Field 2km	On small tree in ditch with some more trees between fields with high grass, 1km away from sea	8m	From 2013 on
	Field 4km	On small tree in ditch with some more trees between fields with high grass, 4km away from sea	10m	From 2013 on
	Forest 2km	On tree in forest, widely spaced large trees, bushes and tall grass in openings, 3km away from sea	10m	From 2013 on
	Forest 4km	On tree in forest, widely spaced large trees, bushes and tall grass in openings, 0.5km away from sea	4m	From 2013 on

Table 4-1 Previous station locations (top), current sensor sites for the assessment of the urban bias (middle) as well as sensors depicting the rural surroundings (bottom) in Haparanda.

The complete temperature dataset as well as all metadata was provided by the Swedish Meteorological and Hydrological Institute (SMHI). The metadata consists of archived protocols written by the observers as well as reports written by people at the SMHI supervising the measurements and the observers. Mean monthly temperature data derived from daily averages showed no gaps since the beginning of the measurements, whereas minimum and maximum temperatures are missing between 1951 and 1960. Before 1914, the daily average was calculated using the Edlund formula ([T08 + T14 + 5*T21] / 7) whereas from then on, the Ekholm-Modéns formula was used ([aT07 + bT13 + cT19 + dTx + eTn] / 100; coefficients included are based on the respective month and geographical position of the met station - see Moberg and Bergström (1997) for details). Since the installation of AWS, daily average is calculated as the arithmetic mean of all measured values. Even though several studies show that a change in calculation of mean temperatures might cause inhomogeneities (e.g. Tuomenvirta, 2001; Begert *et al.*, 2005), Moberg and Bergström (1997) reject that there is a considerable impact, at least in case of the Swedish temperature data they worked with.

4.2.3 Application of HOMER for bias identification

The homogeneity of the Haparanda record was tested using the HOMER package in "R" (Mestre *et al.*, 2013). HOMER is based on the comparison of different climate stations, and the application of the program requires several data processing steps. The Haparanda dataset was used as candidate time series, and reference data were downloaded from the SMHI explorer (SMHI, http://opendata-catalog.smhi.se/explore/) and KNMI explorer (KNMI, http://climexp.knmi.nl/). The original data are provided by the Finnish, Swedish and Norwegian meteorological services. In order to acquire suitable reference station data, a search radius was applied with Haparanda as its centre. Due to a lack of sufficient data close to Haparanda, the radius needed gradual adaption. Finally, 22 stations within a range of 500km distance to Haparanda were found which could be used for analysis, including four stations that reach back to before 1880 (see Fig. 4-2).

Figure 4-2 Haparanda and reference stations (black dots) used for the homogenization attempt with HOMER. The starting dates of operation are given as well.

We used the HOMER break point detection to search for shifts within the time series. HOMER is capable of performing a pairwise detection as well as a joined detection when comparing the time series provided by the user. Breaks are detected based on statistical tests (like students t-test, maximum likelihood ratio) which check for a significant change in the data. This is coupled with an optimization scheme to assess the position most probable for the break, a moving window approach being one possibility for such a procedure (Venema *et al.*, 2012a). As a second step, we compared the findings with the relocation dates from the Haparanda metadata to check for compliance.

Unfortunately, the application of HOMER did not provide reliable indications of any relocation break points or environmental influence when performing both detection methods. Reasons for this are the great distances between Haparanda and the reference stations, the various climates included such as maritime and continental as well as the fact that there are too few records reaching back in time as long as they should in order to enable a good comparison. In addition to that, if there were break points of minor size, HOMER might not detect them since it is more moderate in terms of identifying inhomogeneities. This approach was therefore abandoned.

4.2.4 Temperature sensor network

In order to examine the potential relocation bias in the Haparanda temperature record, a network of temperature sensors (HOBO Pro v2 U23-001 in radiation shields RS1, Onset Computer Corporation, Bourne, MA 02532, USA) was installed considering the historical station locations (see Table 4-1). Due to construction changes at the previous station locations, some adaptions had to be made. While the living house of the first station location (1859-1942) is still there, it was not possible to re-install a sensor at the window cage where the original measurements took place. Instead, a sensor was placed on a free-standing lamp post 40 meters away from the original site. At the second location (1942-1977), several buildings were constructed since the met station was located here and the sensor was placed in a location ~100 m to the east, to resemble the description of the site according to meta-data. Since two of the three residential areas are practically identical to their appearance back in 1977, we simply placed the sensors close to the original station locations. The third residential site did change, however, but since this site closely resembled the first residential area, no additional sensor was deployed there and it will not be dealt with separately in the following.

All sensors were set to record a sample every 30min. Analysis of a pre-deployment 22 day inter-instrument comparison, over a −4 to 18°C range, found the mean difference based on 10 minute data to be <0.05°C, with <5% exceeding ±0.1°C (max. 10 min difference is 0.3°C). These inter-sensor differences are neglected as they are rather small. Data from this sensor network was collected between 01.07.2013 and 30.06.2015 (data collection is on-going) generating a total of two complete years used in analysis in this paper.

In addition, smaller temperature sensors (HOBO Tidbit v2 Data Logger, Onset Computer Corporation, Bourne, MA 02532, USA) were placed in several locations around Haparanda in order to assess the rural temperature variability. These sensors measure with the same accuracy and frequency as the U23 sensors. However, the Tidbit sensors were only protected from direct insolation by a white plastic cover which is directly applied to the sensor. In order to minimize

radiation influences, only the night-time (minimum) temperatures were taken into account in this analysis. In total, five such sensors were installed in the outlying rural areas of different openness (forest/field), two in the north-west of Haparanda in 2 and 4 km distance to the village, and three in the south-west towards the Baltic Sea to capture potential maritime influences in 1 and 3 km distance as well as one at the shoreline (see Fig. 4-1, Table 4-1).

4.2.5 Data analysis

The half-hourly sensor data were averaged to daily mean temperature (TM), and the lowest and highest of the 48 measurements each day were used to define the daily minimum (TN) and maximum (TX) temperatures, respectively. Actual maximum and minimum temperature may occur between the half hour measuring intervals, resulting in a small negative bias for TX and a small positive one for TN. Due to logger storage limitations, it was not possible to achieve a higher temporal resolution and avoid this problem. TM, TN and TX were then used to calculate seasonal and annual averages. The monthly values were subsequently used to assess and correct the long station record, which is only available at monthly resolution. Besides, these allow a good graphical presentation of differences throughout the year.

As the current automatic weather station (AWS) is situated outside the village to avoid urban influence (Andersén, 2010), the corresponding sensor (U23) was chosen as a reference. To evaluate the AWS U23 as a rural reference, its monthly data were compared with the Tidbit sensors surrounding the village. This was done by calculating the residuals from the mean of all rural sites considering night-time (minimum) temperatures to avoid radiation biases:

$$\Delta T_{min(site)} = T_{min(Tidbit\ site\ or\ U23\ AWS)} - T_{min\_average(all\ sensors)}$$

As a second step, the difference between each former met station site and the AWS location was calculated:

$$\Delta T_{max/avg/min(site)} = T_{max/avg/min(site)} - T_{max/avg/min(AWS)}$$

A pairwise t-test was performed to evaluate whether sensor differences are significant. The method was chosen according to a similar comparison of parallel measurements (Gallo, 2005). Monthly and seasonal confidence intervals (CI) were calculated for every sensor considering 95% confidence levels (CL).

4.2.6 Correction for relocation bias

The differences among the monitored historical met station sites were used to correct for the relocation bias in the long station record (Fig. 4-3). The current location (AWS, 2008-2014) is considered free of urban influences and no correction was applied. The previous Residential 1+2 (1977-2008) and River sites (1942-1977) were corrected considering the temperature residuals between the representative sensors and the AWS site in order to account for the UHII. However, this simple way of generating a correction factor was not applicable to the initial station location. Considering the history of Haparanda, the village centre was already constructed at the time of station installation in 1859, but the urban area around the site grew substantially during the following 82 years of operation at this site. To account for this urban growth, half of the calculated difference between the centre sensor and the AWS sensor was regarded to be existent from the beginning on, the other half gradually added in the following years, with the intent of representing the increase in urban influence. This is a rather crude method of accounting for the urban bias in the early part of the long Haparanda record, but the lack of metadata information and parallel measurements prevent validation of other, more sophisticated, approaches. Furthermore, the initial Haparanda station was installed in a window cage, making an additional temperature bias, for example due to anthropogenic heat release, likely. Due to a lack of metadata, this bias is not addressed in this study, but this type of issues are common in early observational records and should be considered when relying on long term data.

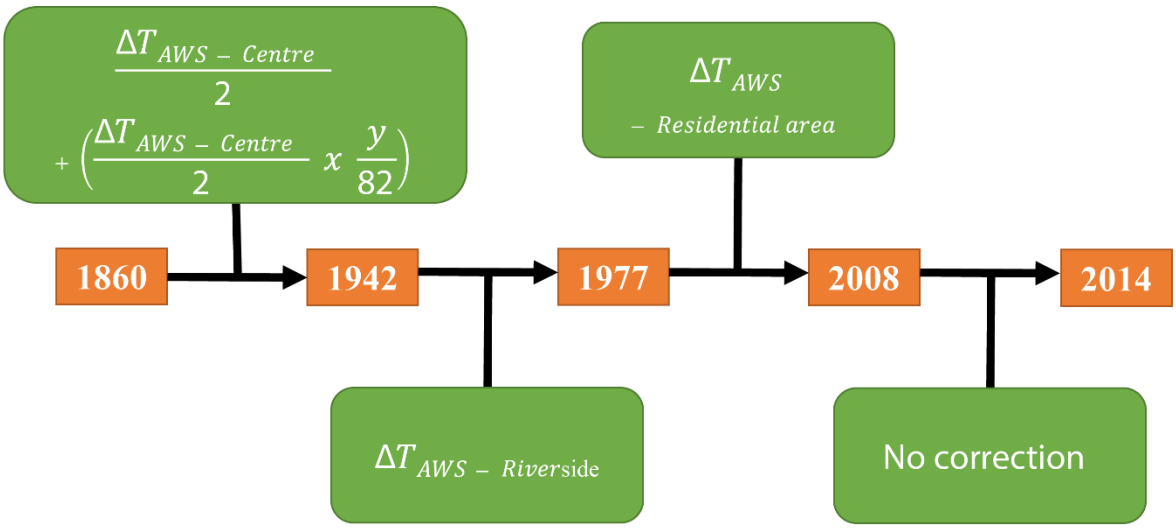

Figure 4-3 Correction of the relocation bias based on parallel sensor measurements in Haparanda. The long record starts in 1860 with the first year of complete data and was subsequently adjusted with regard to the following three major relocations.

4.3 Results

4.3.1 Haparanda temperature differences

In order to assess the rural temperature patterns and to evaluate the U23 sensor installed at the AWS as a rural reference, monthly TN of the AWS and Tidbit sensors are plotted as anomalies from the average of all sensors (Fig. 4-4). The most striking deviations are the high sea shore temperatures, and the low inland field temperatures in about 4km distance to the village. The seashore site was particularly warm in July (1.5 ± 0.3°C) and August (1.7 ± 0.3°C) whereas in winter the differences are much smaller. The 4km field site is on average 1.4 ± 0.3°C colder than the mean of all sensors reaching a maximum in August of 2.2 ± 0.3°C. However, the 4km forest site, located just 500 m from the seashore, is instead consistently warmer (annual average 0.4 ± 0.1°C), even though the differences from the mean of all data are not always significant. The 2km field and 2km forest sites show smaller residuals (all months ≤ 0.5°C), though they display inverse patterns, with the field being slightly warmer in summer and cooler during the other seasons. The AWS temperatures are similar to the mean of all sensors, with only 3 months deviating significantly.

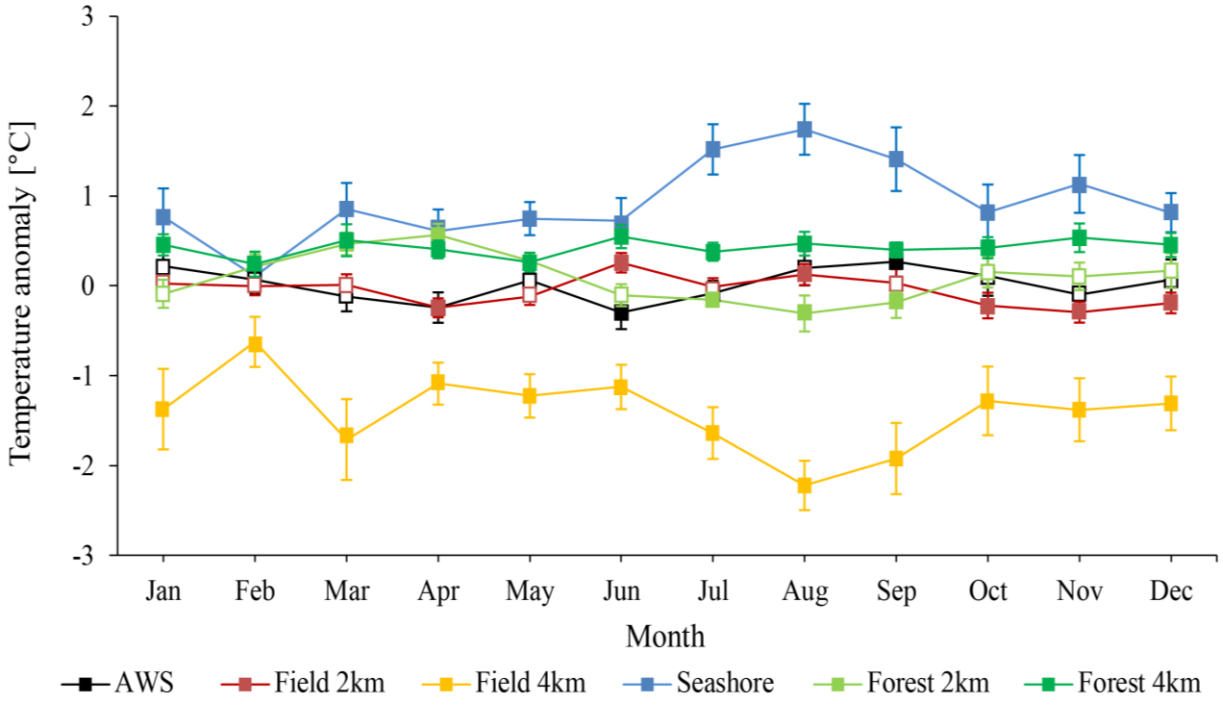

Figure 4-4 Seasonal pattern of temperature deviations recorded at Haparanda sensors over two years. Monthly temperatures shown as anomalies from the mean of all sensors. Error bars display the variance as 95% confidence intervals. Filled squares mark significant deviations.

In order to examine potential differences associated with the relocations of the Haparanda met station, the TX, TM and TN residuals relative to the modern AWS site were analysed (Fig. 4-5). The differences vary both seasonally and diurnally and are most pronounced in summer and during night (TN). In TM and TN, every former station location displays positive monthly deviations, revealing the UHII. The village centre is characterised by maximum deviations reaching 2.2 ± 0.5°C and 0.8 ± 0.1°C in July TN and TM, respectively. The riverside sensor shows TN to be similar to the centre during warm season but different values in the cold season. In comparison to AWS, the residential area is ~0.4 ± 0.2°C warmer throughout the year. In general, TN and TM patterns are relatively similar considering all sensors, with TM displaying less pronounced differences.

A comparison of maximum temperatures at the centre and river sites reveals a larger difference in summer compared to winter, obviously showing a distinct seasonal dependence. The riverside is more than half a degree cooler than the AWS site in summer, but deviates by just 0.1-0.2 ± 0.2°C from December to February. The centre shows temperatures similar to the AWS site, with the largest deviation equal to 0.3 ± 0.1°C in November, and no other monthly value exceeding 0.2°C. Regarding the residential areas, the pattern is similar with temperatures deviating no more than 0.2 ± 0.2°C in any month when compared to the AWS. Overall, the deviations are largest in the minimum temperatures, less so in mean and maximum temperatures, with the AWS being constantly cooler than all sites regarded with the exception of the warm season in TX.

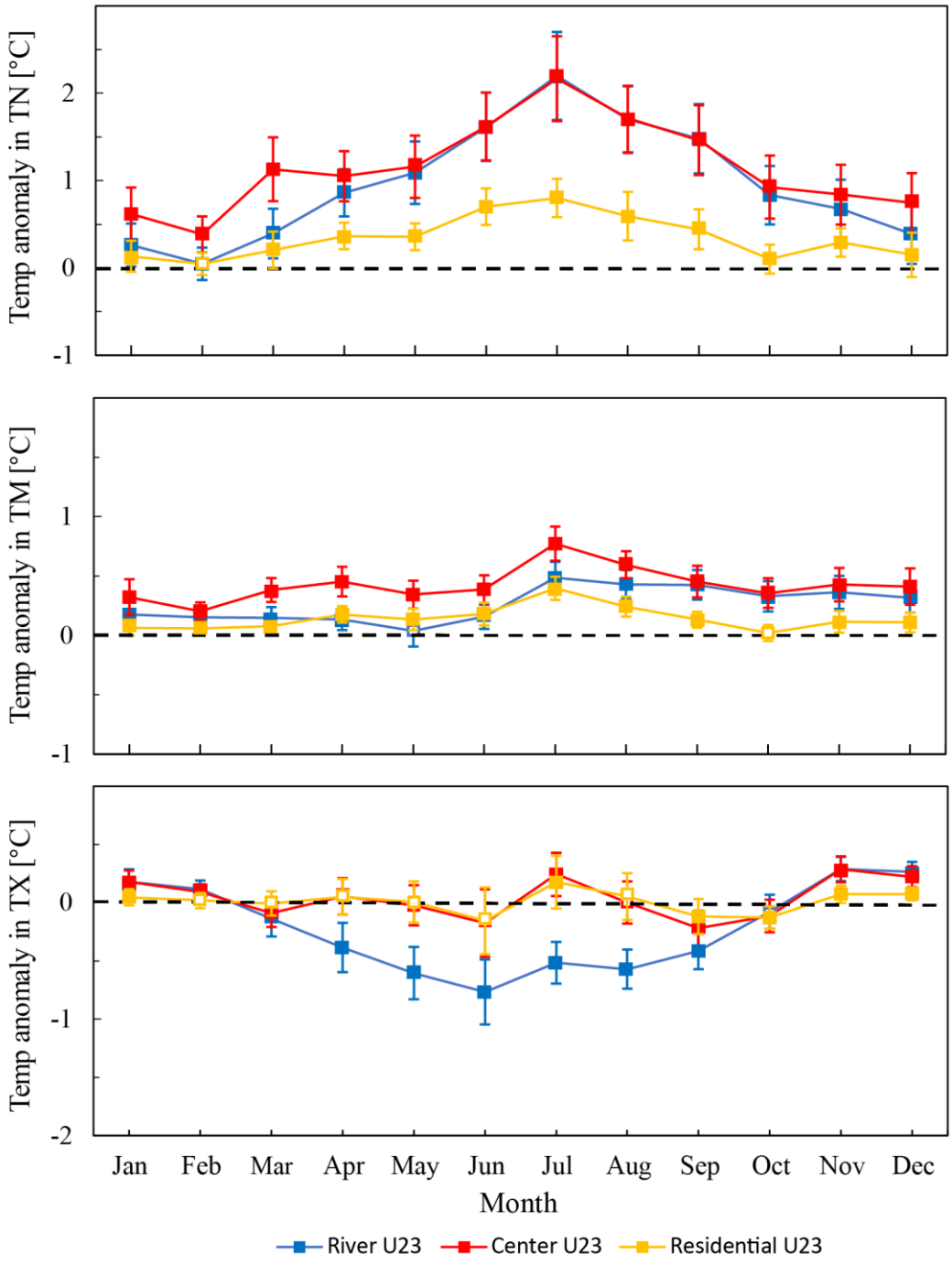

Figure 4-5 Temperature residuals between the historical thermometer locations and the current AWS station location. Monthly TX, TM and TN deviations including 95% error bars calculated over two years are shown. The residential values are an average of two sensors. Significant deviations are displayed as filled squares.

4.3.2 Adjustment of the long Haparanda station record

The relocation bias in the long temperature series is removed for each month using the temperature residuals from sensor network (as detailed in Fig. 4-3). A seasonal overview is presented in the following (Fig. 4-6), considering monthly mean, minimum and maximum

temperatures. Furthermore, an exemplary course of the residual applied to the time series is displayed later (Fig. 4-7).

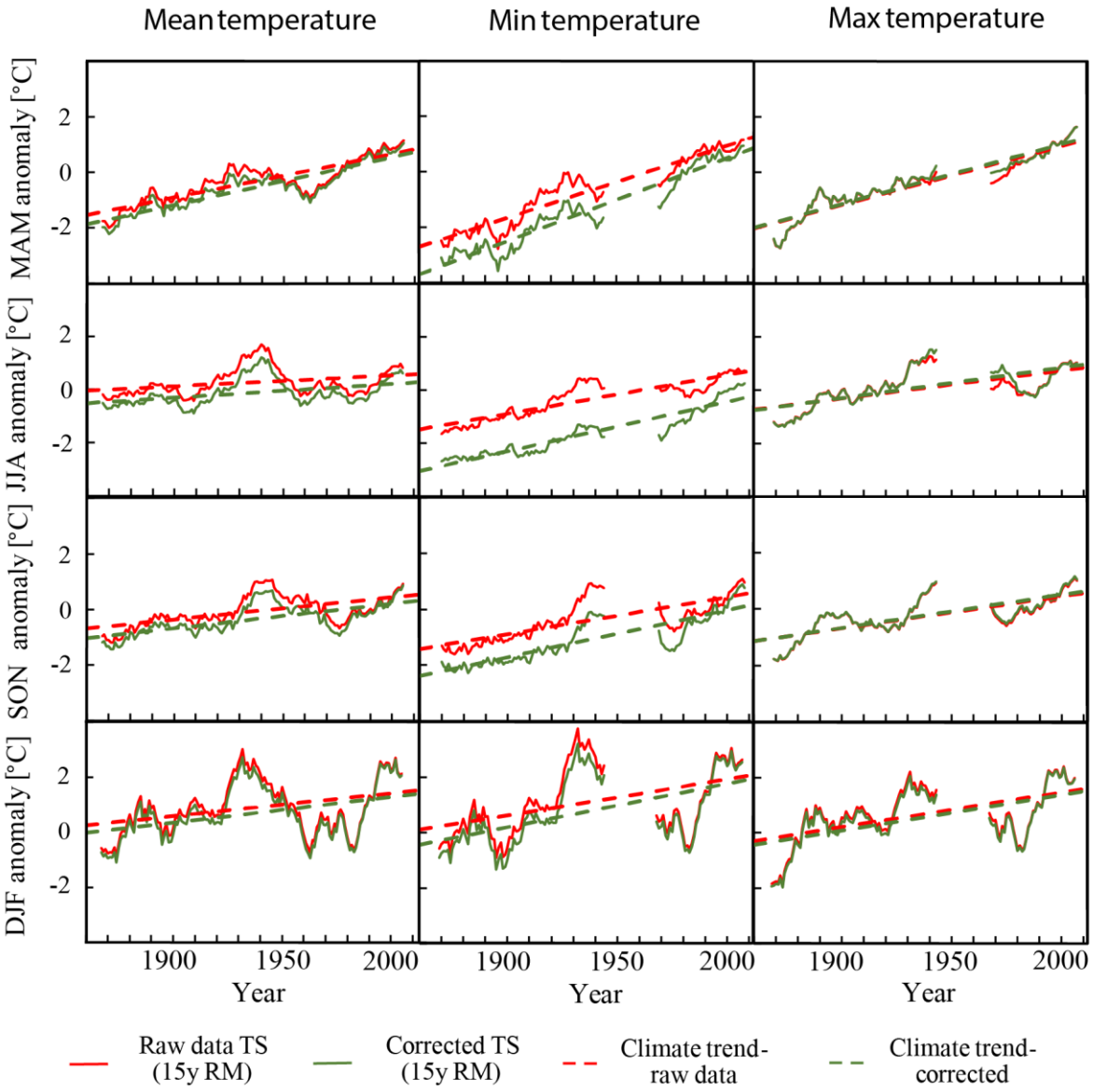

Figure 4-6 Raw and adjusted seasonal TM, TN and TX time series of the long Haparanda station. Curves are smoothed using a 15-year running mean, dashed lines display linear trends over the period 1860 - 2014. Temperatures are plotted as anomalies relative to the climate period from 1961 - 1990. The gap in TN and TX is due to missing data.

The correction generally lowered the temperatures, implying that the measured values were too high before (see Fig. 4-6). As the UHII is most pronounced in the village centre (station location 1859-1942), slightly lower at the riverside (1942-1978), and lowest in the residential area (1978-2008), the difference between raw and adjusted values decreases gradually towards present. The UHII was strongest during summer and in TN, and smallest during winter and in maximum temperatures. One exception to this pattern was found at the riverside location in

spring and summer TX, revealing a slightly positive correction and hence the corrected time series to appear above the original one during that time. As the bias is larger in the earlier part of the record, the warming trend of the corrected data increased compared to the uncorrected (Table 4-2). This was most pronounced in TN where the annual trend rose from 0.18°C/10years to 0.21°C/10years over the whole period of 155 years. As consequence to the corrections made, the new trends show the largest increase in summer and the least in TX.

PARAMETER	SPRING	SUMMER	AUTUMN	WINTER	YEAR
			Uncorrected		
TX	0.23	0.11	0.14	0.15	0.16
TN	0.26	0.15	0.14	0.14	0.18
TM	0.17	0.04	0.10	0.11	0.11
			Corrected		
TX	0.23	0.13	0.14	0.16	0.17
TN	0.29	0.18	0.17	0.17	0.21
TM	0.19	0.06	0.11	0.12	0.12
			Difference		
TX COR-UNCOR	0.00	0.02	0.00	0.01	0.01
TN COR-UNCOR	0.03	0.03	0.03	0.03	0.03
TM COR-UNCOR	0.02	0.02	0.01	0.01	0.01

Table 4-2 Trends in corrected and uncorrected seasonal and annual TX, TN, and TM time series. Temperature trends in °C/10years calculated over the period 1860-2014 are shown.

The trends for the period from 1901 to 2000 were analysed as well. The overall pattern proofs to be similar to the 155 year period already discussed, indeed displaying more severe differences regarding the trends. An annual trend increase by 0.07°C/10years and 0.09°C/10years in summer could be observed for TN, respectively. Comparing the corrected and the original record revealed a substantial rise in trend of 0.03°C/10years in annual mean temperatures, resulting from the strong correction in the early part of the record. Only maximum temperatures show no difference if the 20th century is considered instead of the whole 155 year record.

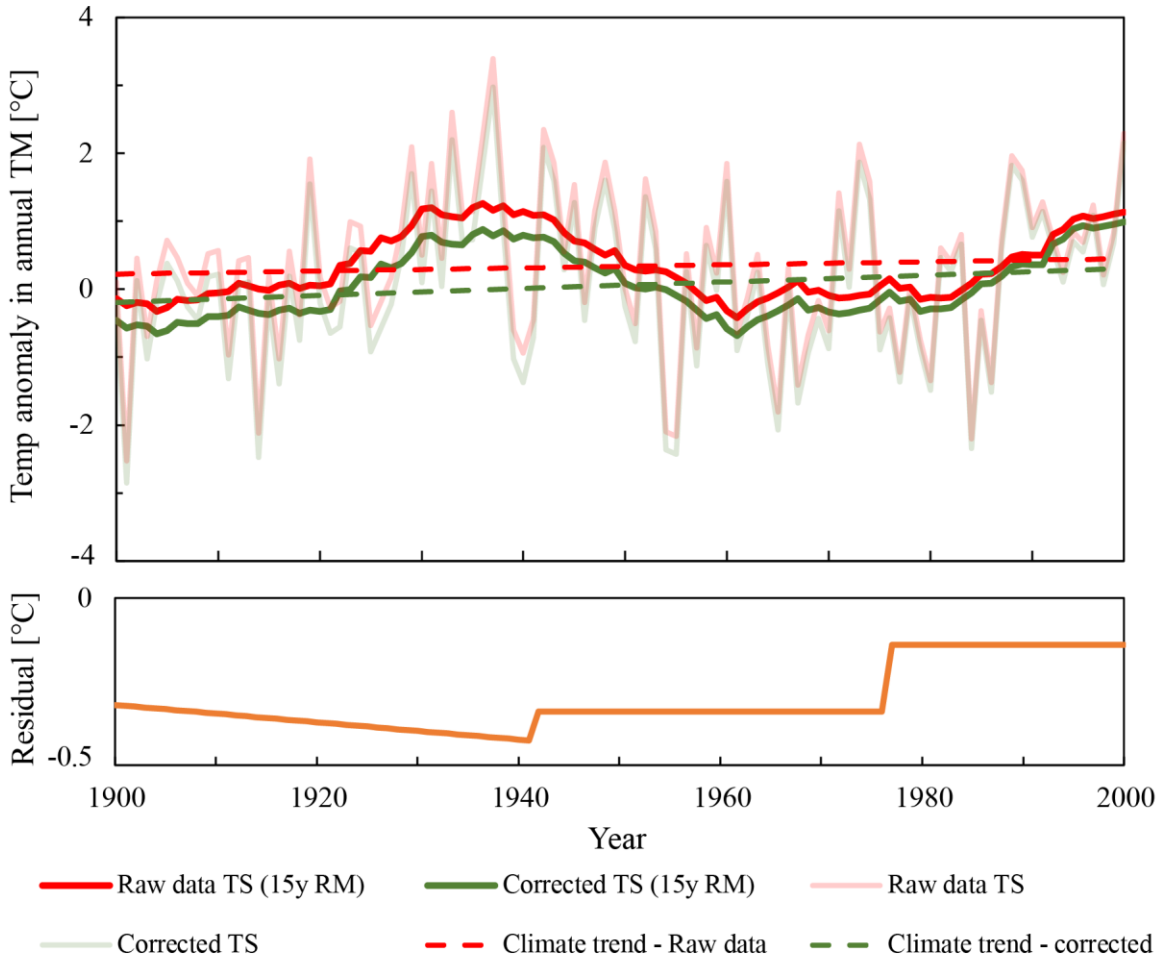

Figure 4-7 Raw and adjusted annual mean temperatures of the Haparanda station record with smoothed curves as a 15-year running mean. Dashed lines display linear trends over the period from 1901 - 2000. Temperatures are plotted as anomalies relative to the climate period from 1961 - 1990. The residual used for obtaining the corrected series is shown below.

4.4 Discussion

4.4.1 Suitability of the rural reference

The comparison of the temperature sensors revealed a significant thermal variability in the village of Haparanda as well as in its rural surroundings, with most pronounced differences in summer nights (TN). As one of the objectives of this study was to identify UHI, identification and verification of a representative rural reference is crucial. Temperature variability within pre-defined rural areas can, however, be substantial, e.g. due to changing land cover as well as vegetation type, height and density (Grimmond *et al.*, 1993; Hawkins *et al.*, 2004; Lindén, 2011; Lindén *et al.*, 2015b). In addition, the increased heat capacity of water can have moderating effects on rural temperature variability (Oke, 1987). Since the landscape is flat without any abrupt changes in altitude, the topography is assumed to be insignificant in the analysis.

These influences also seem to be important in Haparanda, where the seashore location showed considerably higher TN than the other rural stations. The considerably lower TN in the open inland field compared to the forested sites indicated radiative cooling to be an important factor of rural temperature variability as well (Hawkins *et al.* (2004). The site of the current AWS in Haparanda, surrounded by a young forest stand and installed according to standard protocol for AWS stations (Andersén, 2010), did not differ significantly from the rural mean TN. We interpreted this as proof of no indication of urban influences on the current AWS site. This conclusion is, however, limited as the rural variability of TM and TX could not be examined in the rural network since direct insolation effects on the Tidbit sensors bias the results. As the spatial differences in the urban sensor network is most pronounced in TN, it appears likely tough that the deviations from the rural mean are similar or lower in TM and TX, implying that the AWS sensor is area-representative as a rural reference.

4.4.2 Determining the urban bias

The analysis of a sensor network over two years revealed a significant long term bias in Haparanda due to differing UHII in relation to the AWS as a rural reference. This bias is not confined to a certain season but persistent throughout the year. As frequently reported in urban climate studies, the UHI was most pronounced in the urban centre, and decreased with building density (e.g. Stewart and Oke, 2012). In line with existing evidence (Klysik and Fortuniak, 1999; Morris *et al.*, 2001; Huang *et al.*, 2008), UHI is also most pronounced in minimum temperatures during summer. The long-term summer urban TN bias in Haparanda (1.8°C) equals approximately half of the summer UHI reported from large cities under optimum conditions such as Lodz, Poland; 700,000 inhabitants (Klysik and Fortuniak, 1999) and Melbourne, Australia; 4,000,000 inhabitants (Morris *et al.*, 2001), and approximately one-third of the ΔTM found in the town of Hania, Greece; 100,000 inhabitants (Kolokotsa *et al.*, 2009), even though not being directly comparable due to different measurement procedures. This shows that the influence of the urban area on temperatures needs to be carefully considered also for smaller urban settlements.

The town of Tornio, population 22 000, is located on the Finnish side of the Torne river across from Haparanda, with a small commercial centre 500 m towards north east of the sensor placed by the river and could thus potentially influence temperatures. However, the population density of Tornio is very low, 18 inhabitants/km^2 for the whole municipality and the actual population in the near vicinity of the measurements used in this study is very low as well. A study by (Lindén *et al.*, 2015a) found significant correlations between mainly non-urban temperatures and built/paved elements in the surroundings up to a distance of 1000 m, and source areas

between 30 – 500 m have been found to be most representative in studies of the urban climate (Hart and Sailor, 2009; Li and Roth, 2009; Yokobori and Ohta, 2009; Lindén, 2011). Tornio has a low population density and in combination with its location > 500 m downwind it is assumed to not have a significant influence on the climate of Haparanda.

In sub-arctic Haparanda, strong summertime solar radiation generates spatially heterogeneous heating of paved and vegetated surfaces during daytime. This is emphasized by a non-existing sunset for most of June. Even in July and May, the duration of a day is never below 17 hours. The differing radiation absorption along with the heat capacity are the basis of the severe site-specific differences in nocturnal cooling. As the mid-winter sun rises only about 3° over the horizon in Haparanda and daylight is limited to less than 5 hours, impact of direct and diffuse solar radiation is minimal during the cold season. The smaller, but still significant, bias found in winter (TX = 0.2, TM = 0.3, TN = 0.6°C) likely results from anthropogenic heat release, as is also reported both in the small village of Barrow (population: 4,200), Alaska (Hinkel and Nelson, 2007) but also in the large city of Seoul (population: 10,000,000), Korea (Kim and Baik, 2005).

The sensor placed at the Haparanda riverside is located downwind from the village centre considering the prevailing wind direction (Bergström, 2007). The TN bias found at this site is thus likely a combination of warming from the central urban area as well as a result of the water energy balance particularly during summer and autumn. The lower winter and spring TM/TN bias at the riverside is likely due to the fact that the river is frozen from late autumn until May (see Persson, 2012). The cold bias in summer TX is likely due to the greater thermal capacity of the water, moderating daytime warming (Hathway and Sharples, 2012). The slightly cooler TN in winter is explained by the sensor's location further away from buildings (~35m) and reduced wind protection supporting air mass exchange and cooling (Bonan, 2000; Benzerzour *et al.*, 2011). In the residential area, the mix of rural and urban elements generates a lower, but still significant urban bias, as also found in Toulouse (population: 450,000), France (Houet and Pigeon, 2011, http://www.ncbi.nlm.nih.gov/pubmed/21269746), for example.

Since the sea proved to be an important factor for local temperature pattern, the sites within Haparanda and the AWS site outside the village might be influenced differently according to their distance to the seashore, even though they are several kilometres away. Therefore, a difference in temperature between these locations might not exclusively be caused by the degree of urbanization in their vicinity. With increasing proximity to the sea, a compensatory impact for urban warming is likely to occur, though the extent might be limited due to the existing

distance. Nevertheless, the correction succeeds in eliminating the relocation bias no matter the source.

4.4.3 Adjusting the long Haparanda temperature record

The results from the sensor network demonstrated a significant urban warming in a small urban settlement. The categorization of village met stations as "rural" in global databases (e.g. NOAA, ftp://ftp.ncdc.noaa.gov/pub/data/ghcn/v3/), implying that data from those locations are free from urban biases, needs to be reconsidered, at least for Northern Europe. Our sensor measurements indicate that the repeated relocations of the Haparanda station have gradually reduced the bias caused by different UHII, and a removal of relocation bias, even though strengthening the warming trend, is thus needed to improve data reliability.

The identification and adjustment of relocation bias is not feasible using classical homogenization tools, such as HOMER, due to the lack of suitable long reference station records in its vicinity. The application of HOMER to the Haparanda station record revealed no break points that are in line with meta-information. The only way to handle relocation biases in such an environment seems to be a monitoring of spatial temperature patterns by running a detailed network of temperatures sensors as done in this study.

This basic correction approach based on parallel measurements mounted at the old met station locations has some weaknesses. The correction procedure applied here is based on the assumption that the sensor measurements are representative for the UHII throughout station history. Historical maps and photos were used to evaluate the building structure and land cover, indicating very similar and partly identical structures since the first relocation in 1942. Analysis of this meta-information also demonstrated that urban growth has taken place at the outskirts of the village, indicating that our sensor measurements are representative for this period. Population growth may have generated an increased anthropogenic activity including traffic. However, Haparanda has long been a centre for trade, with high activity in the village centre throughout the 20th century, and traffic has in previous studies proven to have very limited influence offside the main roads (Pigeon *et al.*, 2007), and is therefore unlikely an important heat source in the small centre of Haparanda. Historical photographs and maps also show that during the initial 82 years of the Haparanda record the village centre structure was already similar to today, though this period is likely to have seen considerable changes in street paving and the heating of buildings. The gradual increase in impermeable ground (e.g. paving of streets) up until the 1940s would likely affect the urban energy balance to some extent. However, since the sensor was placed on a lamp post above a meadow and the old station was

installed outside a house above a meadow as well, the direct influence of the surrounding ground cover is not causing a bias. During the course of the Haparanda station changes, alterations in the anthropogenic heat sources are also likely to have occurred. Information that would enable correction for this potential anthropogenic bias is unfortunately not available but it can be argued that for example an increased domestic heating today is likely compensated by improved isolation in modern buildings. Furthermore, the influence of anthropogenic sources on temperatures have been found very limited outside of dense urban centres, especially when all weather conditions are regarded (Allen *et al.*, 2011). Since historic sources (see chapter 2.1) indicate that building structure and human activity in the village centre was relatively similar at the initiation of the Haparanda station an influence on urban temperatures likely existed in the village centre from the start. However, due to the growth in surroundings as well as changes in surroundings and activity, the bias at station initiation was not likely of the same magnitude. In order to avoid an over-estimation of the bias, it was therefore assumed to equal only 50% of the current urban bias at the station's initiation in 1860, and gradually increasing to reach 100% at the time of relocation in 1942. This simplistic approach reduces the risk of overestimating the early bias. It is possible, however, that the window cage placement in the original location caused some additional warm bias due to building heat leakage and insolation effects, particularly during summer, but such biases can only be handled usefully by parallel measurements (Böhm *et al.*, 2009). For instance, Nordli *et al.* (1997) found no effect on winter TM in their Nordic dataset for instruments having been moved from a window cage to a free-standing screen, but a rise in summer TM of 0.0-0.3°C.

In Haparanda, the relocation bias is consistently negative, and homogenization led to an increased temperature trend in minimum temperatures by up to 0.3°C/10y over the whole met station measurement period. A consistently negative relocation bias was also found in an North Atlantic climatological dataset (Tuomenvirta, 2001), and an increased temperature trend after homogenization has been reported in Switzerland (Begert *et al.*, 2005), Spain (Brunet *et al.*, 2006), China (Yan *et al.*, 2010; Yang *et al.*, 2013) and Iran (Rahimzadeh and Zavareh, 2014), for example. Since meteorological stations generally moved from centres to the outskirts or out of the urban area, the gradual warming caused by steady urbanization which enhances the warming trend is reduced. Relocation procedures are usually accomplished to reduce the urban influence and as a result, the original time series contains less urban warming towards present. By correcting for the relocation bias, the UHII bias is recovered in the adjusted dataset, thus resulting in an increased warming trend (Zhang *et al.*, 2014). This study shows that also smaller

urban settlements such as towns and villages need to be carefully evaluated to avoid an UHII bias in long term temperature trends.

4.5 Conclusions

Based on two years of parallel measurements at ten locations, a substantial UHI was found in the village of Haparanda in northern Sweden. The UHII increases towards the village centre and is strongest in minimum temperatures during summer. The analysis of historical locations of the Haparanda meteorological station shows that the long temperature record from this village contains a bias caused by station relocations from the urban centre towards the outlying forest area, reaching 1.8°C in summer minimum temperatures and 0.4°C as an annual mean. We here used the temperature residuals between the different station locations to remove the relocation bias from the 155-year Haparanda record. Since the bias is stronger during earlier periods, data homogenization increased the warming trend in the temperature record by up to 0.03°C/10y over the whole period. As efforts to reduce non-climatic influences on met stations records generally increased towards present, it is possible that similar trend-limiting biases are inherent to other relocated station records. This specific homogenization method is time consuming and requires detailed monitoring data, and is therefore not applicable to large scale datasets. However, the Haparanda example might indicate that relocation biases are also important in records from other smaller towns and villages, and shows how such biases can be adjusted without relying on nearby reference stations.

4.6 References

Aguilar E, Auer I, Brunet M, Peterson TC, Wieringa J (2003). Guidelines on climate metadata and homogenization. *WMO/TD* **1186**.

Allen L, Lindberg F, Grimmond CSB (2011). Global to city scale urban anthropogenic heat flux: model and variability. *International Journal of Climatology* **31**: 1990-2005.

Andersén M (2010). Allmän beskrivning av OBS2000-stationerna. Norrköping, Sweden, Swedish Meteorological and Hydrological Institute (SMHI).

Arnfield AJ (2003). Two decades of urban climate research: a review of turbulence, exchanges of energy and water, and the urban heat island. *International Journal of Climatology* **23**: 1-26.

Auer I, Böhm R, Jurkovi A, Orlik A, Potzmann R, Schöner W, Ungersböck M, Brunetti M, Nanni T, Maugeri M, Briffa K, Jones P, Efthymiadis D, Mestre O, Moisselin J-M, Begert M, Brazdil R, Bochnicek O, Cegnar T, Gajic-capka M, Zaninovi K, Majstorovi e, Szalai S, Szentimrey T, Mercalli L (2005). A new instrumental precipitation dataset for the greater alpine region for the period 1800-2002. *International Journal of Climatology* **25**: 139-166.

Begert M, Schlegel T, Kirchhofer W (2005). Homogeneous temperature and precipitation series of Switzerland from 1864 to 2000. *International Journal of Climatology* **25**: 65-80.

Benzerzour M, Masson V, Groleau D, Lemonsu A (2011). Simulation of the urban climate variations in connection with the transformations of the city of Nantes since the 17th century. *Building and Environment* **46**: 1545-1557.

Bergström H (2007). Wind resource mapping of Sweden using the MIUU-model. *Wind Energy Report*. Uppsala, Sweden, Uppsala University.

Böhm R, Jones PD, Hiebl J, Frank D, Brunetti M, Maugeri M (2009). The early instrumental warm-bias: a solution for long central European temperature series 1760–2007. *Climatic Change* **101**: 41-67.

Bonan GB (2000). The microclimates of a suburban Colorado (USA) landscape and implications for planning and design. *Landscape and Urban Planning* **49**: 97-114.

Brunet M, Saladié O, Jones P, Sigró J, Aguilar E, Moberg A, Lister D, Walther A, Almarza C (2006). A case-study/guidance on the development of long-term daily adjusted temperature datasets. *WMO/TD* **1425**.

Dimoudi A, Nikolopoulou M (2003). Vegetation in the urban environment: microclimatic analysis and benefits. *Energy and Buildings* **35**: 69-76.

Esper J, Frank D, Büntgen U (2007). On selected issues and challenges in dendroclimatology. *A changing world: challenges for landscape research*. Kienast, F, Wildi, O,Ghosh, S, Springer**:** 113-132.

Freitas L, Pereira MG, Caramelo L, Mendes M, Nunes LF (2013). Homogeneity of monthly air temperature in Portugal with HOMER and MASH. *Quarterly Journal of the Hungarian Meteorological Service* **117**: 69-90.

Fujibe F (2009). Detection of urban warming in recent temperature trends in Japan. *International Journal of Climatology* **29**: 1811-1822.

Gallo KP (2005). Evaluation of Temperature Differences for Paired Stations of the U.S. Climate Reference Network. *Journal of Climate* **18**: 1629-1636.

Grimmond CSB, Oke TR, Cleugh HA (1993). The role of "rural" in comparisonsof observed suburban-rural flux differences. *Exchange Processes at the Land Surface for a Range of Space and Time Scales*, Yokohama, IAHS.

Hansen J, Ruedy R, Sato M, Imhoff W, Lawrence D, Easterling DR, Peterson TC, Karl T (2001). A closer look at United States and global surface temperature change. *Journal of Geophysical Research* **106**: 23947-23963.

Hart MA, Sailor DJ (2009). Quantifying the influence of land-use and surface characteristics on spatial variability in the urban heat island. *Theoretical and Applied Climatology* **95**: 397-406.

Hathway EA, Sharples S (2012). The interaction of rivers and urban form in mitigating the Urban Heat Island effect: A UK case study. *Building and Environment* **58**: 14-22.

Hawkins TW, Brazel AJ, Stefanov WL, Bigler W, Saffell EM (2004). The Role of Rural Variability in Urban Heat Island Determination for Phoenix, Arizona. *Journal of Applied Meteorology* **43**: 476-486.

He Y, Jia G, Hu Y, Zhou Z (2013). Detecting Urban Warming Signals in Climate Records. *Advances in Atmospheric Sciences* **30**: 1143-1153.

Hederyd O (1993). Tornedalens historia: Haparanda efter 1809 : kommunhistoria utgiven med anledning av Haparandas 150-årsjubileum. Haparanda.

Hinkel KM, Nelson FE (2007). Anthropogenic heat island at Barrow, Alaska, during winter: 2001–2005. *Journal of Geophysical Research* **112**: 1-12.

Hinkel KM, Nelson FE, Klene AE, Bell JH (2003). The urban heat island in winter at Barrow, Alaska. *International Journal of Climatology* **23**: 1889-1905.

Houet T, Pigeon G (2011). Mapping urban climate zones and quantifying climate behaviors--an application on Toulouse urban area (France). *Environmental Pollution* **159**: 2180-2192.

Huang L, Li J, Zhao D, Zhu J (2008). A fieldwork study on the diurnal changes of urban microclimate in four types of ground cover and urban heat island of Nanjing, China. *Building and Environment* **43**: 7-17.

Jones PD, Lister D, Li Q (2008). Urbanization effects in large-scale temperature records, with an emphasis on China. *Journal of Geophysical Research* **113**: 1-12.

Jones PD, Wigley TML (2010). Estimation of global temperature trends: what's important and what isn't. *Climatic Change* **100**: 59-68.

Kim Y-H, Baik J-J (2005). Spatial and Temporal Structure of the Urban Heat Island in Seoul. *Journal of Applied Meteorology* **44**: 591-605.

Klysik K, Fortuniak K (1999). Temporal and spatial characteristics of the urban heat island of Lodz, Poland. *Atmospheric Environment* **33**: 3885-3895.

KNMI - Koninklijk Nederlands Meteorologisch Instituut. *KNMI Climate Explorer*. http://climexp.knmi.nl/. Access: May and June 2014

Kolokotsa D, Psomas A, Karapidakis E (2009). Urban heat island in southern Europe: The case study of Hania, Crete. *Solar Energy* **83**: 1871-1883.

Kottek M, Grieser J, Beck C, Rudolf B, Rubel F (2006). World Map of the Köppen-Geiger climate classification updated. *Meteorologische Zeitschrift* **15**: 259-263.

LandmaterietSweden - *Landmateriet Sweden Database*. https://www.lantmateriet.se/en/. Access: 12.09.2015

Li RM, Roth M (2009). Spatial variation of the canopy-level urban heat island in Signapore. *The seventh International Conference on Urban Climate*. Yokohama, Japan, International Association for Urban Climate.

Lindén J (2011). Nocturnal Cool Island in the Sahelian city of Ouagadougou, Burkina Faso. *International Journal of Climatology* **31**: 605-620.

Lindén J, Esper J, Holmer B (2015a). Using Land Cover, Population, and Night Light Data for Assessing Local Temperature Differences in Mainz, Germany. *Journal of Applied Meteorology and Climatology* **54**: 658-670.

Lindén J, Grimmond CSB, Esper J (2015b). Urban warming in villages. *14th EMS Annual Meeting & 10th European Conference on Applied Climatology (ECAC)*. Auer, I. Prague, Czech Republic, Advances in Science & Research.

Magee N, Curtis J, Wendler G (1999). The Urban Heat Island Effect at Fairbanks, Alaska. *Theoretical and Applied Climatology* **64**: 39-47.

Mestre O, Domonkos P, Picard F, Auer I, Robin S, Lebarbier E, Böhm R, Aguilar E, Guijarro J, Vertachnik G, Klancar M, Dubuisson B, Stepanek P (2013). HOMER: a homogenization software - methods and applications. *Quarterly Journal of the Hungarian Meteorological Service* **117**: 47-67.

Moberg A, Bergström H (1997). Homogenization of Swedish temperature data - Part III - The long temperature records from Uppsala and Stockholm. *International Journal of Climatology* **17**.

Morris CJG, Simmonds I, Plummer N (2001). Qualification of the Influences of Wind and Cloud on the Nocturnal Urban Heat Island of a Large City. *Journal of Applied Meteorology* **40**: 169-182.

NOAA - National Oceanic and Atmospheric Administration. *GHCN - Global Historical Climatology Network*. ftp://ftp.ncdc.noaa.gov/pub/data/ghcn/v3/. Access: May 2014

Nordli PØ, Alexandersson H, Frich P, Førland EJ, Heino R, Jónsson T, Tuomenvirta H, Tveito OE (1997). The effect of raditation screens on Nordic time series of mean temperature. *International Journal of Climatology* **17**: 1667-1681.

Odencrants R (1945). Haparanda stad 100 år: Minnesskrift på uppdrag av Haparanda stad. Uppsala.

Oke TR (1982). The energetic basis of the urban heat island. *Quarterly Journal of the Royal Meteorological Society* **108**: 1-24.

Oke TR (1987). Boundary Layer Climates, Taylor & Francis Ltd.

Oke TR (2006). Initial Guidance to obtain representative meteorological observations at urban sites. *WMO/TD* **1250**: 1-47.

Parker DE (2005). A Demonstration That Large-Scale Warming Is Not Urban. *Journal of Climate* **19**: 2882-2895.

Parker DE (2010) Urban heat island effects on estimates of observed climate change. *WIREs Climate Change* **1**, 123-133.

Persson G (2012). Islossning i Torneälven. *Hydrologi* **118**: 1-25.

Pigeon G, Legain D, Durand P, Masson V (2007). Anthropogenic heat release in an old European agglomeration (Toulouse, France). *International Journal of Climatology* **27**: 1969-1981.

Rahimzadeh F, Zavareh MN (2014). Effects of adjustment for non-climatic discontinuities on determination of temperature trends and variability over Iran. *International Journal of Climatology* **34**: 2079-2096.

Ren G, Zhou Y, Chu Z, Zhou J, Zhang A, Guo J, Liu X (2008). Urbanization Effects on Observed Surface Air Temperature Trends in North China. *Journal of Climate* **21**: 1333-1348.

Rizwan AM, Dennis LYC, Liu C (2008). A review on the generation, determination and mitigation of Urban Heat Island. *Journal of Environmental Sciences* **20**: 120-128.

SMHI - Swedish Meteorological and Hydrological Institute. *SMHI Climate Explorer*. http://opendata-catalog.smhi.se/explore/. Access: February 2015

StatisticsSweden - *Official Swedish statistics database*. www.scb.se. Access: September 2015

Steeneveld GJ, Koopmans S, Heusinkveld BG, van Hove LWA, Holtslag AAM (2011). Quantifying urban heat island effects and human comfort for cities of variable size and urban morphology in the Netherlands. *Journal of Geophysical Research* **116**: 1-14.

Stewart ID, Oke TR (2012). Local Climate Zones for Urban Temperature Studies. *Bulletin of the American Meteorological Society* **93**: 1879-1900.

Syrakova M, Stefanova M (2008). Homogenization of Bulgarian temperature series. *International Journal of Climatology* **29**: 1835-1849.

Trenberth KE, Jones PD, Ambenje P, Bojariu R, Easterling DR, Klein Tank AMG, Parker DE, Rahimzadeh F, Renwick JA, Rusticucci M, Soden BJ, Zhai P (2007). Observations: Surface and Atmospheric Climate Change. *Climate Change 2007: The Physical Science Basis. Contribution of Working Group I to the Fourth Assessment Report of the Intergovernmental Panel on Climate Change*. Solomon, S, Qin, D, Manning, M, Chen, Z, Marquis, M, Averyt, KB, Tignor, M,Miller, HL. Cambridge; New York.

Tuomenvirta H (2001). Homogeneity adjustments of temperature and precipitation series - Finnish and Nordic data. *International Journal of Climatology* **21**: 495-506.

Venema V, Mestre O, Aguilar E, Auer I, Guijarro J, Domonkos P, Vertachnik G, Szentimrey T, Stepanek P, Zahradnicek P, Viarre J, Müller-Westermeier G, Lakatos M, Williams CN, Menne MJ, Lindau R, Rasol D, Rustemeier E, Kolokythas K, Marinova T, Andresen L, Acquaotta F, Fratianni S, Cheval S, Klancar M, Brunetti M, Gruber C, Prohom M, Likso T,

Esteban P, Brandsma T (2012a). Benchmarking homogenization algorithms for monthly data. *Climate of the Past* **8**: 89-115.

Venema V, Mestre O, Aguilar E, Guijarro J, Domonkos P, Vertachnik G, Szentimrey T, Stepanek P, Zahradnicek P, Viarre J, Müller-Westermeier G, Lakatos M, Williams CN, Menne MJ, Lindau R, Rasol D, Rustemeier E, Kolokythas K, Marinova T, Andresen L, Acquaotta F, Fratianni S, Cheval S, Klancar M, Brunet M, Gruber C, Prohom M, Likso T, Esteban P, Brandsma T, Willet K (2012b). Detecting and repairing inhomogeneities in datasets, assessing current capabilities. *Bulletin of the American Meteorological Society* **93**: 951-954.

Vertachnik G, Dolinar M, Bertalanic R, Klancar M, Dvorsek D, Nadbath M (2015). Ensemble homogenization of Slovenian monthly air temperature series. *International Journal of Climatology* **35**: 4015-4026.

Wasserman A (2009). Haparanda historiska utveckling - från by, köping och till stad. *Institutionen för Industriell ekonomi och samhällsvetenskap*. Luleå, Luleå Tekniska Universitet. **BSc**.

Weng Q, Lu D (2008). A sub-pixel analysis of urbanization effect on land surface temperature and its interplay with impervious surface and vegetation coverage in Indianapolis, United States. *International Journal of Applied Earth Observation and Geoinformation* **10**: 68-83.

Yan Z, Li Z, Qingxiang I, Jones PD (2010). Effects of site change and urbanisation in the Beijing temperature series 1977–2006. *International Journal of Climatology* **30**: 1226-1234.

Yang P, Ren G, Liu W (2013). Spatial and Temporal Characteristics of Bejing Urban Heat Island Instensity. *Journal of Applied Meteorology and Climatology* **52**: 1803-1816.

Yokobori T, Ohta S (2009). Effect of land cover on air temperatures involved in the development of an intra-urban heat island. *Climate Research* **39**: 61-73.

Zhang L, Ren G, Ren Y, Zhang A, Chu Z, Zhou Y (2014). Effect of data homogenization on estimate of temperature trend: a case of Huairou station in Bejing Municipality. *Theoretical and Applied Climatology* **115**: 365-373.

5 Detection and elimination of UHI effects in long temperature records from villages – A case study from Tivissa, Spain

Manuel Dienst[1], Jenny Lindén[2], Òscar Saladié[3], Jan Esper[1]

[1]Department of Geography, Johannes Gutenberg University, Mainz, Germany

[2]IVL – Swedish Environmental Research Institute, Gothenburg, Sweden

[3]Departament of Geography, Universitat Rovira i Virgili, Vila-seca, Spain

Urban Climate – in review

5.1 Introduction

As far back as Roman times, people started to consider the climate in cities to be different and hence thought about ways to address that in town planning (Rykwert, 1988). Though urban climate is not completely understood even today, great progress has been made to identify underlying processes and their implications for local climatic conditions. One major issue in that regard is the establishment of an urban heat island (UHI), a rise in urban temperatures compared to the rural surroundings (Landsberg, 1981). The amplified warming is mainly caused by the introduction of new materials and a change in geometry as well as anthropogenic heat release as summarized by Rizwan et al. (2008). Although there are inter-urban variations, outgoing longwave radiation is usually lower in cities due to radiation trapping within narrow streets with high buildings (Unger, 2004). In addition, the introduction of new materials changes the heat capacities and might lower albedo values, which is an essential part of UHI formation (Giridharan et al., 2004). Naturally, this urbanization causes the amount of vegetation and bare soil to decrease as they are replaced by sealed surfaces, lowering the cooling or more specifically the latent heat flux originating from evapotranspiration (Oke, 1982). Wind speed is usually lowered in urban canyons and hence ventilation is limited, not only preventing a removal of pollutants in cities but also intensifying the urban warming (Dimoudi and Nikolopoulou, 2003).

UHIs have been reported from cities all over the world (e.g. Saaroni *et al.*, 2000; Kim and Baik, 2004; Gaffin *et al.*, 2008; Emmanuel and Krüger, 2012). Many studies have also indicated that continued urbanization gradually increases the UHI (e.g. Brandsma *et al.*, 2003; Zhou *et al.*, 2004; Ghazanfari *et al.*, 2009; Hamdi *et al.*, 2009). This might have implications for meteorological measurements and especially for long temperature time series, since many stations were initially located in urban areas. Correction for the urban impact in long time series has in several studies had a considerable effect on the recent warming trends (e.g. Balling Jr and Idso, 1989; Kato, 1996; Wang and Ge, 2012). The development of UHIs has been confirmed also in small urban settlements like villages, though studies are still few (e.g. Hinkel *et al.*, 2003; Szegedi *et al.*, 2013), implying temperature records originating from these locations are possibly biased.

Nowadays, the siting of meteorological stations is carefully regulated in order to minimize the impact of site specific features such as nearby slopes, buildings or vegetation (WMO, 2011). This procedure aims at reducing non-climatic impacts as well as representing the regional rather than the site-specific climate. Unfortunately, the records are influenced by other factors as well, e.g. changes in observing staff, variations in observing times, changes in instrumentation, or

relocations (Böhm *et al.*, 2009). The potential for anthropogenic bias is high in century long temperature records, since the stations tended to be originally placed within the urban centres in order to provide high accessibility for manual read outs, moving gradually to a more rural surrounding in the course of their history. Relocating a station proved to have the most substantial effects on temperature records, since this results in a significant change in station environment (e.g. Tuomenvirta, 2001; Brunet *et al.*, 2006a). In order to produce high-quality long term temperature data, a homogenization is usually performed, aiming to remove these inadvertent alterations (Venema *et al.*, 2012). One widely used homogenization method is the HOMER script which executes a statistical analysis of temperature time series and performs a comparison between these records, assessing breakpoints and differences among the series which can later be eliminated by adjusting a record to the overall regional climate signal indicated by the other records (Freitas *et al.*, 2013; Mestre *et al.*, 2013).

In this study, we identify and correct for UHI effects in a century long time series relying on temperature data gathered in all historical sites of the meteorological station in the village Tivissa in Spain. In a former study, we used a similar approach to assess and remove the relocation bias in a long temperature record from a village in Sweden (Dienst *et al.*, 2017), mainly because statistical homogenization failed due to a lack of suitable reference stations. The Tivissa time series has previously been partly homogenized using the HOMER method, and an additional aim in this study is to compare the results of both correction approaches.

5.2 Study area and methods

5.2.1 Study area

Tivissa is situated in the Autonomous Region of Catalonia in the North-eastern part of Spain, with the river Ebro running in 6km distance to the West and the Mediterranean Sea in 12km distance to the South-east (see Fig. 5-1). The village is located at the foot of the Serra de Llaberia and Muntanyes de Tivissa-Vendellòs at an altitude of 315m a.s.l. The landscape is dominated by hilly and mountainous terrain, valleys being mostly used for agriculture and the mountain slopes covered by open forests. Based on the updated Köppen & Geiger climate classification by Kottek *et al.* (2006), the region is regarded as a warm temperate climate zone with dry and hot summers (Csa).

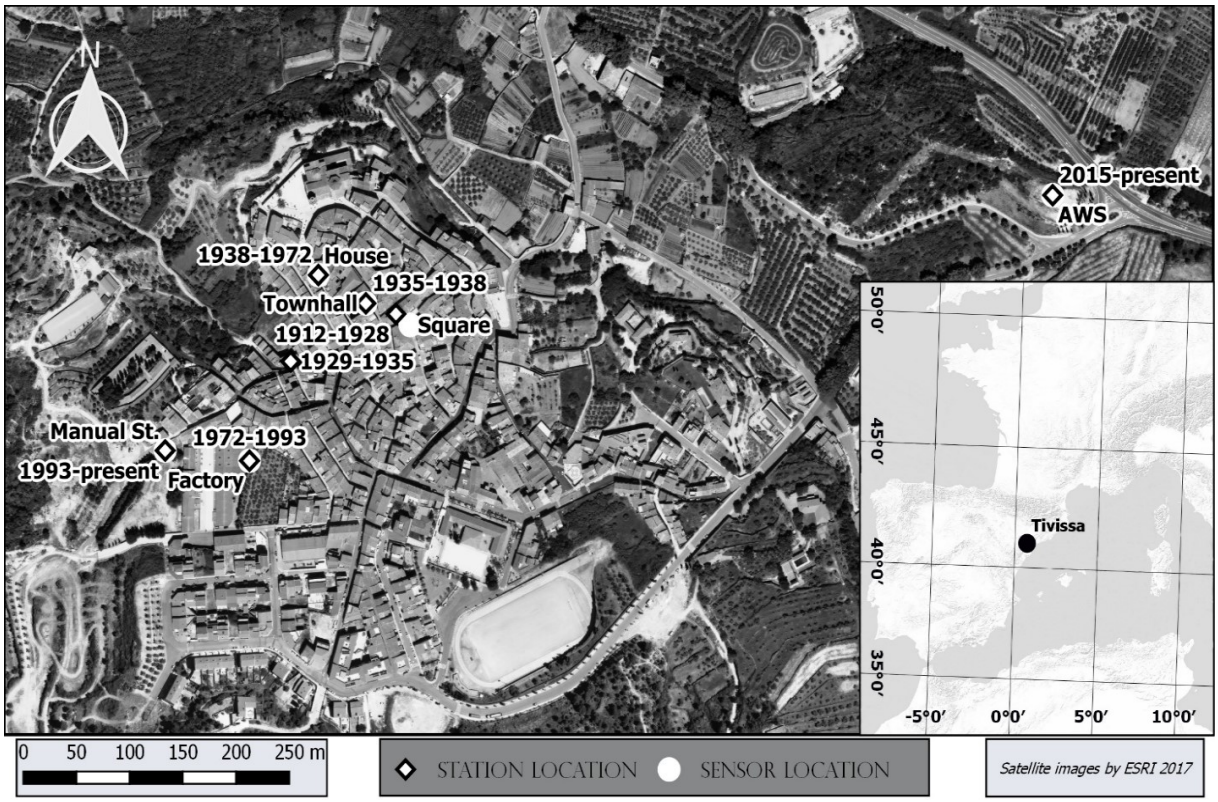

Figure 5-1 Measurements in Tivissa. Historical meteorological station sites with interval of operation and sensor placements close to these sites (main map). Location of the village in Spain (side map).

Despite having a history that dates back to Iberian and Roman times, the village is dominated by the medieval centre nowadays. White and brownish one- to three-storey houses exist alongside or integrated in the medieval structures, with narrow streets and alleys in-between. The expansion of the village was limited during the 20th century and mainly took place to the south-west of the centre in the 80s, introducing a new residential area. Only few houses have been built beginning of this century next to this expansion. In 1910, population size of the village was 2400 inhabitants, but declined afterwards, especially after the Spanish Civil War. Since the 21st century, Tivissa is home to 1400 people, but still shrinking.

5.2.2 Meteorological station history and dataset

With measurements starting in 1911 (precipitation) and 1912 (temperature), respectively, and still running, the meteorological station in Tivissa provides one of the longest temperature records in Spain, outside of the large cities. Saladié *et al.* (2013) worked on reconstructing the history of the meteorological station which will be detailed in the following and refers to Table 5-1 and Figure 5-1 regarding locations and measurement periods. A Hellmann device for precipitation was installed after setting up the station in 1911 and a Tonnelot maximum and

minimum thermometer to measure temperatures one year later (Jardí, 1923). Instruments have been protected with a screen ever since, being very similar to a Stevenson screen. This screen was replaced in 1972 by a new one of the same type. Apart from a change in screening, several relocations took place during the course of the station's history. First, measuring started on the roof terrace of a building in approximately 7m height above ground in the village centre (Roof 1). From 1929 to 1935, the station was situated 150m away in a similar location and was set up the same way (Roof 2), although this time a lawn was adjacent to the house in the North. A different site was chosen for the following three years, when measurements were performed on the flat roof of the town hall clock tower in a height of 15m (Town hall). In 1938, the station moved to the roof terrace of a building again, very similar to the first two locations, where it stayed until 1972 (Roof 3). Until 1950, every relocation was coupled with a change in observer as well. In 1950, a change in observer took place but the station remained in the same place. The observer, head of a local company, moved the station out of the centre to his factory in 250m distance to the former site in order to insure better accessibility and maintenance 22 years later. Although todays' manual station is still located at the factory, it has experienced minor relocations within the factory before moving to its final spot, most of the time being situated on an elevated concrete surface (3m height) east of the great factory halls (Factory). Unfortunately, the dates of these minor relocations have not been reported. The final change was performed in 1993 with the station being relocated to a lawn west of the factory halls where measuring is still taking place (Manual Station), albeit the fact that an automatic weather station was installed east of the village in 600m distance to the centre in 2015. Nowadays, the manual station is seen about by the former observers' son and is part of the network run by the Spanish Meteorological Service, while the automatic station is maintained by the Meteorological Service of Catalonia. Information on relocations and changes in observing staff is based on documents completed by the observers or members of the meteorological agencies, as well as derived from personal conversation with them. The temperature datasets along with metadata was provided by Meteorological Service of Catalonia.

	LOCATION	SITE DESCRIPTION	ALT	PERIOD
MET STATION	Roof 1	on the roof terrace of a house in the centre of the village	317m	1912-1928
	Roof 2	on the roof terrace of a house in the centre of the village	317m	1929-1935
	Town hall	on the clock tower of the town hall (approx. 12m height)	318m	1935-1938
	Roof 3	on the roof terrace of a house in the centre of the village	314m	1938-1972
	Factory	mainly: on paved concrete slightly elevated, factory hall to the west and vineyard to the east; afterwards: several undocumented smaller relocations within the factory took place – placement somewhere between first location and manual station	318m	1972-1993
	Manual Station	on lawn, some trees around, factory hall in 20m distance	310m	1993-today
U23 SENSORS	Square	on lamp post on square (20x10m), parking space nearby, three story buildings	301m	From 2015 on
	Town hall	on metal post next to old met station location	318m	From 2015 on
	Roof	on railing next to old station position (Roof 3)	314m	From 2015 on
	Factory	on post where old station was located, now small olive trees to the east	318m	From 2015 on
	Manual Station	in screen of current manual station	310m	From 2015 on
	AWS	on post of AWS, bare ground, some trees nearby as well as a road and a street	314m	From 2015 on

Table 5-1 Metadata on meteorological station and sensor set-up. Site-specific descriptions and operation details for historical as well as current measurements.

The temperature data from Tivissa used in this study consists of a minimum and maximum temperature record spanning from September 1912 to December 2016. The time series is continuous for 104 years, although a total of 17 months have been disregarded because of missing data.

5.2.3 Current measurements

A set of temperature sensors was installed in the village to depict the current climatic conditions in all past locations of the meteorological station. The sensor network consists of six sensors which measure temperature and relative humidity. Figure 5-1 and Table 5-1 give an overview on recent measurements in Tivissa. Even though the station moved three times within the centre in the period from 1912 to 1972, it was only possible to install sensors in two of these locations, the top of the town hall clock tower (Town hall) and the roof terrace where the station has been situated from 1938 onwards (Roof). Being very similar to the later one and very close as well, we estimate the first two locations to be well depicted by the one sensor placed on the roof terrace. Due to a lack of information on smaller relocations within the factory and since the station was located east of the factory halls for most of the time, we chose this spot to be

representative until 1992 (Factory). To depict the recent situation, one sensor was placed within the screen of the current manual station (Manual Station). An additional sensor was set up in the central square of the village (Square), trying to assess the presumably maximum UHI intensity in the village while another one was placed outside the village at the current automatic weather station in order to serve as rural reference (AWS).

The sensors installed are of the same type and are protected by a radiation shield (HOBO Pro v2 U23-001 with RS1, Onset Computer Company), except for the one sensor located within the screen of the manual station. For analysis, daily mean (T_{mean}), minimum (T_{min}) and maximum (T_{max}) temperatures were derived from the dataset. Since the measuring interval was set to 30min, the mean was calculated using the 48 daily values and maximum and minimum set as the highest and lowest ones, respectively. Unfortunately, actual minimum and maximum temperatures might differ slightly because they could occur within these intervals. Monthly and annual temperatures are simple averages of the daily values and are essential for the correction as it is based on monthly data. The data of this survey is comprised of two full years spanning from October 2015 to September 2017.

To assess the UHI in the village and a possible impact on the temperature record in Tivissa, a rural reference is crucial. The current AWS site was selected to host the reference sensor since it is located outside the village and should meet all requirements detailed by the WMO (2011) to serve as a representative site.

5.2.4 The correction approach

To correct the time series for an urban impact at different times, the record needed to be split in several periods according to its past locations detailed in chapter 2.2. The warming was quantified relying on the current measurement data and removed from the original time series. In total, the meteorological station was installed at seven sites in Tivissa. The first two sites as well as the fourth were located in the centre of Tivissa on roof terraces being represented by the current sensor on the respective roof terrace. A correction factor at these locations was assessed by subtracting the daily mean, minimum and maximum temperatures measured at the AWS from the ones of the according location ($T_{Location} - T_{AWS}$). Monthly, seasonal and annual values were later derived from the daily ones. Since the AWS sensor is assumed to be free of an urban influence, the resulting anomaly equals the site specific anthropogenic impact, with negative values suggesting a downward and positive values an upward correction of the original time series ($T_{Temperature\ record} + T_{Anomaly}$). The other periods were treated identically with due regard to the change in representative sensors, using the town hall, factory and current manual station sensors depending on the period considered.

5.2.5 Comparison to HOMER output

The introduced procedure focussing on the removal of UHI influence, i.e. the relocation bias, is mainly dependent on two major elements. On the one hand, existing metadata has to be thoroughly investigated in order to exactly determine the various measurement sites the meteorological station was located at as well as the corresponding time intervals. On the other hand, the site-specific climate needs to be assessed to determine the anthropogenic influence at the respective locations. In contrast, statistical homogenization based on the HOMER approach heavily relies on additional station data from the region that the target time series could be compared with. This comparison will result in suggestions on how to correct the data to make it more similar to the overall climate signal of the region. MeteoCat has previously homogenized the minimum and maximum temperature records from Tivissa. Since both approaches aim to improve the dataset, it is an interesting issue to compare the generated data and discuss the differences in altering the original dataset, with one approach being more site-specific and the other one more targeted at the overall bias in the data. Although technically not correct since both approaches work towards the same goal, we will subsequently address our approach as correction and the HOMER approach as homogenization to avoid confusion.

The comparison was performed by first assessing the correction factors for each year, implying the values being added or subtracted from the original time series as suggested by the automated homogenization or the manual correction (chapter 2.4), respectively. In a second step, the correction factors from the correction were subtracted from the ones produced by homogenization, resulting in a residual that reveals the discrepancy between the two methods. Due to the scarcity of other records before 1950, homogenized data is only available from that year onwards, reducing the period of overlapping data to 67 years.

Since many studies focus on mean temperatures, we chose to include these as well by calculating the mean of T_{min} and T_{max}. However, this has only been performed for yearly averages. In order to smooth the data allowing for better visual assessment of trends and changes, a 10-year spline was applied to the original, the homogenized as well as the corrected time series as presented by Cook and Peters (1981).

5.3 Results

In this chapter, we first address the spatial variations in the Tivissa sensor dataset, particularly focussing on the urban heat island effect. The UHI intensity will then be used to correct the

dataset for urban influence and hence the relocation bias during different time periods. In the following, the corrected record is compared to the one produced through statistical homogenization relying on HOMER.

5.3.1 Spatial temperature patterns

To illustrate site-specific differences and the UHI intensity at all urban locations, we calculated the differences using the AWS sensor outside the village as rural reference. Figure 5-2 shows that inter-seasonal variance is very distinct in ΔT_{max}. The overall pattern reveals a mostly significant warming compared to the AWS at all sites that is most distinct in summer and secondly in spring, even reaching 1.8 °C and 1.2 °C at the factory site, respectively. A similar, but slightly weaker warming is detected at the square in the village centre. Both locations display a very strong discrepancy between spring/summer and autumn/winter ΔT_{max} that does not occur again for any other location or parameter. In winter, the temperature discrepancy for the square even falls below zero (-0.2 °C). Seasonal temperatures on the roof terrace and at the manual station are not very different with all values in a range of 0 °C to 0.5 °C, the only exception being summer ΔT_{max} at the manual station (0.7 °C). Another feature is the town hall temperatures, showing similar values as the AWS (below 0.2 °C) regardless of the season.

In general, the distribution of data in ΔT_{mean} is smaller compared to the other parameters, i.e. inter-seasonal as well as differences among the sensors are less pronounced. Temperatures at the factory still display the largest seasonal variations, especially in summer (0.7 °C) and winter (-0.2 °C), with winter being the only negative anomaly in ΔT_{mean} at all. As in ΔT_{max}, the sensors at the roof terrace and at the town hall show almost no seasonal differences. Overall, summer is again the season displaying highest values at all locations but the town hall, with a peak value of 1.1 °C at the square. All locations except for the factory show significantly higher seasonal anomalies in ΔT_{min} of at least 0.4 °C. A unique feature in ΔT_{min} is found at the factory, displaying exclusively lower temperatures than the sensor at the AWS (-0.5 °C as a yearly average). There is less seasonality in minimum temperatures compared to the other two parameters, with differences less than 0.4 °C at each site, except for the factory. The square in the centre develops the most substantial warming with an anomaly of more than 1.5 °C in summer. The variance in the dataset for each location is higher in comparison to ΔT_{mean}, but similar to ΔT_{max}.

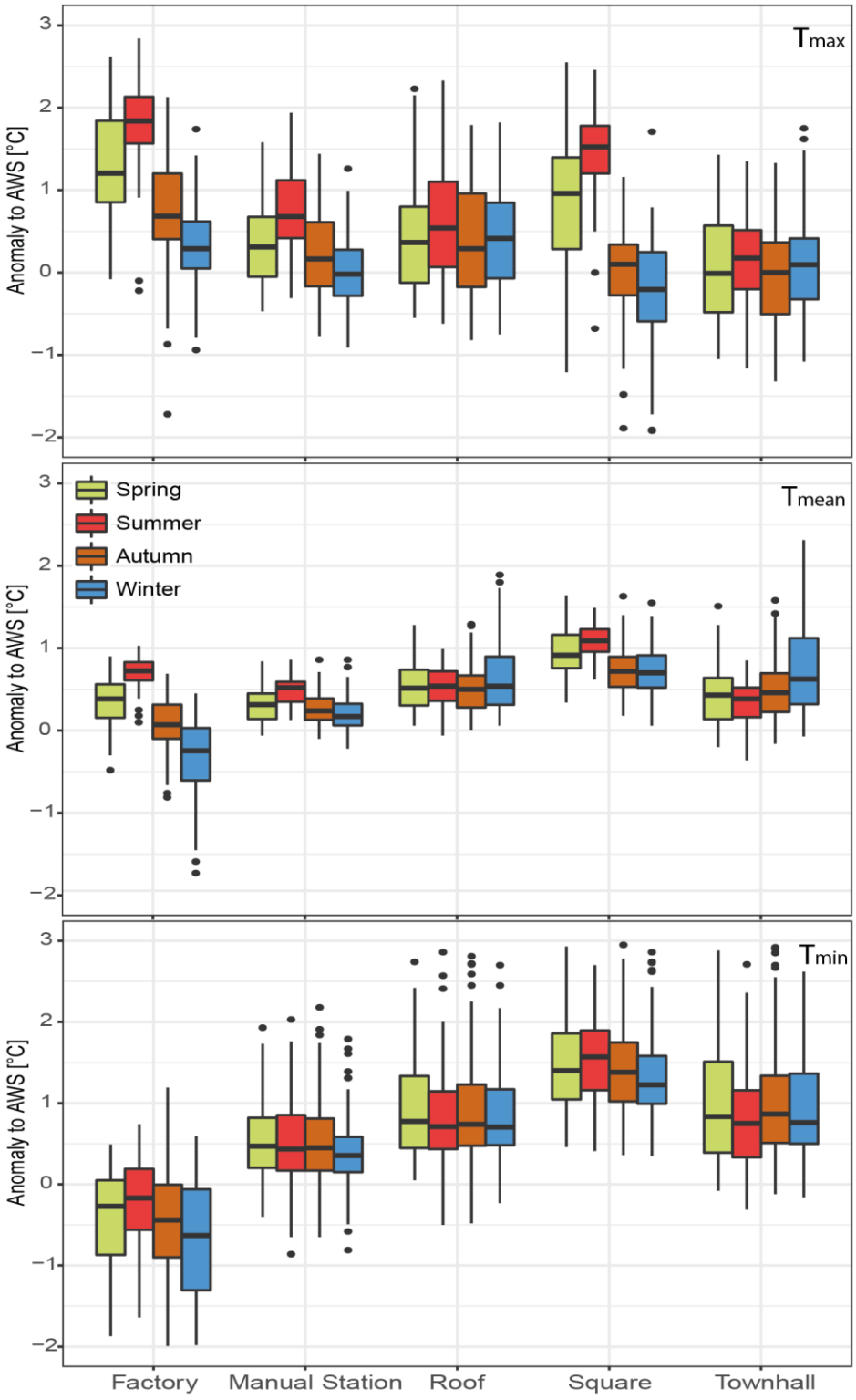

Figure 5-2 UHI intensity in Tivissa. Seasonal maximum (top), mean (middle) and minimum (bottom) temperatures at all sensor sites displayed as anomalies to the rural reference sensor (AWS) based on daily data. Boxplots display the median (black middle line), the upper and lower quartile including 50% of the data (coloured box) and whiskers (vertical lines) including the other 50%. Values beyond 1.5 times the interquartile range are plotted as outliers and are excluded from the whiskers, thus reducing the amount of data within.

5.3.2 Eliminating the relocation bias

Since the spatial temperature analysis revealed distinct differences between the rural reference and the other locations, a correction of the record is necessary. The quantification of this spatial variability now serves as the key to produce a Tivissa record free of relocation bias. Differences derived from the inter-sensor comparison were used for correction of the various time periods when the station was situated in varying locations throughout the village, as shown in Figure 5-3. A substantial downwards correction of at least 0.5 °C is applied for the first 60 years of the T_{min} record when the station was located within the centre of the village. For the same time period, the correction in T_{max} is considerably lower in all seasons, especially from 1935 until 1938 (town hall clock tower), when differences are close to zero. To account for the relocation to the factory in 1972, a strong downward correction is applied to T_{max}, while T_{min} is corrected upwards in order to account for the nocturnal cooling mentioned in chapter 3.1. From 1993 onwards, the current manual station was in use and, in consequence, the original temperatures are lowered again by about 0.5 °C or less in T_{min}, though not as much in T_{max} except for a distinct correction in summer.

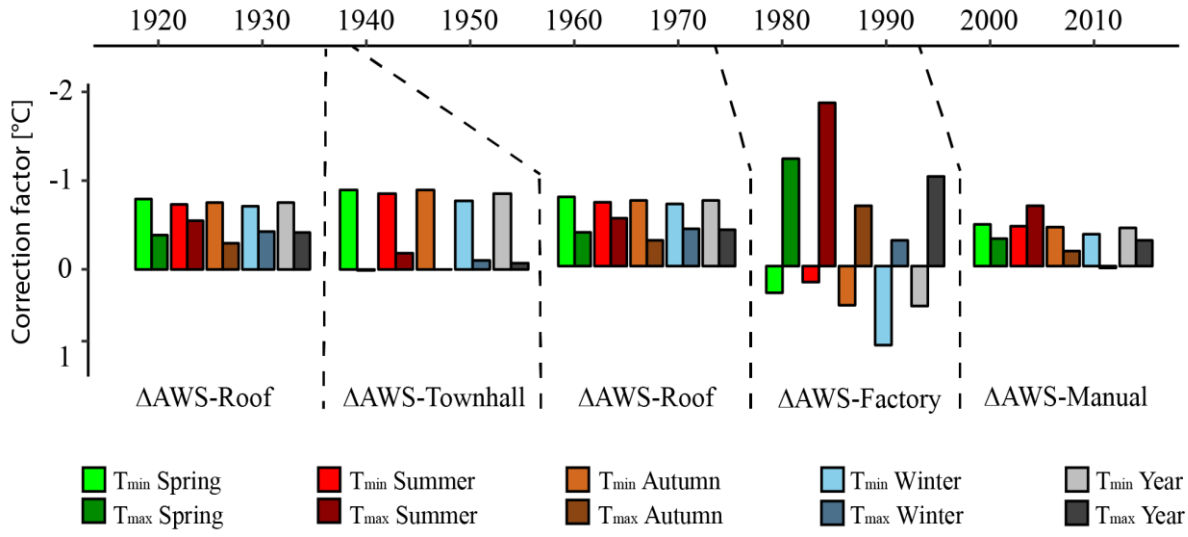

Figure 5-3 Time series adjustment. Corrections applied to the minimum and maximum temperature series according to the different measuring periods.

Correcting the more than 100 year-long records affected T_{min} and T_{max} time series differently, with an increasing warming trend in T_{min}, while the trend in T_{max} was unchanged or reduced compared to the original temperature record (Figure 5-4). Before correction, trends in minimum temperatures were not very distinct except for summer (0.08 °C/10 years). The correction increased trends to above 0.1 °C per decade in all seasons, a doubling or more of the original trend. This is especially true for winter, where correction causes a tenfold increase in the trend,

from 0.01 to 0.11 °C/10 years. Although summer T_{min} was least affected, it displayed the strongest overall warming. While the warming trend was most pronounced in summer for T_{max} as well (0.21 °C/10 years), the correction substantially reduced this to 0.14 °C per decade. Summer temperatures were thus most affected by the correction. A slight downwards change of trend lines did occur for spring and autumn, although original and corrected trend patterns are almost the same in autumn. Overall, uncorrected warming trends were far stronger in T_{max} than in T_{min}, but the correction resulted in aligning the temperature trends of T_{min} and T_{max} by enhancing the first and reducing the latter. Winter T_{max} is an exception since the existent trend was increased from 0.13 °C to 0.17 °C per decade after the correction.

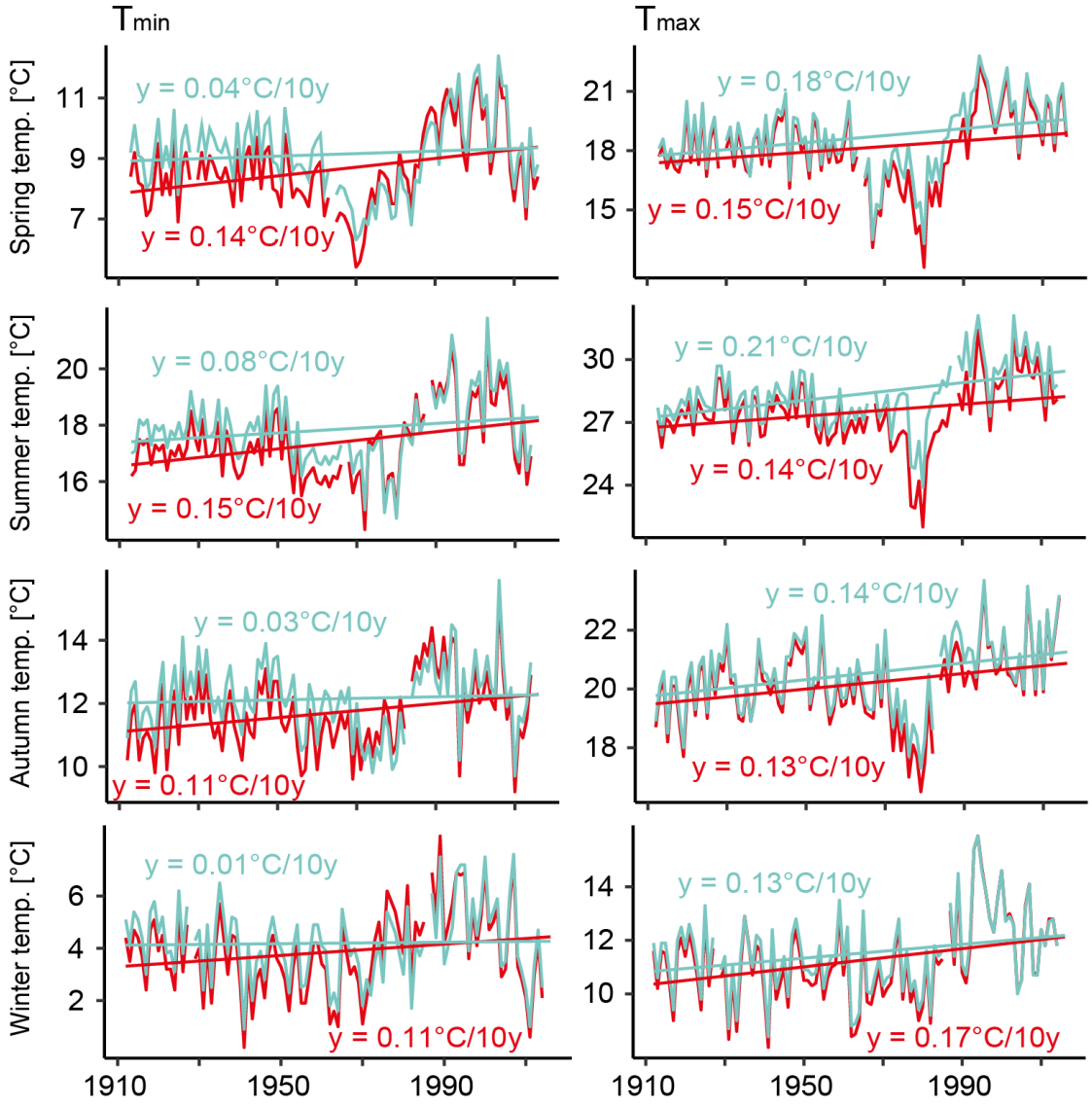

Figure 5-4 Trend changes after adjustment. Original (turquoise) and corrected (red) seasonal temperature time series and the corresponding decadal trends from spring to winter. Minimum temperatures displayed on the left, maximum temperatures on the right side.

5.3.3 Comparison of correction and homogenization approach

In order to assess the differences between the relocation bias correction introduced here and the one based on statistical homogenization, both records are plotted along with the original time series in Figure 5-5. The dashed lines mark the years when relocations took place.

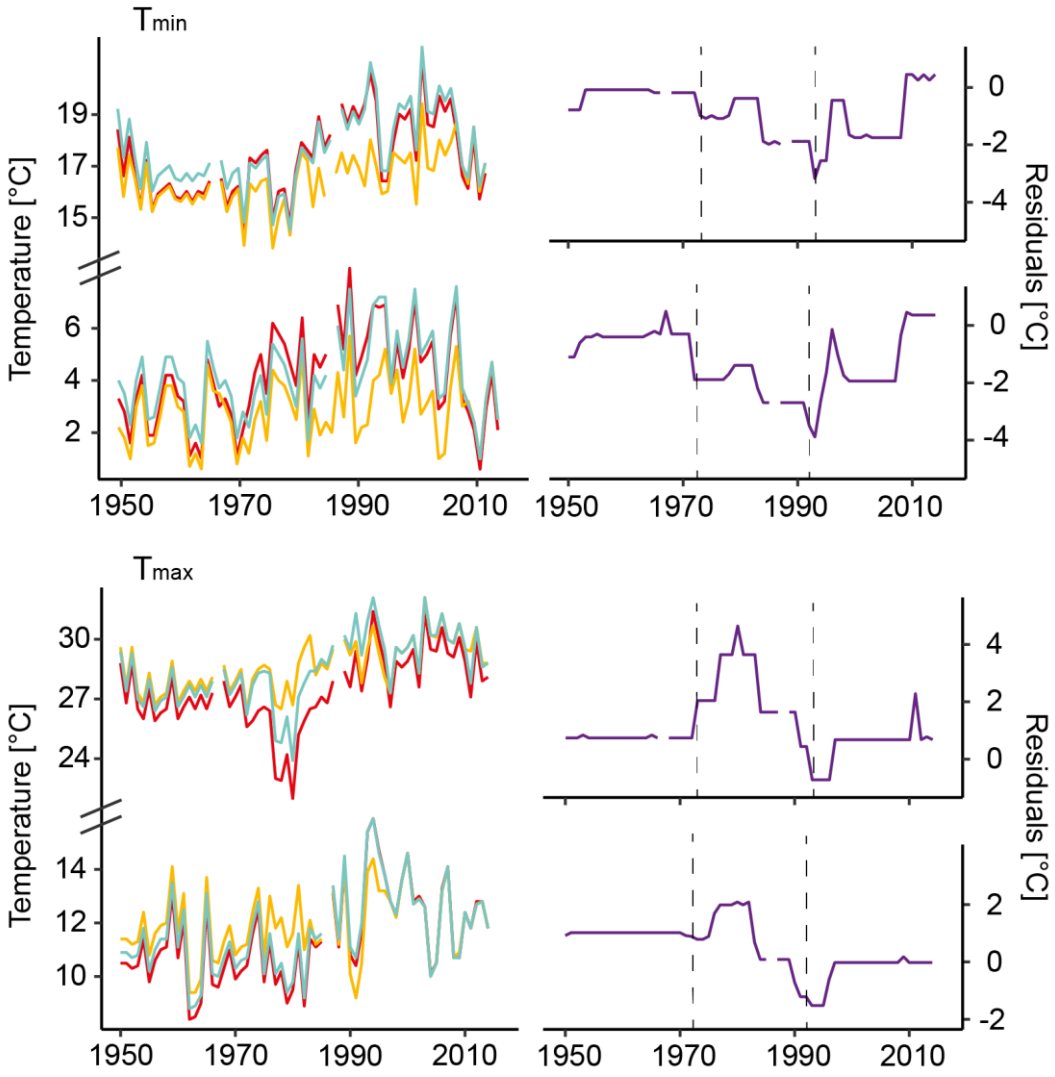

Figure 5-5 Differences in adjustment results. Comparison of corrected (red) and homogenized (orange) time series with the original one (turquoise). Minimum temperatures are displayed at the top, maximum temperatures at the bottom, with both showing the summer as well as the winter record. The difference of the correction values ($\Delta CorrValue_{correctedTS\text{-}homogenizedTS}$) are displayed as a residual (purple) next to the various time series. The dashed lines indicate relocations.

In general, the homogenized dataset is characterised by a stronger downwards adjustment in T_{min} and mostly upwards one in T_{max}. The biases indicated by the two methods are often reversed. The changes applied to the original dataset show some agreement between homogenized and corrected record until 1972 and from 2009 onwards. In-between, the severe change in the homogenized dataset results in a discrepancy of approx. -2 °C for many years and

peak values of more than -3 °C in 1991/1992, although decreasing one year later. In summer T_{max}, the corrected time series displays lower temperatures for the whole period while the homogenized one does the opposite until 1984. The corresponding differences are almost constantly ~ 0.7 °C until 1973 and from 1997 onwards due to the more positive adjustment in the corrected record if compared to the homogenized series. Within the 20 years from 1972 until 1992, this discrepancy is much more pronounced with values reaching approx. 4 °C. This is particularly true for the years around 1980, when original data show a distinct cooling that is still incorporated in the corrected record, but strongly upwards corrected by homogenization. Although the overall pattern in winter is similar, it is characterised by some other features as well. While the difference between the correction values is stronger in the beginning (~ 1 °C), it lasts until 1975 and is less pronounced thereafter, never exceeding 2.1 °C. Differences are almost negligible from 1984 to 1989 as well as after 1997, but a substantial downwards correction in the homogenized record causes the values to drop (~ 1.5°C) temporarily in the beginning of the 90's.

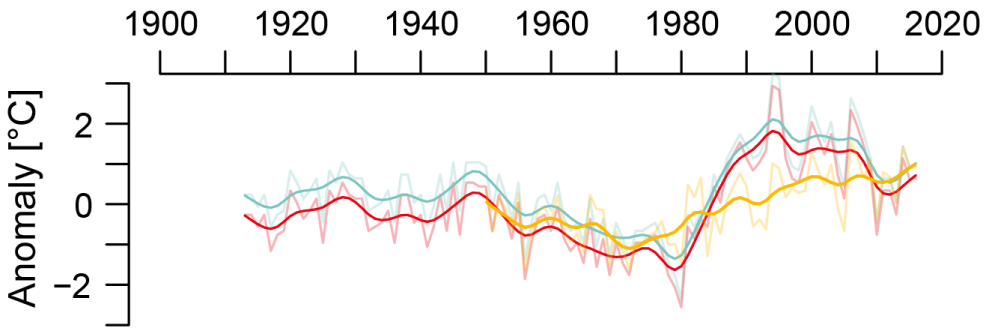

Figure 5-6 20th century trend comparison. Annual mean temperature record for Tivissa (turquoise) along with the corrected (red) and homogenized (orange) series. All records are shown as anomalies to the original series for the reference period 1950-1959. The light graphs indicate the absolute values while the thick lines illustrate the smoothed versions using a 10-year spline.

Since many studies focus on the development of mean temperatures in the 20th and 21st century, Figure 5-6 details the implications homogenization and relocation elimination have on the yearly average time series. A 10-year spline was applied to all data in order to emphasize long-term variability. The corrected record continuously stays below the original one. The difference is stronger in the beginning (~ 0.5°C) and reduced towards recent times (~ 0.3°C), leading to an increase in warming trend. The general pattern of the temperature record is not changed when applying the correction for the relocation bias. However, application of the statistical homogenisation method introduces clear changes of the pattern. While showing good agreement with the corrected record for more than a decade, a drastic change can be observed

from the late 1970s until the beginning of the 21st century, when homogenized values first overshoot the cooler period in original and corrected record by 0.5°C and more, but later undershoot them by approx.. 1.5°C around 1990. These huge differences are a result of the steep temperature increase in the original dataset during the 1980s, a feature that homogenization strongly mitigated by replacing it with an extended though reduced rise in temperatures. In recent years, homogenized and original data are almost the same.

5.4 Discussion

In this chapter, we first discuss the observed temporal and spatial variability in urban microclimates in Tivissa. Subsequently, we discuss and evaluate the implications our correction has for the Tivissa temperature record and address the partly severe differences compared to the homogenized time series.

5.4.1 Urban warming in Tivissa

The Spanish village Tivissa was found to develop a consistent UHI that is most pronounced in summer and least in winter, but detectable in almost every season and parameter examined in this study. This finding is not in line with other evidence from the Mediterranean claiming the UHI intensity to be strongest in winter (Montavez2000, Papanastasiou2011). A further investigation has to be carried out in order to explain this discrepancy. The square in the village centre is most affected by urban warming, with summer temperatures revealing a difference of more than 1 °C in ΔT_{mean} and 1.5 °C in both ΔT_{min} and ΔT_{max}, if compared to the AWS location that serves as rural reference. These intensities are comparable to UHIs found in larger cities such as Utrecht (300,000 inhabitants) with a nocturnal UHI of 1.5 °C (Brandsma and Wolters, 2012), Manaus (2,000,000 inhabitants) with 0.7 °C and 1.6 °C in summer T_{min} and T_{max}, respectively (de Souza and dos Santos Alvalá, 2014), Chennai (4,700,000 inhabitants) with 2.5 °C (Devadas and Rose, 2009) or Volos (200,000 inhabitants) with 2 °C mean maximum UHI intensity in summer (Papanastasiou and Kittas, 2012). However, other cities like Seoul or New York show much higher maximum intensities with 3-4 °C on average in a year (Kim and Baik, 2002; Gedzelman *et al.*, 2003). While low sky view factors and hence radiation trapping usually contribute to additional warming in densely built areas (Hamdi and Schayes, 2008), same as anthropogenic heat sources (Pigeon *et al.*, 2007), UHI intensities observed at the central square in Tivissa, especially in ΔT_{max}, are comparably small in autumn and winter. Since regional wind activity as well as cloud cover are increased (European Climate Assessment & Dataset, https://www.ecad.eu) and the sun shines from a lower angle during wintertime, higher

wind speeds and stronger urban shading effects likely mitigate the UHI intensity as also found by Morris *et al.* (2001) and Emmanuel *et al.* (2007).

Other sites show interesting patterns as well. In ΔT_{max}, almost no UHI formation is detectable at the town hall site. Since the sensor is positioned on top of the clock tower and above roof-level, winds are stronger compared to lower levels in the urban area (Nakamura and Oke, 1988), thus likely mitigating heating through accelerated ventilation as also described by Ramponi *et al.* (2014). The large variance, with lowest nocturnal temperatures and among the highest daytime temperatures, found at the factory site are likely caused by a complex combination of underlying processes. The sensor was placed above a concrete platform with a paved surface covered by a roof and the factory buildings to the West and a small field of low trees, formerly a vineyard, to the East. Low heat capacities of stone, concrete and metal accelerate warming during daytime when solar radiation is highest, but contribute to a rapid cooling after sundown, thus contributing to high T_{max} and low T_{min}. In addition, nocturnal anthropogenic warming is likely negligible because activity at the factory stops at night. Since spatial and temporal differences in hilly and mountainous terrain are often caused by local topography and climatology, e.g. cold air flows as described by Barry (2008) or Poulos and Zhong (2008), the factory site might be affected by this. As the terrain slopes westwards, cool downhill air flows are trapped at the factory buildings within the roof-covered area that is open to the East. During day, ventilation is presumably impeded which amplifies warming. Although the manual station sensor is only about 50 m away, it displays a completely different pattern. Here, the overall UHI intensity is low but not negative, with ΔT_{min} amounting to almost 0.5 °C in all seasons but winter. The open placement on a lawn with some distance to urban structures minimizes warming influence while at the same time preventing a pooling of cold air as the terrain slopes further westbound.

Given the intensities of the UHI in Tivissa, these findings signify the need to treat villages as urban areas instead of being a part of the rural landscape. The village urban warming is more intense in T_{min} than in T_{max}. This is in line with many findings from all over the world (e.g. Klysik and Fortuniak, 1999; Kim and Baik, 2002; Wilby, 2003). Substantially lower inter-seasonal differences in T_{min} compared to T_{max} imply a strong decoupling of nighttime UHI intensity from seasonal behaviour.

5.4.2 Implications of time series adjustment

The consistent UHI effect found in Tivissa at all examined locations confirms the need to correct for anthropogenic warming incorporated in the dataset by accounting for station

relocations. Since all past locations of the meteorological station are characterised by their own microclimatic conditions, the record was adjusted in accordance to the historical placement of the Tivissa station. We here refer to the correction of warm bias as an elimination of the relocation bias rather than a removal of gradual warming caused by the growth of a city as addressed by Jones *et al.* (2008) or Fujibe (2011).

In T_{min}, the correction resulted in a substantial rise in warming trend over the last >100years. Although urbanization effects likely have a minor impact on temperature records on a larger scale (Jones *et al.*, 1990; Peterson *et al.*, 1999), elimination of anthropogenic influence leading to a rise in trend is confirmed by other studies from Northern Scandinavia (Tuomenvirta, 2001) or China (Yang *et al.*, 2013). The reason for this amplification in trend is found in the movement of the meteorological station and its historical placement in Tivissa. Initially located within the village and hence influenced by urban warming effects, a stronger downwards correction had to be applied in the beginning. The placement in the factory in the 1970s led to an inverse correction since accelerated cooling at night compared to the rural reference made an upwards adjustment inevitable. Although the station moved to the manual station location of today 20 years later which resulted in a downwards correction again, the UHI affecting the measurements is lower compared to the first locations. Zhang *et al.* (2014) point out that this increase in warming trend might as well be caused by a recovery of the urban warming related to the steady growth of an urban area that would otherwise be mitigated by the relocations to less urbanized areas towards today. However, we estimate this to be very unlikely in the Tivissa case, because population has declined rather than increased from 1910 onwards and only small changes have occurred regarding building structure within the last 100 years.

Correcting for the relocation bias generated less change in the T_{max} than in the T_{min} trend, with the exception of correcting for the microclimate at the more recent factory site. The strong downwards correction in T_{max} for the time when the station was located at this site even caused a decreased trend in spring and summer.

Since the factory site seems to be of great importance to the correction and the resulting warming trend, a follow-up study needs to further clarify the site-specific climatology and offer a better insight in daily cooling and warming patterns. Nevertheless, a strong increase in warming trend for T_{min} and less distinct patterns in T_{max} are similar to the findings considering a long-term temperature record from a Swedish village (Dienst *et al.*, 2017).

5.4.3 Evaluating the correction approach

Since the homogenized and the corrected time series revealed some severe differences, a closer look on the varying patterns is inevitable in order to understand the reasons for this discrepancy as well as try to determine strengths and weaknesses of both approaches.

Considering T_{min}, a good agreement between homogenized and manually corrected record was found in the beginning, both indicating an additional warming in the original record and hence suggesting a downwards correction. For the 20 years the station was located at the factory, both approaches adjust the temperature record differently, with our correction undoing presumably cooler conditions and the homogenization removing an assumed strong impact of non-climatic related warming.

The unsteady residual during that time originates from changes in the correction factor suggested by homogenization. Since it is known that the station had undergone minor relocations within the factory, a varying correction factor supposedly better addresses this time interval. As a result, the factory sensor might be representative for most time but not the entire period. However, there is no indication for a strong downwards correction as suggested by homogenization either, because not only the factory site data contradict that finding, but also data gathered at the current manual station close to the factory show only a small warming influence at the maximum. In addition, no changes to the screen or the protection of the instruments in general were applied during its placement at the factory that might explain a strong amplified warming. Hence, we advise against the severity of the intervention suggested by homogenization. Nevertheless, since the discrepancy is strongest around 1980, a solely short-term inhomogeneity is still the main reason for this offset. Besides, the strong adjustment in homogenization persists after 1993, when the station was moved to the current location (manual station), but becomes insignificant after 15 years. Since there is no site-specific or historical evidence to support why it has not changed the year it was moved to this location, we consider our correction to be more reasonable from 1993 onwards. Finally, an urban warming influence is still present at the current manual station site that is not captured in the homogenized version.

As comparison of the historical station sites only indicate enhanced warming in T_{max}, our correction lowers temperatures in the overall dataset. Statistical homogenization agrees after mid-1980s with this adjustment, but suggests an upwards adjustment prior to this. Again, evidence to support the alteration suggested by homogenization are lacking in the metadata, especially since possible impacts like insufficient sheltering would result in a rise in T_{max} and

hence imply an inverse adjustment (Brunet *et al.*, 2006a). Additional ventilation at the roof terrace, as explained for the clock tower in chapter 4.1, might have lowered T_{max}, but sensor measurements instead indicated a slight warming to be present in some seasons nonetheless. Similar to T_{min}, the 20 years of measurements within the factory cause large discrepancies in corrections suggested by the two methods, potentially linked to the poorly documented station movements within the factory. Homogenization considers the bias in T_{max} after relocating the station to its current spot to be negligible and while we agree this is true for winter, an urban warming influence is still present in summer. In addition, homogenization does not capture the relocation in 1993 as the time series is adjusted several years later.

The warmer period in the 1980s following a longer period of cooler temperatures is incorporated in the corrected record as well and has not been removed by means of relocation bias elimination. In general, global temperatures depict that pattern as well (Hartmann *et al.*, 2013). The general temperature decrease, beginning in the 1950s, has been connected to global dimming and hence reduced incoming solar radiation due to higher aerosol concentrations caused by anthropogenic air pollution (Wild *et al.*, 2007; Wild, 2009). These studies trace the strong increase in the 1980s back to the introduction of filters used in power plants, industrial production, traffic, etc., and other devices that have reduced this impact, allowing the warming trend caused by increased greenhouse gas emissions to stand out again. However, the temperature increase of more than 2 °C in one decade as found in Tivissa, even if to some extent caused by a distinct drop in T_{max} beforehand, is unlikely, since such a drastic change in climate does not occur in other records from Spain (see Brunet *et al.*, 2006b). This strange feature, however, seems to be not or only slightly related to relocations, as our approach fails to address it properly. Since the sheltering did not change and the observer stayed the same during that time, we struggle to find reasons for this phenomenon. Regardless of the cause, statistical homogenization with the HOMER method removes this increase and hence indicates a warming since 1980 similar to that of other Spanish temperature series.

Apart from that, relative homogenization is only applicable if sufficient reference records are available in the region. While this is true from 1950 onwards, our method is capable of improving the data before that time, boosting its utilization when it comes to long-term temperature records.

5.5 Conclusions

The local climate of Tivissa has been investigated for a two-year-period with a set of six temperature sensors placed within and outside the village in order to reveal whether it is affected by urban warming. A persistent UHI was detected that has its maximum intensity in the warm season and overall during nighttime. Hosting a meteorological station, Tivissa likely has a temperature record containing this warm bias. Certainly, as the station was relocated several times within the village, the magnitude of this influence varies over time. We eliminated these site-specific impacts resulting from relocations by adjusting the century long record based on recent measurements carried out at the historical locations of the station. Overall, the correction lowered temperatures for most part of the record, addressing the inherent warming and resulting in a substantial increase in warming trend in T_{min} regardless of the season, while trends in T_{max}, except for winter, were inversely affected. Since the Tivissa time series has been homogenized from 1950 onwards relying on statistical comparison with reference records from the region, we compare these results with the ones from our correction approach based on in-situ measurements. In general, both adjustments show only small agreement, especially from mid-70s until mid-90s when the station was located at a factory. The relocation bias elimination better addresses exact site-specific differences, reduces the risk of overcorrection related to relative homogenization, and is able to proof that even the recent measurement site is biased by anthropogenic warming, a feature lost in the homogenized data. However, homogenization is able to remove the unreasonably steep warming trend incorporated in the original data during the 80s while our correction fails to do so, possibly due to other influences on measurements not detailed in metadata. Finding an explanation for this feature is still pending, because common error sources like a change in observer or screening have not been reported for the time intervals with peculiar data. Since relocations and alterations in site-specific climatology are generally known to be the main cause for substantial biases in time series, we estimate the correction based on in-situ measurements to be a good approach to produce enhanced temperature data. While both methods remove specific undesired impacts, they seem to fail covering others, resulting in improved time series that still do not succeed in recovering the real historical climatological data. Further research needs to be carried out by extending the comparison to other sites in order to better understand differences between the methods of data adjustment and their underlying reasons.

5.6 References

Balling Jr RC, Idso SB (1989). Historical temperature trends in the United States and the effect of urban population growth. *Journal of Geophysical Research* **94**: 3359-3363.

Barry RG (2008). Mountain weather and climate. Cambridge, Cambridge University Press.

Böhm R, Jones PD, Hiebl J, Frank D, Brunetti M, Maugeri M (2009). The early instrumental warm-bias: a solution for long central European temperature series 1760–2007. *Climatic Change* **101**: 41-67.

Brandsma T, Können GP, Wessels HRA (2003). Empirical estimation of the effect of urban heat advection on the temperature series of De Bilt (The Netherlands). *International Journal of Climatology* **23**: 829-845.

Brandsma T, Wolters D (2012). Measurement and Statistical Modeling of the Urban Heat Island of the City of Utrecht (the Netherlands). *Journal of Applied Meteorology and Climatology* **51**: 1046-1060.

Brunet M, Saladié O, Jones P, Sigró J, Aguilar E, Moberg A, Lister D, Walther A, Almarza C (2006a). A case-study/guidance on the development of long-term daily adjusted temperature datasets. *WMO/TD* **1425**.

Brunet M, SaladiÉ O, Jones P, SigrÓ J, Aguilar E, Moberg A, Lister D, Walther A, Lopez D, Almarza C (2006b). The development of a new dataset of Spanish Daily Adjusted Temperature Series (SDATS) (1850–2003). *International Journal of Climatology* **26**: 1777-1802.

Cook ER, Peters K (1981). The smoothing spline: A new approach to standardizing forest interior tree-ring width series for dendroclimatic studies. *Tree-Ring Bulletin* **41**: 45-53.

de Souza DO, dos Santos Alvalá RC (2014). Observational evidence of the urban heat island of Manaus City, Brazil. *Meteorological Applications* **21**: 186-193.

Devadas MD, Rose AL (2009). Urban factors and the intensity of heat island in the city of Chennai. The seventh International Conference on Urban Climate. Yokohama.

Dienst M, Lindén J, Engström E, Esper J (2017). Removing the relocation bias from the 155-year Haparanda temperature record in Northern Europe. *International Journal of Climatology* **37**: 4015-4026.

Dimoudi A, Nikolopoulou M (2003). Vegetation in the urban environment: microclimatic analysis and benefits. *Energy and Buildings* **35**: 69-76.

Emmanuel R, Krüger E (2012). Urban heat island and its impact on climate change resilience in a shrinking city: The case of Glasgow, UK. *Building and Environment* **53**: 137-149.

Emmanuel R, Rosenlund H, Johansson E (2007). Urban shading—a design option for the tropics? A study in Colombo, Sri Lanka. *International Journal of Climatology* **27**: 1995-2004.

Freitas L, Pereira MG, Caramelo L, Mendes M, Nunes LF (2013). Homogeneity of monthly air temperature in Portugal with HOMER and MASH. *Quarterly Journal of the Hungarian Meteorological Service* **117**: 69-90.

Fujibe F (2011). Urban warming in Japanese cities and its relation to climate change monitoring. *International Journal of Climatology* **31**: 162-173.

Gaffin SR, Rosenzweig C, Khanbilvardi R, Parshall L, Mahani S, Glickman H, Goldberg R, Blake R, Slosberg RB, Hillel D (2008). Variations in New York city's urban heat island strength over time and space. *Theoretical and Applied Climatology* **94**: 1-11.

Gedzelman SD, Austin S, Cermak R, Stefano N, Partridge S, Quesenberry S, Robinson DA (2003). Mesoscale aspects of the Urban Heat Island around New York City. *Theoretical and Applied Climatology* **75**: 29-42.

Ghazanfari S, Naseri M, Faridani F, Aboutorabi H, Farid A (2009). Evaluating the effects of UHI on climate parameters (A case study for Mashhad, Khorrasan). *International Journal of Energy and Environment* **3**: 94-101.

Giridharan R, Ganesan S, Lau SSY (2004). Daytime urban heat island effect in high-rise and high-density residential developments in Hong Kong. *Energy and Buildings* **36**: 525-534.

Hamdi R, Deckmyn A, Termonia P, Demarée GR, Baguis P, Vanhuysse S, Wolff E (2009). Effects of Historical Urbanization in the Brussels Capital Region on Surface Air Temperature Time Series: A Model Study. *Journal of Applied Meteorology and Climatology* **48**: 2181-2196.

Hamdi R, Schayes G (2008). Sensitivity study of the urban heat island intensity to urban characteristics. *International Journal of Climatology* **28**: 973-982.

Hartmann DL, Klein Tank AMG, Rusticucci M, Alexander LV, Brönnimann S, Charabi YA-R, Dentener FJ, Dlugokencky EJ, Easterling DR, Kaplan A, Soden BJ, Thorne PW, Wild M, Zhai P (2013). Observations: Atmosphere and Surface. IPPC Report: 159-254.

Hinkel KM, Nelson FE, Klene AE, Bell JH (2003). The urban heat island in winter at Barrow, Alaska. *International Journal of Climatology* **23**: 1889-1905.

Jardí R (1923). Deu anys d'observacions termopluviomètriques a Tivissa. Barcelona.

Jones PD, Groisman PY, Coughlan M, Plummer N, Wang W-C, Karl TR (1990). Assessment of urbanization effects in time series of surface air temperature over land. *Nature* **347**: 169-172.

Jones PD, Lister D, Li Q (2008). Urbanization effects in large-scale temperature records, with an emphasis on China. *Journal of Geophysical Research* **113**: 1-12.

Kato H (1996). A Statistical Method for Seperating Urban Effect Trends from Observed Temperature Data and its Application to Japanese Temperature Records. *Journal of the Meteorological Society of Japan* **74**: 639-653.

Kim Y-H, Baik J-J (2002). Maximum Urban Heat Island Intensity in Seoul. *Journal of Applied Meteorology* **41**: 651-659.

Kim YH, Baik JJ (2004). Daily maximum urban heat island intensity in large cities of Korea. *Theoretical and Applied Climatology* **79**: 151-164.

Klysik K, Fortuniak K (1999). Temporal and spatial characteristics of the urban heat island of Lodz, Poland. *Atmospheric Environment* **33**: 3885-3895.

Kottek M, Grieser J, Beck C, Rudolf B, Rubel F (2006). World Map of the Köppen-Geiger climate classification updated. *Meteorologische Zeitschrift* **15**: 259-263.

Landsberg HE (1981). The Urban Climate. New York, Academic Press.

Mestre O, Domonkos P, Picard F, Auer I, Robin S, Lebarbier E, Böhm R, Aguilar E, Guijarro J, Vertachnik G, Klancar M, Dubuisson B, Stepanek P (2013). HOMER: a homogenization software - methods and applications. *Quarterly Journal of the Hungarian Meteorological Service* **117**: 47-67.

Morris CJG, Simmonds I, Plummer N (2001). Qualification of the Influences of Wind and Cloud on the Nocturnal Urban Heat Island of a Large City. *Journal of Applied Meteorology* **40**: 169-182.

Nakamura Y, Oke TR (1988). Wind, Temperature and Stability Conditions in an East-West Oriented Urban Canyon. *Atmospheric Environment* **22**: 2691-2700.

Oke TR (1982). The energetic basis of the urban heat island. *Quarterly Journal of the Royal Meteorological Society* **108**: 1-24.

Papanastasiou DK, Kittas C (2012). Maximum urban heat island intensity in a medium-sized coastal Mediterranean city. *Theoretical and Applied Climatology* **107**: 407-416.

Peterson TC, Gallo KP, Lawrimore JH, Owen TW, Huang A, McKittrick DA (1999). Global rural temperature trends. Papers in Natural Resources.

Pigeon G, Legain D, Durand P, Masson V (2007). Anthropogenic heat release in an old European agglomeration (Toulouse, France). *International Journal of Climatology* **27**: 1969-1981.

Poulos G, Zhong S (2008). An observational history of small-scale katabatic winds in Mid-Latitudes. *Geography Compass* **2**: 1798-1821.

Ramponi R, Gaetani I, Angelotti A (2014). Influence of the urban environment on the effectiveness of natural night-ventilation of an office building. *Energy and Buildings* **78**: 25-34.

Rizwan AM, Dennis LYC, Liu C (2008). A review on the generation, determination and mitigation of Urban Heat Island. *Journal of Environmental Sciences* **20**: 120-128.

Rykwert J (1988). The Idea of a Town: The Anthropology of Urban Form in Rome, Italy and the Ancient World. Princeton, Princeton University Press.

Saaroni H, Ben-Dor E, Bitan A, Potchter O (2000). Spatial distribution and microscale characteristics of the urban heat island in Tel-Aviv, Israel. *Landscape and Urban Planning* **48**: 1-18.

Saladié Ò, Salvat Salvat J,Anton Clavé S (2013). Diseño de un itinerario turístico en Tivissa a partir de la estación meteorológica. *Investigaciones Geográficas*: 119-133.

Szegedi S, Toth T, Kapocska L, Gyarmati R (2013). Examinations on the meteorological factors of urban heat island developement in small and medium-sized towns in Hungary. *Carpathian Journal of Earth and Environmental Sciences* **8**: 209-214.

Tuomenvirta H (2001). Homogeneity adjustments of temperature and precipitation series - Finnish and Nordic data. *International Journal of Climatology* **21**: 495-506.

Unger J (2004). Intra-urban relationship between surface geometry and urban heat island: review and new approach. *Climate Research* **27**: 253-264.

Venema V, Mestre O, Aguilar E, Guijarro J, Domonkos P, Vertachnik G, Szentimrey T, Stepanek P, Zahradnicek P, Viarre J, Müller-Westermeier G, Lakatos M, Williams CN, Menne MJ, Lindau R, Rasol D, Rustemeier E, Kolokythas K, Marinova T, Andresen L, Acquaotta F, Fratianni S, Cheval S, Klancar M, Brunet M, Gruber C, Prohom M, Likso T, Esteban P, Brandsma T, Willet K (2012). Detecting and repairing inhomogeneities in datasets, assessing current capabilities. *Bulletin of the American Meteorological Society* **93**: 951-954.

Wang F,Ge Q (2012). Estimation of urbanization bias in observed surface temperature change in China from 1980 to 2009 using satellite land-use data. *Chinese Science Bulletin* **57**: 1708-1715.

Wilby RL (2003). Past and projected trends in London's urban heat island. *Weather* **58**: 251-260.

Wild M (2009). Global dimming and brightening: A review. *Journal of Geophysical Research* **114**.

Wild M, Ohmura A, Makowski K (2007). Impact of global dimming and brightening on global warming. *Geophysical Research Letters* **34**.

WMO (2011) Guide to Climatological Practices - Third Edition.

Yang Y-J, Wu B-W, Shi C-E, Zhang J-H, Li Y-B, Tang W-A, Wen W-A, Zhang H-Q, Shi T (2013). Impacts of Urbanization and Station-relocation on Surface Air Temperature Series in Anhui Province, China. *Pure and Applied Geophysics* **170**: 1969-1983.

Zhang L, Ren G, Ren Y, Zhang A, Chu Z, Zhou Y (2014). Effect of data homogenization on estimate of temperature trend: a case of Huairou station in Bejing Municipality. *Theoretical and Applied Climatology* **115**: 365-373.

Zhou L, Dickinson RE, Tian Y, Fang J, Li Q, Kaufmann RK, Tucker CJ, Myneni RB (2004). Evidence for a significant urbanization effect on climate in China. *Proceedings of the National Academy of Sciences USA* **101**: 9540-9544.

6 Conclusions and prospects

The quality of temperature data is a great issue in today's climate research because it determines the ability to quantify and evaluate past and recent climate variability, and hence contributes to the discussion about current global warming. However, the reliability of temperature records is sometimes imperilled, as meteorological measurements might contain signals not caused by climate exclusively, but by manmade features, which is particularly true for long time series as demonstrated for the Alpine region (Auer *et al.*, 2007). This thesis introduced ways of assessing the anthropogenic impact related to UHI formation in long temperature time series as well as a correction approach for the biased data.

First, this work shows that villages are indeed characterised by significantly warmer temperatures than their rural surroundings, and minimum temperatures are most influenced in that regard. The maximum UHI intensity decreases from northern to southern Europe and persists throughout the year, although seasonal intensity varies with a more prominent UHI in winter in the Mediterranean but otherwise stronger summertime effect. This finding might be linked to less evapotranspirative cooling in the rural area during summer due to arid conditions in the Mediterranean that is supported by solely slight correlations between vegetation coverage and local cooling. However, the local river mitigates warming at nighttime, while this effect is absent in the central and northern European sites. Since an increase in the amount of built-up area causes a significant rise in temperatures at all sites, and each village is home to a meteorological station characterised as rural, a revaluation of rural sites is essential in order to avoid using UHI affected data as bias-free reference.

In a second step, the thesis proves that the over 200 yearlong temperature record from the city of Brno, Czech Republic, contains a bias related to the UHI effect at past measurement sites of the meteorological station. A new approach is introduced based on recent temperature data and land cover assessment to correct the time series for this bias. Since additional warming originating from urban structures is most pronounced in warm season minimum temperatures, corrections are also strongest during that time of the year. Applying the correction lowers temperatures particularly in the early part of the record, because the historical measurement sites were situated within the city centre and thus were exposed to significant anthropogenic warming. With the station moving out of the centre in the 20th century and hence correction factors becoming almost negligible, confirming the record's reliability from that point onwards,

the corrected time series shows an overall amplified warming trend if compared to the original dataset. As the stepwise relocation of meteorological stations from the centre to the rural surroundings is a characteristic of many long temperature records, any of these are likely biased in the same way, raising the question whether past warming in general might be even stronger.

Following this, the Haparanda station serves as an example for a village station being relocated several times with a tendency of moving to less urbanized sites. These relocations are addressed by means of temperature measurements at each historical measurement site. Substantial urban warming effects, particularly in summer nighttime temperatures, exist at the sites investigated and thus are incorporated in the temperature dataset. Eliminating the relocation bias leads to similar results as in Brno, with a stronger correction in the early and a lesser one in the recent part of the record. The implication is once more an increasing warming trend for the corrected time series. Because of the station's remoteness and the length of the record, the correction method introduced here offers a good alternative to enhance temperature data if homogenization based on reference records is not applicable.

In addition to the work in Haparanda, the temperature time series from the Spanish village Tivissa possibly contains a bias related to relocation measures in its century long history as well. Indeed, measurements display a strong warming in Tivissa at various past measurement sites particularly at nighttime, although one urban location cools down faster than even the rural reference station due to cool air pooling at nighttime. Removing the impact of site-specific climatology leads to increasing trends in minimum but decreasing ones in maximum temperatures. As temperature data has been homogenized from 1950 onwards, a comparison with the newly introduced correction approach was performed, revealing at times substantial differences between both adjusted time series. The analysis shows that the relocation bias elimination is a good way of addressing site-specific differences but has its limitations to consider other impacts. At the same time, it shows relative homogenization has weaknesses particularly regarding the magnitude and timing of applied correction factors.

The implications of this thesis are diverse. It serves as an important contribution to the assessment of urban heat islands in villages and site-specific climatology in various locations throughout Europe using similar set-ups and measurement techniques. The quantification of the maximum UHI intensity shows that warming is remarkably high in comparison to larger cities, considering the small sizes and low population densities in the settlements. Following these findings, it states to treat rural station data from villages with great care as measurements are influenced by additional anthropogenic warming. Furthermore, it offers a new approach to

quantify and eliminate the relocation bias, particularly evoked by varying UHI intensities at past measurement locations by relying on recent temperature measurements. In addition, long temperature time series, particularly in remote places, often lack reference stations, hence rendering the application of relative homogenization techniques impossible. Therefore, the method might be seen as a basic homogenization approach to enhance contaminated records by addressing the relocation bias that is known to have the most significant impact on data, even though it lacks the ability to capture other influences on the dataset like changes in screening or observing staff. If relocations are not explicitly detailed in metadata, the method might not be suitable. Besides relying on well-documented metadata, the approach needs a sophisticated set-up and is very time-consuming, limiting its application to several selected sites.

Finally, two findings need further consideration. A feature that all long records introduced here have in common is the warming influence particularly in the early part of the record due to the placement of stations in the centre of the urban area. The implication is the necessity of a downwards correction in temperatures at least during the 19th century. As proxy data evidence indicates cooler temperatures during that time as well (Frank *et al.*, 2007), this thesis adds another possible explanation for the observed discrepancy between measured and reconstructed temperatures, in addition to the argument of insufficient sheltering and hence solar bias in the station data (e.g. Nicholls *et al.*, 1996; Nordli *et al.*, 1997).

Furthermore, additional research needs to be carried out in order to address the point Zhang *et al.* (2014) make for their study, stating that the intensified warming after a correction for site-specific differences, i.e. relocation biases, is simply a recovery of the urban warming caused by the steady growth of a city. They explain the urban warming has been supressed in the original data by relocating the station to more rural sites, lessening the UHI effect on measurements towards today. While this might be true for cities with intense growth over the past centuries, it should be of little importance for villages, particularly if they have not changed very much from the installation of the meteorological station until today, as is true for the ones investigated in this thesis. Although it might hold true for the Brno record to some extent, this thesis nonetheless suggests warming trends in long temperature records are actually more severe than known to this point.

Bibliography

Aguilar E, Auer I, Brunet M, Peterson TC, Wieringa J (2003). Guidelines on climate metadata and homogenization. *WMO/TD* **1186**.

Alcoforado MJ, Andrade H (2005). Nocturnal urban heat island in Lisbon (Portugal): main features and modelling attempts. *Theoretical and Applied Climatology* **84**: 151-159.

Auer I, Böhm R, Jurkovic A, Lipa W, Orlik A, Potzmann R, Schöner W, Ungersböck M, Matulla C, Briffa K, Jones P, Efthymiadis D, Brunetti M, Nanni T, Maugeri M, Mercalli L, Mestre O, Moisselin J-M, Begert M, Müller-Westermeier G, Kveton V, Bochnicek O, Stastny P, Lapin M, Szalai S, Szentimrey T, Cegnar T, Dolinar M, Gajic-Capka M, Zaninovic K, Majstorovic Z, Nieplova E (2007). HISTALP—historical instrumental climatological surface time series of the Greater Alpine Region. *International Journal of Climatology* **27**: 17-46.

Begert M, Schlegel T, Kirchhofer W (2005). Homogeneous temperature and precipitation series of Switzerland from 1864 to 2000. *International Journal of Climatology* **25**: 65-80.

Berkowicz R, Palmgren F, Hertel O, Vignati E (1996). Using measurements of air pollution in streets for evaluation of urban air quality — meterological analysis and model calculations. *Science of The Total Environment* **189-190**: 259-265.

Böhm R (1998). Urban bias in temperature time series - A case study for the city of Vienna, Austria. *Climatic Change* **38**: 113-128.

Böhm R, Jones PD, Hiebl J, Frank D, Brunetti M, Maugeri M (2009). The early instrumental warm-bias: a solution for long central European temperature series 1760–2007. *Climatic Change* **101**: 41-67.

Bornstein R, Lin Q (2000). Urban heat islands and summertime convective thunderstorms in Atlanta: three case studies. *Atmospheric Environment* **34**: 507-516.

Brunekreef B, Holgate ST (2002). Air pollution and health. *The Lancet* **360**: 1233-1242.

Brunet M, Saladié O, Jones P, Sigró J, Aguilar E, Moberg A, Lister D, Walther A, Almarza C (2006). A case-study/guidance on the development of long-term daily adjusted temperature datasets. *WMO/TD* **1425**.

Chang C-R, Li M-H, Chang S-D (2007). A preliminary study on the local cool-island intensity of Taipei city parks. *Landscape and Urban Planning* **80**: 386-395.

Chen X-L, Zhao H-M, Li P-X, Yin Z-Y (2006). Remote sensing image-based analysis of the relationship between urban heat island and land use/cover changes. *Remote Sensing of Environment* **104**: 133-146.

Chow W, Roth M (2006). Temporal dynamics of the urban heat island of Singapore. *International Journal of Climatology* **26**: 2243-2260.

Conti S, Meli P, Minelli G, Solimini R, Toccaceli V, Vichi M, Beltrano C, Perini L (2005). Epidemiologic study of mortality during the Summer 2003 heat wave in Italy. *Environ Res* **98**: 390-399.

Coseo P, Larsen L (2014). How factors of land use/land cover, building configuration, and adjacent heat sources and sinks explain Urban Heat Islands in Chicago. *Landscape and Urban Planning* **125**: 117-129.

Devadas MD, Rose AL (2009). Urban factors and the intensity of heat island in the city of Chennai. *The seventh International Conference on Urban Climate*. Yokohama.

Dewan AM, Yamaguchi Y (2009). Land use and land cover change in Greater Dhaka, Bangladesh: Using remote sensing to promote sustainable urbanization. *Applied Geography* **29**: 390-401.

Dimoudi A, Kantzioura A, Zoras S, Pallas C, Kosmopoulos P (2013). Investigation of urban microclimate parameters in an urban center. *Energy and Buildings* **64**: 1-9.

Dixon PG, Mote TL (2003). Patterns and Causes of Atlanta's Urban Heat Island–Initiated Precipitation. *Journal of Applied Meteorology* **42**: 1273-1284.

Döös BR (2002). Population growth and loss of arable land. *Global Environmental Change* **12**: 303-311.

Elminir HK (2005). Dependence of urban air pollutants on meteorology. *Sci Total Environ* **350**: 225-237.

Esper J, Cook ER, Schweingruber FH (2002). Low-frequency signals in long tree-ring chronologies for reconstructing past temperature variability. *Science* **295**: 2250-2253.

Ferreira MJ, de Oliveira AP, Soares J (2010). Anthropogenic heat in the city of São Paulo, Brazil. *Theoretical and Applied Climatology* **104**: 43-56.

Frank D, Büntgen U, Böhm R, Maugeri M, Esper J (2007). Warmer early instrumental measurements versus colder reconstructed temperatures: shooting at a moving target. *Quaternary Science Reviews* **26**: 3298-3310.

Fujibe F (2009). Detection of urban warming in recent temperature trends in Japan. *International Journal of Climatology* **29**: 1811-1822.

Giridharan R, Ganesan S, Lau SSY (2004). Daytime urban heat island effect in high-rise and high-density residential developments in Hong Kong. *Energy and Buildings* **36**: 525-534.

Giridharan R, Kolokotroni M (2009). Urban heat island characteristics in London during winter. *Solar Energy* **83**: 1668-1682.

Grimmond CSB, Oke TR (2002). Turbulent Heat Fluxes in Urban Areas: Observations and a Local-Scale Urban Meteorological Parameterization Scheme (LUMPS). *Journal of Applied Meteorology* **41**: 792-810.

Hamdi R, Schayes G (2008). Sensitivity study of the urban heat island intensity to urban characteristics. *International Journal of Climatology* **28**: 973-982.

Hansen J, Ruedy R, Sato M, Imhoff W, Lawrence D, Easterling DR, Peterson TC, Karl T (2001). A closer look at United States and global surface temperature change. *Journal of Geophysical Research* **106**: 23947-23963.

Hinkel KM, Nelson FE, Klene AE, Bell JH (2003). The urban heat island in winter at Barrow, Alaska. *International Journal of Climatology* **23**: 1889-1905.

Homer C, Dewitz J, Yang L, Jin S, Danielson P, Xian G, Coulston J, Herold N, Wickham J, Megown K (2015). Completion of the 2011 National Land Cover Database for the Conterminous United States – Representing a Decade of Land Cover Change Information. *Photogrammetric Engineering & Remote Sensing* **81**: 345-354.

Hua LJ, Ma ZG, Guo WD (2008). The impact of urbanization on air temperature across China. *Theoretical and Applied Climatology* **93**: 179-194.

Jauregui E (1997). Heat island development in Mexico City. *Atmospheric Environment* **31**: 3821-3831.

Jones PD, Groisman PY, Coughlan M, Plummer N, Wang W-C, Karl TR (1990). Assessment of urbanization effects in time series of surface air temperature over land. *Nature* **347**: 169-172.

Kalnay E, Cai M (2003). Impact of urbanization and land-use change on climate. *Nature* **423**: 528-531.

Ketterer C, Matzarakis A (2015). Comparison of different methods for the assessment of the urban heat island in Stuttgart, Germany. *Int J Biometeorol* **59**: 1299-1309.

Kim YH, Baik JJ (2004). Daily maximum urban heat island intensity in large cities of Korea. *Theoretical and Applied Climatology* **79**: 151-164.

Klysik K, Fortuniak K (1999). Temporal and spatial characteristics of the urban heat island of Lodz, Poland. *Atmospheric Environment* **33**: 3885-3895.

Kolokotroni M, Giridharan R (2008). Urban heat island intensity in London: An investigation of the impact of physical characteristics on changes in outdoor air temperature during summer. *Solar Energy* **82**: 986-998.

Kukla G, Gavin J, Karl TR (1986). Urban Warming. *Journal of Climate and Applied Meteorology* **25**: 1265-1270.

Kumar S, Prasad T, Sashidharan NV, Nair SK (2001). Heat island intensities over Brihan Mumbai on a cold winter and hot summer night. *Mausam* **52**: 703-708.

Künzli N, Kaiser R, Medina S, Studnicka M, Chanel O, Filliger P, Herry M, Horak F, Puybonnieux-Texier V, Quénel P, Schneider J, Seethaler R, Vergnaud JC, Sommer H (2000). Public-health impact of outdoor and traffic-related air pollution: a European assessment. *The Lancet* **356**: 795-801.

Landsberg HE (1981). The Urban Climate. New York, Academic Press.

Lee DO (1979). The influence of atmospheric stability and the urban heat island on urban-rural wind speed differences. *Atmospheric Environment (1967)* **13**: 1175-1180.

Lindén J, Esper J, Holmer B (2015). Using Land Cover, Population, and Night Light Data for Assessing Local Temperature Differences in Mainz, Germany. *Journal of Applied Meteorology and Climatology* **54**: 658-670.

Lo CP, Quattrochi DA (2003). Land-Use and Land-Cover Change, Urban Heat Island Phenomenon, and Health Implications: A Remote Sensing Approach. *Photogrammetric Engineering & Remote Sensing* **69**: 1053-1063.

Lopes A, Saraiva J, Alcoforado MJ (2011). Urban boundary layer wind speed reduction in summer due to urban growth and environmental consequences in Lisbon. *Environmental Modelling & Software* **26**: 241-243.

López E, Bocco G, Mendoza M, Duhau E (2001). Predicting land-cover and land-use change in the urban fringe. *Landscape and Urban Planning* **55**: 271-285.

Maragogiannis K, Kolokotsa D, Maria E-A (2011). Study of Night Ventilation Efficiency in Urban Environment: Technical and Legal Aspects. *Scientific Journal of Riga Technical University. Environmental and Climate Technologies* **6**.

McKinney ML (2006). Urbanization as a major cause of biotic homogenization. *Biological Conservation* **127**: 247-260.

Meehl GA, Stocker TF, Collins WD, Friedlingstein P, Gaye AT, Gregory JM, Kitoh A, Knutti R, Murphy JM, Noda A, Raper SCB, Watterson SCB, Weaver AJ, Zhao Z-C (2007). Global Climate Projections. *Climate Change 2007: The Physical Science Basis. Contribution of Working Group I to the Fourth Assessment Report of the Intergovernmental Panel on Climate Change*. Solomon S, Qin D, Manning M, Chen Z, Marquis M, Averyt KB, Tignor M, Miller HL. Cambridge and New York.

Mestre O, Domonkos P, Picard F, Auer I, Robin S, Lebarbier E, Böhm R, Aguilar E, Guijarro J, Vertachnik G, Klancar M, Dubuisson B, Stepanek P (2013). HOMER: a homogenization software - methods and applications. *Quarterly Journal of the Hungarian Meteorological Service* **117**: 47-67.

Moberg A, Bergström H (1997). Homogenization of Swedish temperature data - Part III - The long temperature records from Uppsala and Stockholm. *International Journal of Climatology* **17**.

Montávez JP, Rodríguez A, Jiménez JI (2000). A study of the urban heat island of Granada. *International Journal of Climatology* **20**: 899-911.

Morris CJG, Simmonds I, Plummer N (2001). Qualification of the Influences of Wind and Cloud on the Nocturnal Urban Heat Island of a Large City. *Journal of Applied Meteorology* **40**: 169-182.

Nakagawa T, Tarasov PE, Nishida K, Gotanda K, Yasuda Y (2002). Quantitative pollen-based climate reconstruction in central Japan: application to surface and Late Quaternary spectra. *Quaternary Science Reviews* **21**: 2099-2113.

Nicholls N, Tapp R, Burrows K, Richards D (1996). Historical Thermometer Exposures in Australia. *International Journal of Climatology* **16**: 705-710.

Niyogi D, Pyle P, Lei M, Arya SP, Kishtawal CM, Shepherd M, Chen F, Wolfe B (2011). Urban Modification of Thunderstorms: An Observational Storm Climatology and Model Case Study for the Indianapolis Urban Region*. *Journal of Applied Meteorology and Climatology* **50**: 1129-1144.

Nordli PØ, Alexandersson H, Frich P, Førland EJ, Heino R, Jónsson T, Tuomenvirta H, Tveito OE (1997). The effect of raditation screens on Nordic time series of mean temperature. *International Journal of Climatology* **17**: 1667-1681.

Oke TR (1973). City size and the urban heat island. *Atmospheric Environment* **7**: 769-779.

Oke TR (1987). Boundary Layer Climates, Taylor & Francis Ltd.

Parker DE (2004). Climate: large-scale warming is not urban. *Nature* **432**: 290.

Parker DE (2010) Urban heat island effects on estimates of observed climate change. *WIREs Climate Change* **1**, 123-133

Peterson TC, Easterling DR, Karl TR, Groisman P, Nicholls N, Plummer N, Torok S, Auer I, Boehm R, Gullett D, Vincent L, Heino R, Tuomenvirta H, Mestre O, Szentimrey T, Salinger J, Førland EJ, Hanssen-Bauer I, Alexandersson H, Jones P, Parker D (1998). Homogeneity adjustments ofin situ atmospheric climate data: a review. *International Journal of Climatology* **18**: 1493-1517.

Pigeon G, Legain D, Durand P, Masson V (2007). Anthropogenic heat release in an old European agglomeration (Toulouse, France). *International Journal of Climatology* **27**: 1969-1981.

Quah AKL, Roth M (2012). Diurnal and weekly variation of anthropogenic heat emissions in a tropical city, Singapore. *Atmospheric Environment* **46**: 92-103.

Quereda Sala J, Gil Olcina A, Perez Cuevas A, Olcina Cantos J, Rico Amoros A, Montón Chiva E (2000). Climatic Warming in the Spanish Mediterranean: Natural Trend or Urban Effect. *Climatic Change* **46**: 473-483.

Randall DA, Wood RA, Bony S, Colman R, Fichefet T, Fyfe J, Kattsov V, Pitman A, Shukla J, Srinivasan J, Stouffer RJ, Sumi A, Taylor KE (2007). Cilmate Models and Their Evaluation. *Climate Change 2007: The Physical Science Basis. Contribution of Working Group I to the*

Fourth Assessment Report of the Intergovernmental Panel on Climate Change. Solomon S, Qin D, Manning M, Chen Z, Marquis M, Averyt KB, Tignor M, Miller HL. Cambridge and New York.

Saaroni H, Ben-Dor E, Bitan A, Potchter O (2000). Spatial distribution and microscale characteristics of the urban heat island in Tel-Aviv, Israel. *Landscape and Urban Planning* **48**: 1-18.

Scholz D, Frisia S, Borsato A, Spötl C, Fohlmeister J, Mudelsee M, Miorandi R, Mangini A (2012). Holocene climate variability in north-eastern Italy: potential influence of the NAO and solar activity recorded by speleothem data. *Climate of the Past* **8**: 1367-1383.

Spronken-Smith RA, Oke TR (1998). The thermal regime of urban parks in two cities with different summer climates. *International Journal of Remote Sensing* **19**: 2085-2104.

Steeneveld GJ, Koopmans S, Heusinkveld BG, van Hove LWA, Holtslag AAM (2011). Quantifying urban heat island effects and human comfort for cities of variable size and urban morphology in the Netherlands. *Journal of Geophysical Research* **116**: 1-14.

Stone B (2007). Urban and rural temperature trends in proximity to large US cities: 1951–2000. *International Journal of Climatology* **27**: 1801-1807.

Szegedi S, Toth T, Kapocska L, Gyarmati R (2013). Examinations on the meteorological factors of urban heat island developement in small and medium-sized towns in Hungary. *Carpathian Journal of Earth and Environmental Sciences* **8**: 209-214.

Szymanowski M (2005). Interactions between thermal advection in frontal zones and the urban heat island of Wrocław, Poland. *Theoretical and Applied Climatology* **82**: 207-224.

Tan J, Zheng Y, Tang X, Guo C, Li L, Song G, Zhen X, Yuan D, Kalkstein AJ, Li F (2010). The urban heat island and its impact on heat waves and human health in Shanghai. *Int J Biometeorol* **54**: 75-84.

Tomlinson CJ, Chapman L, Thornes JE, Baker CJ (2012). Derivation of Birmingham's summer surface urban heat island from MODIS satellite images. *International Journal of Climatology* **32**: 214-224.

Torok SJ, Morris CJG, Skinner C, Plummer N (2001). Urban heat island features of southeast Australian. *Australian Meteorological Magazine* **50**: 1-13.

Trouet V, Van Oldenborgh GJ (2013). KNMI Climate Explorer: A Web-Based Research Tool for High-Resolution Paleoclimatology. *Tree-Ring Research* **69**: 3-13.

Tuomenvirta H (2001). Homogeneity adjustments of temperature and precipitation series - Finnish and Nordic data. *International Journal of Climatology* **21**: 495-506.

Unger J (1996). Heat Island intesity with different meteorological conditions in a medium-sized town. *Theoretical and Applied Climatology* **54**: 147-151.

United Nations PD (2017). World Population Prospects. Affairs, DoEaS. New York.

United Nations PD (2018). World Urbanization Prospects. Affairs, DoEaS. New York.

Vogel JL, Huff FA (1978). Relation Between the St. Louis Urban Precipitation Anomaly and Synoptic Weather Factors. *Journal of Applied Meteorology* **17**: 1141-1152.

Wienert U, Kuttler W (2005). The dependence of the urban heat island intensity on latitude - A statistical approach. *Meteorologische Zeitschrift* **14**: 677-686.

Yang P, Ren G, Liu W (2013). Spatial and Temporal Characteristics of Bejing Urban Heat Island Instensity. *Journal of Applied Meteorology and Climatology* **52**: 1803-1816.

Yoshikado H (1994). Interaction of the Sea Breeze with Urban Heat Islands of Different Sizes and Locations. *Journal of the Meteorological Society of Japan. Ser. II* **72**: 139-143.

Zhang J-H, Hou Y, Li G, Yan H, Yang L, Yao F (2005). The diurnal and seasonal characteristics of urban heat island variation in Beijing city and surrounding areas and impact factors based on remote sensing satellite data. *Science in China. Ser. D Earth Sciences* **48**: 220-229.

Zhang L, Ren G, Ren Y, Zhang A, Chu Z, Zhou Y (2014). Effect of data homogenization on estimate of temperature trend: a case of Huairou station in Bejing Municipality. *Theoretical and Applied Climatology* **115**: 365-373.

List of figures

Figure 2-1 Sensor set-up in the three villages. The white squares indicate the sensor locations. Satellite images for Geisenheim and Cazorla have been derived from *Microsoft Bing maps 2017* and for Cazorla from *ESRI map services 2017* 11

Figure 2-2 Seasonal mean temperature values for river, centre and rural U23 sensors in each village. Temperatures are shown as differences to the mean of all sensors. Boxplots display the median (black middle line), the upper and lower quartile including 50% of the data (coloured box) and whiskers (vertical lines) including the other 50%. If a value lies beyond 1.5 times the interquartile range, it is plotted as an outlier and excluded from the whiskers, reducing the amount of data within 16

Figure 2-3 Seasonal minimum temperature values for river, centre and rural U23 sensors in each village. Temperatures are shown as differences to the mean of all sensors. Boxplots display the median (black middle line), the upper and lower quartile including 50% of the data (coloured box) and whiskers (vertical lines) including the other 50%. If a value lies beyond 1.5 times the interquartile range, it is plotted as an outlier and excluded from the whiskers, reducing the amount of data within 17

Figure 2-4 Coefficients of determination shown for three different types of land cover in each village. Seasonal temperatures were correlated with the specific land cover in four different radii. Filled dots indicate significant correlations on a 90%-level 19

Figure 2-5 Regression analysis for selected types of land cover in a specific radius which revealed strong and significant correlations with temperature. The equations display the rise or decrease in temperature per percent increase in type of land cover 20

Figure 3-1 Location of the 11 current measurement stations and historical measurement sites in the area of Brno 37

Figure 3-2 Seasonal air temperature variability based on daily data from June 2011 to February 2015 of rural (n=3, left) as well as urban stations with 41-75% (n=6, middle) and >75% sealed areas (n=2, right), respectively. Temperatures are displayed as anomalies, more specifically as differences to the mean of all sensors. Data exceeding 1.5 times the interquartile range are removed from the whiskers and shown as outliers 42

Figure 3-3 Coefficients of determination for seasonal average (a, b) und minimum temperatures (c, d, e) correlated with selected types of land cover (BU = Building, TV= Total Vegetation and

SA = Sealed Areas) relative to different distances to the stations. Selection was based on the correlation strength and importance of each land cover for later analysis 43

Figure 3-4 Regression analysis based on the relation between the percentage of built-up area within the station surroundings of 300 m radius and spring TN (R^2-Value 0.48*) and 500 m radius and TM (R^2-Value 0.80**), respectively. Spring temperatures were selected due to exceptionally high R^2-values 44

Figure 3-5 Measured and corrected Brno MAM record from 1850 until 2000. Data from the 19th century (left) and 20th century (right) are displayed separately to illustrate the strong corrections in the beginning and the minor changes in the later part. Spring season was selected due to the strongest relation to building density 46

Figure 4-1 Meteorological station (white squares) and sensor locations (white dots) in Haparanda. Dates indicate periods of historical station positions including overlap periods among residential sites. AWS is the current station location. An outline of the urban area 1946 is displayed as well (white line). *Maps from ESRI 2014* 60

Figure 4-2 Haparanda and reference stations (black dots) used for the homogenization attempt with HOMER. The starting dates of operation are given as well 63

Figure 4-3 Correction of the relocation bias based on parallel sensor measurements in Haparanda. The long record starts in 1860 with the first year of complete data and was subsequently adjusted with regard to the following three major relocations 66

Figure 4-4 Seasonal pattern of temperature deviations recorded at Haparanda sensors over two years. Monthly temperatures shown as anomalies from the mean of all sensors. Error bars display the variance as 95% confidence intervals. Filled squares mark significant deviations 67

Figure 4-5 Temperature residuals between the historical thermometer locations and the current AWS station location. Monthly TX, TM and TN deviations including 95% error bars calculated over two years are shown. The residential values are an average of two sensors. Significant deviations are displayed as filled squares 69

Figure 4-6 Raw and adjusted seasonal TM, TN and TX time series of the long Haparanda station. Curves are smoothed using a 15-year running mean, dashed lines display linear trends over the period 1860 - 2014. Temperatures are plotted as anomalies relative to the climate period from 1961 - 1990. The gap in TN and TX is due to missing data 70

Figure 4-7 Raw and adjusted annual mean temperatures of the Haparanda station record with smoothed curves as a 15-year running mean. Dashed lines display linear trends over the period from 1901 - 2000. Temperatures are plotted as anomalies relative to the climate period from 1961 - 1990. The residual used for obtaining the corrected series is shown below 72

Figure 5-1 Measurements in Tivissa. Historical meteorological station sites with interval of operation and sensor placements close to these sites (main map). Location of the village in Spain (side map) 87

Figure 5-2 UHI intensity in Tivissa. Seasonal maximum (top), mean (middle) and minimum (bottom) temperatures at all sensor sites displayed as anomalies to the rural reference sensor (AWS) based on daily data. Boxplots display the median (black middle line), the upper and lower quartile including 50% of the data (coloured box) and whiskers (vertical lines) including the other 50%. Values beyond 1.5 times the interquartile range are plotted as outliers and are excluded from the whiskers, thus reducing the amount of data within 93

Figure 5-3 Time series adjustment. Corrections applied to the minimum and maximum temperature series according to the different measuring periods 94

Figure 5-4 Trend changes after adjustment. Original (turquoise) and corrected (red) seasonal temperature time series and the corresponding decadal trends from spring to winter. Minimum temperatures displayed on the left, maximum temperatures on the right side 95

Figure 5-5 Differences in adjustment results. Comparison of corrected (red) and homogenized (orange) time series with the original one (turquoise). Minimum temperatures are displayed at the top, maximum temperatures at the bottom, with both showing the summer as well as the winter record. The difference of the correction values ($\Delta CorrValue_{correctedTS\text{-}homogenizedTS}$) are displayed as a residual (purple) next to the various time series. The dashed lines indicate relocations 96

Figure 5-6 20th century trend comparison. Annual mean temperature record for Tivissa (turquoise) along with the corrected (red) and homogenized (orange) series. All records are shown as anomalies to the original series for the reference period 1950-1959. The light graphs indicate the absolute values while the thick lines illustrate the smoothed versions using a 10-year spline 97

List of Tables

Table 2-1 Overview on the different sensors positioned in every village 15

Table 3-1 Location of the 11 current measurement stations and historical measurement sites in the area of Brno 38

Table 3-2 Classification of those land cover types in the wider area of Brno that have been considered in this study 39

Table 3-3 Regression equations and R^2-values for LC buildings and temperature relation 45

Table 3-4 Overview of the historical measurement periods of the Brno meteorological station, together with the built fraction in a 500 m radius around the past measuring locations derived from historical maps drawn in the years listed in column three. Columns 4-8 display the quantified heat bias in different seasons caused by nearby buildings based on the equations shown in table 2-3 45

Table 4-1 Previous station locations (top), current sensor sites for the assessment of the urban bias (middle) as well as sensors depicting the rural surroundings (bottom) in Haparanda 61

Table 4-2 Trends in corrected and uncorrected seasonal and annual TX, TN, and TM time series. Temperature trends in °C/10years calculated over the period 1860-2014 are shown 71

Table 5-1 Metadata on meteorological station and sensor set-up. Site-specific descriptions and operation details for historical as well as current measurements 89

Curriculum vitae

Not available in online version.

Not available in online version.

Not available in online version.